From the Clinic of Internal Medicine I

of the University of Lübeck

Director: Prof. Dr. med. Dr. h.c. Hendrik Lehnert

"Layered Interactions of Systemic and Brain Effects by Thyroid Hormones"

Dissertation for Fulfilment of Requirements

for the Doctoral Degree

of the University of Lübeck

from the Department of Natural Sciences

Submitted by

Lisbeth Harder

from Ingolstadt, Germany

Lübeck 2018

First referee: Herr Prof. Dr. Jens Mittag
Second referee: Herr Prof. Dr. Olaf Hiort
Date of oral examination: 14. November 2018
Approved for printing: Lübeck, 5. April 2019

Erklärung

Ich versichere, dass ich die Dissertation ohne fremde Hilfe angefertigt und keine anderen als die angegebenen Hilfsmittel verwendet habe. Weder vorher noch gleichzeitig habe ich andernorts einen Zulassungsantrag gestellt oder diese Dissertation vorgelegt. Ich habe mich bisher noch keinem Promotionsverfahren unterzogen.

Lübeck, den 22.06.2018

(Lisbeth Harder)

Publications

Parts of this thesis were already published in peer-reviewed journals due to priority reasons.

Included in this thesis:

Hoefig, C. S.*, Harder, L.*, Oelkrug, R., Meusel, M., Vennström, B., Brabant, G., & Mittag, J. (2016). Thermoregulatory and Cardiovascular Consequences of a Transient Thyrotoxicosis and Recovery in Male Mice. *Endocrinology, 157*(7), 2957-2967. doi:10.1210/en.2016-1095 *contributed equally

Harder, L., Schanze, N., Sarsenbayeva, A., Kugel, F., Köhrle, J., Schomburg, L., Mittag, J., & Hoefig, C. S. (2018). In vivo Effects of Repeated Thyronamine Administration in Male C57BL/6J Mice. *European Thyroid Journal, 7*(1), 3-12.

Harder, L., Dudazy-Gralla, S., Müller-Fielitz, H., Hjerling Leffler, J., Vennström, B., Heuer, H., & Mittag, J. (2018). Maternal Thyroid Hormone is Required for Parvalbumin Neurone Development in the Anterior Hypothalamic Area. *J Neuroendocrinol*. doi:10.1111/jne.12573

Not included in this thesis:

Hoefig, C. S., Jacobi, S. F., Warner, A., Harder, L., Schanze, N., Vennström, B., & Mittag, J. (2015). 3-Iodothyroacetic acid lacks thermoregulatory and cardiovascular effects in vivo. *Br J Pharmacol, 172*(13), 3426-3433. doi:10.1111/bph.13131

Renko, K., Hoefig, C. S., Dupuy, C., Harder, L., Schwiebert, C., Köhrle, J., & Schomburg, L. (2016). A Nonradioactive DEHAL Assay for Testing Substrates, Inhibitors, and Monitoring Endogenous Activity. *Endocrinology, 157*(12), 4516-4525. doi:10.1210/en.2016-1549

Oelkrug, R., Herrmann, B., Geissler, C., Harder, L., Koch, C., Lehnert, H., Oster, H., Kirchner, H., & Mittag, J. (2017). Dwarfism and insulin resistance in male offspring caused by alpha1-adrenergic antagonism during pregnancy. *Mol Metab, 6*(10), 1126-1136. doi:10.1016/j.molmet.2017.06.016

Johann, K., Reis, M. C., Harder, L., Herrmann, B., Gachkar, S., Mittag, J., & Oelkrug, R. (2018). Effects of sildenafil treatment on thermogenesis and glucose homeostasis in diet-induced obese mice. *Nutr Diabetes, 8*(1), 9. doi:10.1038/s41387-018-0026-0

Content

Summary

Thyroid hormones (THs) are engaged in numerous peripheral and central processes, including growth, energy metabolism, thermogenesis and cardiovascular control but also brain function and development. Consequently, TH diseases have manifold and often devastating effects, if not treated appropriately. Deciphering the interactions of THs on the different layers of regulation is therefore of particular importance to ensure optimal treatment of TH disorders and to prevent impairments during development. The present thesis addresses these areas by investigating the influence of THs and its metabolites on peripheral processes in the body as well as the importance of THs for brain development.

Consequences of acute TH action can be observed in patients treated with thyroxine after thyroidectomy, who suffered from an initial period of overtreatment. However, the basic consequences of such a transient thyrotoxicosis are only partly understood and were therefore analysed in a mouse model. As expected, a TH induced hyperthermia was observed in the animals, but interestingly the data excluded the interscapular brown adipose tissue as primary source of the heat production. Furthermore, the heart showed hypertrophy and tachycardia upon thyrotoxicosis and surprisingly bradycardia after recovery, indicating a transient hypothyroid state in the heart, most likely due to the rapid decline of serum 3,3',5-triiodo-L-thyronine during recovery. For the clinical routine, these findings emphasise the need of close monitoring of thyrotoxic patients to avoid cardiac events. To test whether the iodine-free TH derivative T_0AM contributes to these effects, the compound was administered *in vivo*. The data suggested that T_0AM is rather a degradation product than of biological relevance.

Besides these acute effects in the adult, TH is also fundamental for brain development, which is best illustrated in congenital hypothyroidism leading to irreversible mental retardation in affected new-borns. However, potential neuroanatomical targets and the exact actions of TH during development are still enigmatic. Therefore, parvalbumin neurones in the anterior hypothalamic area were analysed, which are involved in cardiovascular control and a potential target of TH during brain development. The data revealed that these GABAergic interneurones rely on TH receptor α1 signalling during their post-mitotic phase from embryonic day 12 until birth, but not postnatally, to ensure proper development. These findings strengthen the connection between maternal thyroid function and offspring blood pressure control. They also reveal the first clear neuroanatomical target of maternal TH signalling, which adds evidence on the impact of maternal thyroid disease on the offspring and the importance of routinely screening pregnant women.

Zusammenfassung

Schilddrüsenhormone (SDH) sind in zahlreiche peripherere und zentrale Prozesse eingebunden, einschließlich Wachstum, Energiehaushalt, Thermoregulation und Kontrolle des Herzkreislaufsystems, aber auch in die Aufrechterhaltung von Gehirnfunktionen und Gehirnentwicklung. Folglich haben Schilddrüsenerkrankungen vielfältige und häufig schwerwiegende Krankheitsbilder, wenn sie nicht entsprechend behandelt werden. Das Entschlüsseln der Interaktionen von SDH auf verschiedenen Ebenen der Regulation ist daher von besonderer Bedeutung, um eine optimale Behandlungen von Schilddrüsen-erkrankungen sicherzustellen und dem Auftreten von Entwicklungsstörungen vorzubeugen. Die vorliegende Dissertation befasst sich mit diesen Themengebieten durch die Untersuchung des Einflusses von SDH und seinen Metaboliten auf periphere Prozesse im Körper, genauso wie die Bedeutung von SDH für die Gehirnentwicklung.

Auswirkungen akuter SDH-Wirkung können bei Patienten beobachtet werden, die nach einer Thyreoidektomie mit Thyroxin behandelt werden und dabei eine initiale Überbehandlung erleiden. Trotzdem sind die grundlegenden Konsequenzen solch einer transienten Thyreotoxikose nur teilweise verstanden und wurden deshalb in einem Mausmodel analysiert. Wie erwartet wurde eine SDH-induzierte Hyperthermie in den Tieren hervorgerufen, aber interessanterweise schlossen die Daten das interskapuläre braune Fettgewebe als primäre Quelle für die Wärmeproduktion aus. Außerdem zeigte das Herz Hypertrophie und Tachykardie während der Thyreotoxikose und eine überraschende Bradykardie nach der Erholungsphase, was auf einen transienten hypothyreoten Zustand im Herz hindeutet, sehr wahrscheinlich auf Grund des rapide abfallenden 3,3',5-Triiodo-L-thyronin im Serum während der Erholungsphase. Für die klinische Routine unterstreichen diese Ergebnisse die Bedeutung einer engen Überwachung von thyreotoxischen Patienten, zur Vermeidung kardialer Vorfälle. Um zu testen, ob das iodfreie SDH-Derivat T_0AM zu den beschriebenen Prozessen beiträgt, wurde die Substanz *in vivo* injiziert. Die Daten lassen vermuten, dass T_0AM eher ein Abbauprodukt darstellt, anstatt biologische Relevanz zu besitzen.

Neben diesen akuten Effekten im Erwachsenen, sind SDH auch fundamental für die Gehirnentwicklung, was eindrucksvoll am Beispiel der kongenitalen Hypothyreose illustriert werden kann, die zu irreversiblen, mentalen Schäden in betroffenen Neugeborenen führt. Trotzdem sind potentielle neuroanatomische Zielstrukturen und die exakte Wirkweise von SDH in der Entwicklung noch unbekannt. Daher wurden Parvalbuminneurone im anterioren Hypothalamus analysiert, die an der Kontrolle des Herzkreislaufsystems beteiligt

sind und ein potentielles Ziel für SDH darstellen. Die Daten zeigten, dass diese GABAergen Interneurone auf Signale des Schilddrüsenhormonrezeptors α1 während ihrer postmitotischen Phase von Tag 12 der Embryonalentwicklung bis zur Geburt, jedoch nicht mehr postnatal, angewiesen sind, um eine vollständige Entwicklung sicherzustellen. Diese Ergebnisse stärken die Verbindung zwischen mütterlicher Schilddrüsenfunktion und der Kontrolle des Blutdrucks in den Nachkommen. Sie stellen außerdem das erste klare neuroanatomische Ziel für mütterliche Schilddrüsenhormonsignale dar. Dies sind weitere Beweise für die Auswirkungen von mütterlichen Schilddrüsenerkrankungen auf den Nachwuchs und die Wichtigkeit von Routinescreenings in schwangeren Frauen.

1. Introduction

Symptoms of impairments in the thyroid hormone (TH) system such as goiter, a visible swelling of the neck due to an increased thyroid gland, were already described in ancient times, and treatment approaches using seaweed in China or sea salt in Egypt were passed on through generations (Clements et al., 1961). Today TH diseases are very common worldwide, although the prevalence in populations is strongly associated with the iodide status of the respective area. A population-based studies in northeast Germany recently revealed, that the overall prevalence for diagnosed thyroid disorders is 18.9 % (Khattak et al., 2016). An earlier study of the same population concluded that 27.4 % of patients under treatment still display thyroid stimulating hormone (TSH) levels outside of the reference range and 8.7 % of healthy people showed indications of being undiagnosed for TH disorders (Hannemann et al., 2010). This shows undoubtedly that although our knowledge about the multi-layered and exactly orchestrated system underlying TH signalling has increased, it is still of high relevance to further decipher TH interactions with the overall aim to improve screening attempts and treatment paradigms.

1.1. The Endocrine System and the Thyroid Gland

In mammals, a plethora of mechanisms coexist that have to precisely engage with each other for physiological functionality and the overall survival of the organism. This fragile interplay is strongly controlled by two main systems, the nervous system and the endocrine system. The communication of the first is based on electronic decay and synaptic transmission, whereas the second relies on the production and secretion of signal molecules, called hormones. The endocrine system is involved in development, growth, reproduction, energy metabolism, temperature homeostasis and cardiovascular control, all processes known to be influenced by TH. Production and secretion of THs is regulated by a hierarchic three-layer principle, involving the hypothalamus, the pituitary and the thyroid gland (Figure 1). In detail, neurones of the paraventricular nucleus of the hypothalamus secrete thyrotropin-releasing hormone (TRH) to stimulate thyrotrophs in the anterior lobe of the pituitary, which in turn secrete TSH to directly act on THs production and release in the thyroid gland. To control the release of TRH and TSH, TH feeds back on the hypothalamus and the pituitary and thereby reduces further stimulation of the thyroid gland (Morley, 1981; Yen, 2001).

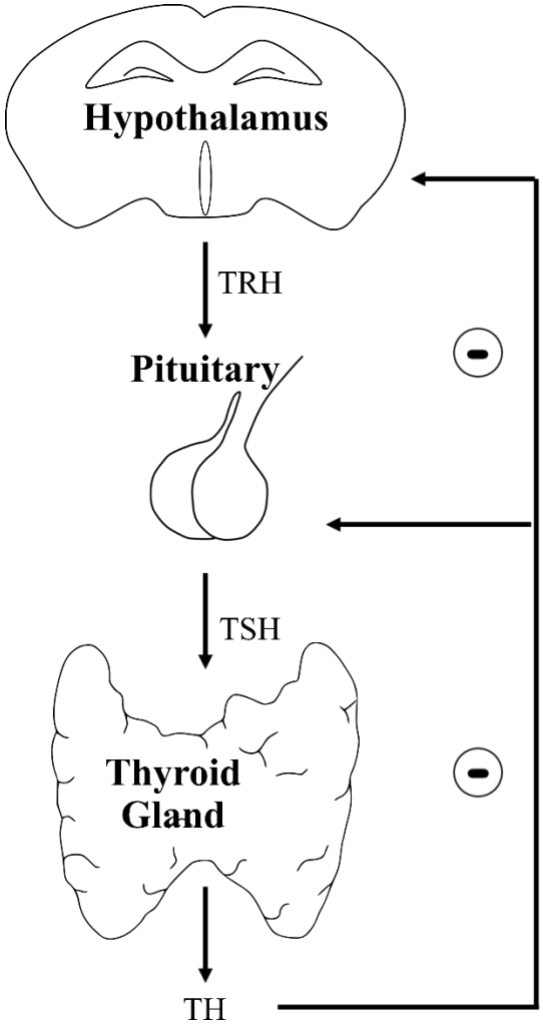

Figure 1: Overview on the regulatory principle of the hypothalamic-pituitary-thyroid-axis. Neurones in the hypothalamus stimulates the pituitary by producing TRH. As reaction, thyrotrophs in the anterior lobe of the pituitary express TSH to stimulate TH production in the thyroid gland. In turn THs repress TRH and TSH expression via a negative feed-back loop. TH, thyroid hormone; TRH, thyrotropin-releasing hormone; TSH, thyroid stimulating hormone.

In humans, the development of the thyroid gland starts three weeks after fertilisation and the generation of the two specific thyroidal cell types, thyroid follicular cells (thyrocytes) and parafollicular cells (C-cells), crucially relies on timely expression of *Pax8, Titf1* and *Foxe1* (Trueba et al., 2005). In its mature state, the thyroid gland consists of two lobes connected by an isthmus and lies in front of the trachea. It is organized in follicle shaped units formed by thyrocytes and filled with colloid, a liquid mainly containing thyroglobulin, synthesised and secreted by thyrocytes, and iodide (Chambard et al., 1987; Vassart, 1972). In the lumen of these thyroid follicles, THs are produced and to a large proportion also stored. The high vascularization of the thyroid tissue assures a simple secretion of THs to the blood stream and their rapid distribution to the respective target tissues (Maenhaut et al., 2000).

1.1.1. Biosynthesis of TH

THs are amino acid derivatives of tyrosine and occur in two main forms, the prohormone 3,3',5,5'-tetraiodo-L-thyronine (T_4, thyroxine) and the biological active form 3,3',5-triiodo-L-thyronine (T_3). For their synthesis iodide is actively transported through the thyrocyte into the follicle lumen (Dai et al., 1996; Royaux et al., 2000). There it is oxidised by the thyroid peroxidase and transferred to tyrosyl residues of thyroglobulin by iodination, creating monoiodotyrosine and diiodotyrosine. These precursors are coupled to each other within the thyroglobulin to form T_3 and T_4 (Taurog et al., 1996). In its bound state, as part of thyroglobulin, T_3 and T_4 can be stored in the follicle lumen. For their release, a proteolytic cleavage of thyroglobulin by cathepsins is necessary (Friedrichs et al., 2003). The free T_4 and to a much smaller extent also the free T_3 are then transported across the cell membrane by TH specific transporters such as the monocarboxylate transport protein 8 (MCT8) and secreted into the blood (Di Cosmo et al., 2010; Nishimura and Naito, 2008). There, the majority of T_4 is tightly bound to transport proteins such as thyroxine-binding globulin, transthyretin or albumin, which leads to a very low turnover rate of 11.2 %/day and a half-life of up to 7 days in humans (Nicoloff et al., 1972; Schussler, 2000). In contrast, the turnover rate of the more loosely bound T_3 is 67.9 %/day leading to a much shorter half-life (Nicoloff et al., 1972). When finally reaching the target tissue, unbound TH uptake again relies on TH transporters. Tissue dependent, the monocarboxclate transport protein 10 (MCT10) (Friesema et al., 2008), the L-type amino acid transporter 1 or 2 (Friesema et al., 2001) and the group of organic anion transporting peptides 1c1 (OATP1c1) (Pizzagalli et al., 2002) have been identified in addition to MCT8 (Friesema et al., 2003) in this context.

To provide sufficient T_3 concentration, despite the low T_3 secretion by the thyroid gland, T_3 is also produced at the level of the target tissues by the conversion of T_4 (Braverman et al., 1970; Pilo et al., 1990). The reaction is catalysed by a group of three selenoenzymes called iodothyronine deiodinases type 1-3 (DIOs 1-3) and each DIO has a preference for inner or outer ring-deiodination(Leonard and Rosenberg, 1981). The peripheral T_4 to T_3 conversion by outer ring-deiodination can be performed by DIO1 and DIO2. In addition, also T_3 and reverse T_3 (rT_3) can function as substrates for both enzymes, producing 3,5-diiodo-L-thyronamine (3,5-T_2) or 3,3'-diiodo-L-thyronamine (3,3'-T_2) respectively. Deiodination of the inner ring is mostly performed by DIO3 but can also be done by DIO1 and is considered as main path of degradation of T_4 and T_3 to rT_3 or 3,3'-T_2, respectively (Köhrle, 2000).

1.1.2. Metabolism and Action of TH

Within the cell T_3 classically executes its function via binding to nuclear TH receptors (TR) (Sap et al., 1986), which act as hormone-inducible transcription factors by forming heterodimers and binding to promotor regions of TH sensitive genes. The binding of a TR complex to TH response elements on the DNA then either activates or represses the respective gene expression (Yen, 2001). Two isoforms of TRs exist (alpha and beta), which are encoded by different genes (*THRA* on chromosome 17 and *THRB* on chromosome 3 in humans, *Thra* on chromosome 11 and *Thrb* on chromosome 14 in mice) and are very conserved among species (Koibuchi and M. Yen, 2016; Lazar, 1993). From each gene, multiple splice variants are described, of which only TRα1, TRβ1 and TRβ2 bind to T_3 as well as to DNA at TH response elements and are therefore considered to be biologically active TRs (Flamant et al., 2017). Besides developmental differences in TR isoform expression, a high tissue specificity is observed among the TR, still there is some expressional overlap between the isoforms (Yen, 2001).

For TRβ1 ubiquitous expression was found, but it exerts a predominant role in liver, whereas TRβ2 is mainly involved in the pituitary-thyroid axis and its feed-back control, auditory function and cone development (Abel et al., 2001; Flores-Morales et al., 2002; Jones et al., 2007). Mice with inactivated TRβ (*Thrb*$^{-/-}$) develop a goiter, have elevated TH and TSH levels and impaired auditory functions, but no overt neurological defects (Forrest et al., 1996). In humans, the resistance to TH (RTHβ) syndrome is known since the 60s, and manifests in reduced responsiveness of specific tissues such as the liver, although TH concentration is strongly increased in the body. 20 years later a cause of the syndrome was identified as various mutations in the THRB gene, which mainly lead to the production of an autosomal dominant protein product with reduced or absent affinity to its ligand T_3. This explains the moderate response of TSH, affected hearing and vision, which all relies on TRβ signalling, whereas the TRα1 depending heart shows tachycardia due to the excessive TH concentration (Refetoff, 1994).

In contrast, TRα1 is predominantly expressed in the brain, the heart, muscle and bone (Bookout et al., 2006; Falcone et al., 1992; Schwartz et al., 1992; Wallis et al., 2010; Wikström et al., 1998). Mice without TRα1 (*Thra1*$^{-/-}$) display lower intrinsic heart rate and a reduced mean body temperature, but normal TH concentration and only slight TSH reduction (Wikström et al., 1998). For a long time, it was assumed that a loss-of-function of TRα1 is not compatible with life in humans, because no patients with mutations in the *THRA* gene had been described. Eventually, in 2012 several such patients were identified, having a

phenotype of mild hypothyroidism with low heart rate and blood pressure, growth and developmental retardation and constipation. At the same time, T_4 concentration was low-normal, T_3 concentration was high-normal and TSH was unchanged, which was interpreted as a selective TH resistance in tissue mainly relying on TRα1 signalling. The obvious phenotypic differences to the *Thra1*$^{-/-}$ model most likely results from the fact that the patients had a dominant negative *THRA* mutation and not just a receptor deficit. (Bochukova et al., 2012; van Mullem et al., 2012). In line with these findings, animal studies have shown that the lack of TRs is far less devastating than the lack of TH itself, which indicates regulatory functions of TRs independent of T_3. Mice devoid of all functional nuclear T_3 receptors (*Thra1*$^{-/-}$/*b*$^{-/-}$) exhibit poor female fertility, hyperactivity of the pituitary-thyroid axis, growth retardation and impaired bone development but show normal longevity, implying that TRs are not crucial for survival (Göthe et al., 1999). In contrast, *Pax8*$^{-/-}$ mice, which develop no functional TH producing follicular cells and are consequently completely athyroid with no endogenous TH production, showed severe mental and growth retardation. They also died shortly after weaning, indicating that the exclusive action of unliganded TRs is fatal. However, the substitution with T_4 extended the survival beyond weaning (Mansouri et al., 1998). Based on this, the current TH signalling model assumes that the transcriptional activity of the TR in its unliganded state (aporeceptor) has the opposite direction as in its liganded state (holoreceptor), meaning gene expression positively regulated by the holoreceptor will be repressed by the aporeceptor and vice versa (Bernal and Morte, 2013).

1.1.3. TH Disorders

Regarding the delicately orchestrated system of TH signalling, described above, it is not surprising that impairments of this system can cause devastating pathologic disorders in the organisms. The most common TH disorder is the reduction of TH, called hypothyroidism, which is defined by increased TSH and reduced free T_4 concentrations for the overt and increased TSH and unchanged free T_3 and free T_4 concentrations for the subclinical form (Allolio and Schulte, 2011). The most common cause to develop hypothyroidism, besides iodine deficiency, is the autoimmune disease Hashimoto thyroiditis, characterised by antithyroid peroxidase or antithyroglobulin antibodies (Allolio and Schulte, 2011; Taylor et al., 2018). Also, some drugs used to treat cardiac arrhythmia, mood disorders and cancer, are associated with an increased risk of hypothyroidism (Cukier et al., 2017; Martino et al., 1984; Shine et al., 2015). Due to the multisystemic influence of TH, multiple symptoms can be cause by overt hypothyroidism such as bradycardia, mild hypertension and narrowed pulse

pressure, weight gain, muscle weakness, tiredness, lethargy, poorer memory and depression, constipation, dry skin and cold intolerance (Allolio and Schulte, 2011). These symptoms are largely reversible by treatment with oral T_4, while in contrast the impairments caused by reduced TH during development are usually irreversible in the offspring. The symptoms of subclinical hypothyroidism are often less pronounced or non-existent; however, it is still under debate whether subclinical hypothyroidism increases cardiovascular risk and mortality and which treatment regime is most beneficial in this context (Pearce et al., 2013).
On the other hand, an abnormally increased action of TH in the body is called thyrotoxicosis, although this term gives no information about the source of TH (De Leo et al., 2016). In the case of elevated synthesis and secretion of TH, the term hyperthyroidism is used, which is defined as undetectable TSH and high T_3 and free T_4 in the overt form, and very low TSH and normal T_3 and free T_4 in the subclinical form (Ross et al., 2016). The most frequent cause for hyperthyroidism is Graves' disease, in which autoreactive TSH receptor antibodies stimulate the TSH receptor of thyroid follicular cells leading to increased TH production, hypertrophy and hyperplasia. Common symptoms of the condition are tachycardia, cardiac insufficiency and elevated blood pressure, tremor, weight loss and impaired glucose tolerance, restlessness and insomnia, diarrhoea, hair loss, heat intolerance and sweating (Allolio and Schulte, 2011). In the case of thyrotoxicosis without hyperthyroidism, comparable symptoms can be evoked by the destruction of thyrocytes or the intentional or unintentional intake of high amounts of TH (De Leo et al., 2016). The majority of these symptoms are reversible by treatment with antithyroid drugs, radioactive iodine ablation or thyroidectomy (Allolio and Schulte, 2011).

1.2. Biosynthesis, Metabolism and Action of Thyronamines (TAM)

In addition to the conversion of T_4 to T_3, which was already described, up to seven other downstream metabolites of T_4 can be produced by deiodination and only differ concerning number and position of their iodine atoms (Figure 2). The physiological role of some of these, so called L-thyronines, is still under discussion. The number of possible downstream metabolites from T_4 gets even bigger considering that in addition to deiodination mutable other modified at the side chains can occur e.g. sulfation, glucuronidation, oxidative deamination or decarboxylation (Wu et al., 2005). Of particular interested in this context are the biological active class of TAMs, which are produced by oxidative decarboxylation and therefore lack the amino acid carboxy group compared to L-thyronines. TAMs have been

known since the 50s, but did not attract much attention until their rediscovery in 2004 (Scanlan et al., 2004). As for L-thyronines, nine different TAMs are possible, based on various numbers and placement of iodine atoms. Among them, the most prominent members are 3-iodothyronamine (3-T_1AM) and the iodine-free TAM (T_0AM), since both were detected in serum and multiple organs of C57BL/6J mice and several other species, so far (Braulke et al., 2008; Scanlan et al., 2004). However, these results are very controversial; while some laboratories were able to detect 3-T_1AM in blood, thyroid, skeletal muscle, adipose tissue and prostate samples of humans (Geraci et al., 2008; Saba et al., 2010), others could not detect endogenous 3-T_1AM and T_0AM in neither mice nor men (Ackermans et al., 2010).

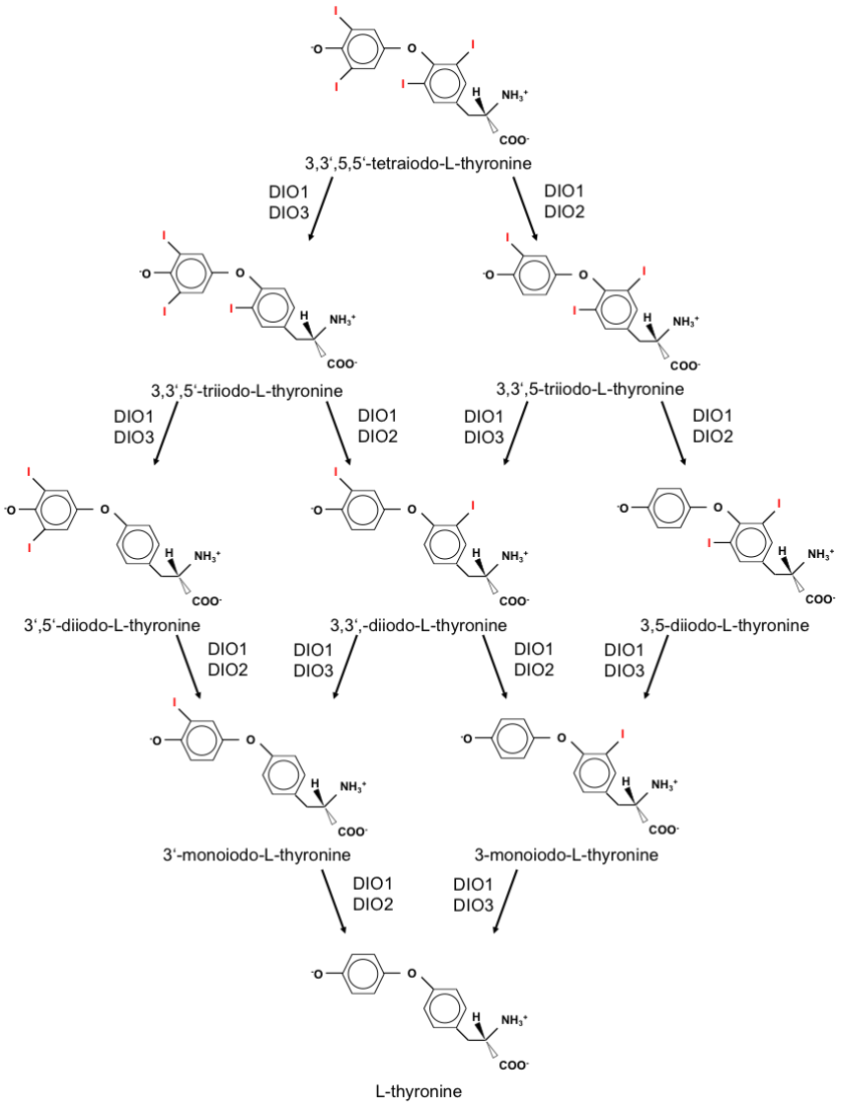

Figure 2: Sequential deiodination of L-thyronines. Nine different L-thyronines can be produced by sequential deiodination. The reaction is catalysed by the group of DIOs, of which DIO2 prefers outer ring deiodination and DIO3 prefers the inner ring deiodination. The DIO1 is able to perform deiodination on both rings. DIO 1-3, iodothyronine deiodinases type 1-3 (modified from (Köhrle, 2002; Piehl et al., 2008; Sakurada et al., 1978)).

Although mechanism and location of endogenous TAM synthesis are still under investigation, based on their structure three possible synthesis pathways are considered: *de novo* synthesis either by oxidative iodination and ether-bond coupling from tyrosine or by iodination from T_0AM, both reactions only observed in the thyroid so far, or decarboxylation and deiodination of T_4 (Hoefig et al., 2016b). At the moment an extrathyroidal synthesis pathway is the most favoured one, because 3-T_1AM is detectable in patients with non-functional thyroid tissue (Hoefig et al., 2011). Therefore, the most likely scenario is proposed by Hoefig et al. who demonstrated that murine intestine is able to synthesise 3-T_1AM from T_4 via the intermediates 3,5-T_2 and 3,5-T_2AM, involving DIO and ornithine decarboxylase (ODC) activity (Figure 3). Interestingly other TAMs such as T_0AM were not detected, indicating a rather fast turnover to other downstream metabolites (Hoefig et al., 2015b; Piehl et al., 2008).

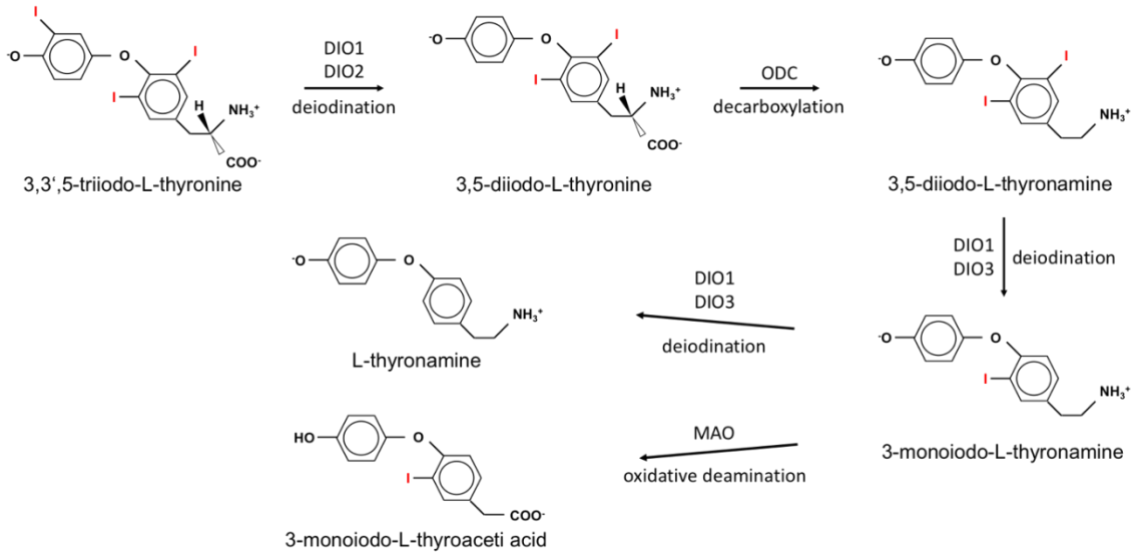

Figure 3: Proposed synthesis pathway for 3-T_1AM and its degradation products T_0AM and TA_1. The preferred pathway for 3-T_1AM production from T_3 is deiodination and decarboxylation to 3,5-diiodo-L-thyronamine, followed by further deiodination or oxidation. DIO 1-3, iodothyronine deiodinases type 1-3; ODC, ornithine decarboxylase; MAO, monoamine oxidase (modified from (Hoefig et al., 2016b)).

Pharmacological effects of 3-T_1AM administration are a rapid dose dependent drop in rectal temperature, heart rate and cardiac output in mice, which lasts six to eight hours. Comparable but weaker reactions were reported upon T_0AM treatment (Scanlan et al., 2004). The very fast onset of effects after TAM administration suggest that they signal is not transmitted via TRs and protein biosynthesis. This is in line with the observation that 3-T_1AM and T_0AM show no affinity to TRα1 or TRβ (Scanlan et al., 2004). Originally the G

protein-coupled receptor trace amine-associated receptor 1 (TAAR1) was believed to be a target of 3-T_1AM; however, *Taar1* knockout (ko) mice showed identical thermoregulatory reactions to 3-T_1AM treatment as controls, which excludes the possibility that these 3-T_1AM effects are mediated by TAAR1 (Panas et al., 2010). Other potential target for TAMs could be the adrenergic receptor α2A or the cold-sensitive transient receptor potential channel melastatin 8, still these need further investigation (Hoefig et al., 2016b).

1.3. TH and Brain Development

TH and its metabolites are not only strongly involved in direct manipulation of body's physiology but already essential during brain development. There, THs were found to be involved in myelination by influencing the expression of myelin proteins; in differentiation of neurones and glia by regulating cell cycle regulators, extracellular matrix proteins, neurotrophins and proteins of the cytoskeleton and in neuronal migration in the cerebral cortex and the hippocampus as well as neurite outgrowth and axonal guidance (Aniello et al., 1991; Balazs et al., 1969; Bernal, 2015). However, even in the adult brain, there are strong indications that neurogenesis relies on TH signalling. In humans, the development of the brain starts during the third week of gestation and extends at least until late adolescence. Within this frame, the time until midgestation and the neonatal phase seems to be crucially relying on TH signalling, given that both are strongly associated with irreversible neuronal deficits in the case of TH deficiency (Bernal, 2015).

T_3 is present in the brain already in week 10, which is early compared to other tissues (Ferreiro et al., 1988). Still, in the first trimester, TH is solely provided by the mother and reaches the foetus via transplacental passage. In detail, an ultrafiltrate of the maternal serum, the coelomic fluid, is reabsorbed by the yolk sac, which is directly connected to the foetal digestive tract and circulation (Contempre et al., 1993). T_4 concentration in the coelomic fluid increases in the course of pregnancy and is positively correlated with maternal serum T_4. Interestingly this correlation was not seen for T_3, indicating that T_3 is mainly metabolised from the maternal T_4 during this time. While total T_4 level in the foetal blood was much lower than in maternal blood, free T_4 in foetal compartments, which is the fraction available for TR stimulation in the target tissue, was comparable to maternal levels. This can be explained by the very low amounts of foetal TH-binding proteins during the first trimester (Calvo et al., 2002). The foetal thyroid gland starts trapping iodine around week 12, at the same time when direct transfer of TH via the placenta into the foetal circulation becomes possible (Calvo et al., 2002; Glinoer, 2001). However, endogenous T_4 is not detectable before

week 18 - 20, which compares to embryonic day 15 (E15) in mice (Glinoer, 2001; Nilsson and Fagman, 2017; Richard and Flamant, 2018). At the end of human pregnancy, when foetal TH production is functional, 30 - 60 % of the circulating TH are still provided by the mother (de Escobar et al., 2008).

Also foetal expression of TRs and DIOs is detectable in the first trimester (Chan et al., 2002). The predominantly expressed DIOs in the foetal brain, 2 and 3, show spatial as well as temporal specificity. Until midgestation, DIO2, catalysing T_4 to T_3 conversion, is highly expressed in the cortex whereas DIO3, catalysing T_3 degradation, is highly expressed in the cerebellum, midbrain, basal ganglia, brain stem, spinal cord and hippocampus. Already around gestational week 18, DIO2 activity leads to a T_3 level comparable to the adult situation in some brain areas, despite the low T_4 circulating level. Meanwhile, other brain areas are protected by DIO3 from excessive T_3 (de Escobar et al., 2008). Animal studies in rats demonstrated in this context, that the locally generated T_3 is mainly produced by astrocytes and tanycytes, surrounding the third ventricle in the hypothalamus, indicating that glia cells not only transfer nutrients but also T_3 to neurones (Guadano-Ferraz et al., 1997).

The transcriptional regulation by T_3 in the developing brain is mainly executed by the ubiquitously expressed TRα1; however, animal studies demonstrated that, with the exception of tanycytes, TRα1 is only expressed in neurones not in glia cells. The first expression of TR in mice was detected on E13.5, which indicates that TRα1 is expressed in immature and post-mitotic, but not proliferating cells (Wallis et al., 2010). In contrast, TRβ expression starts later in development and is more restricted to specific regions e.g. TRβ2 in the retina, cochlea and hypothalamus and TRβ1 in premature oligodendrocytes, as demonstrated in rats (Jones et al., 2007; Sarlieve et al., 2004).

1.3.1. Developmental TH Disorders

Considering the multilayer functions of THs in the developing brain, impaired TH signalling can have devastating effects during development, when it massively interferes with embryonic and postnatal progression. The most common example of insufficient TH signalling in neonates is congenital hypothyroidism (CH), occurring in one of 3500 neonates worldwide (De Felice and Di Lauro, 2004; Kopp, 2002). Repeated reports about an increasing prevalence were explained by changes in ethnicity and lowering of the TSH cut-off (Taylor et al., 2018). Affected neonates have insufficient amounts of TH after birth, which in 85 % of the cases is due to disturbed organogenesis leading to thyroid dysgenesis. The remaining cases result from inborn errors in TH synthesis. Common symptoms of CH are prolonged

jaundice, feeding difficulties, lethargy, constipation, macroglossia, hypothermia, edema, umbilical hernia and a 'hypothyroid facial appearance'. If untreated, CH leads to cretinism, displaying growth retardation, delayed motor development and severe mental impairments. This can largely be avoided by T_4 substitution (> 10 µg/kg body weight/day), starting before the age of three month, hence new-borns in developed countries are routinely screened for increased TSH levels directly after birth (Grüters and Krude, 2011). Alarmingly, more than 70 % of new-borns worldwide are not included in such screening programs and are thereby exposed to the risk of irreversible neurodevelopmental impairments due to undetected hypothyroidism (Ford and LaFranchi, 2014). A well-established animal model for CH is the athyroid *Pax8*$^{-/-}$ mouse, based on the observation that mutations in the thyroid transcription factor *PAX8* are involved in human cases of CH (Mansouri et al., 1998).

Another specific case of postnatal thyroid disorder is the Allen-Herndon-Dudley syndrome (AHDS). Patients suffer from severe psychomotor retardation and show abnormal TH levels (high plasma T_3, low T_4, borderline-high TSH), due to a mutation in the TH transporter MCT8 (Friesema et al., 2004). The MCT8 deficiency prohibits the transport of TH across cell membranes and tissue barriers such as the blood brain barrier (Friesema et al., 2008). Thereby the secretion of TH from the thyroid and the uptake of TH in the brain and in the neurones are disturbed, explaining partly the phenotype of AHDS patients (Di Cosmo et al., 2010). Classical symptoms are hypotonia, decreased muscle mass, hyperreflexia, no or limited speech and spastic paraplegia within the progression of the disease (Schwartz et al., 2005). Interestingly, mice with a *Mct8* ko show the same abnormal TH concentration in serum as patients but do not have deranged neuronal development in the brain (Trajkovic et al., 2007). A possible explanation is that only T_3 transport is diminished in *Mct8* ko mice because T_4 transport can be compensated by other transporters, mainly OATP1C1. Thus, only *Mct8/Oatp1c1* double ko (dko) mice represent a valid mouse model for AHDS research (Mayerl et al., 2014).

In addition to the role of THs in postnatal development, the hormones are also very important in prenatal development. During the maturation of the human foetal thyroid gland (first half of pregnancy), TH is solely provided by the mother; however, substantial placental transfer of TH from the mother to the foetus was demonstrated until term (Chan et al., 2009; Vulsma et al., 1989). An excessive amount of TH in the mother is associated with mental impairments for the child later in life for example attention deficit hyperactivity disorder (Andersen et al., 2014). Overt hyperthyroidism in pregnant women, mainly induced by Graves' disease (Carle et al., 2011) is comparatively rare. Much more frequent is gestational hyperthyroidism, which can occur due to high concentrations of human

chorionic gonadotropin, a weak agonist of the TSH receptor, in the body during the first trimester (Korevaar et al., 2017). In 2016, it was for the first time demonstrated that high maternal free T_4 concentrations are also associated with a lower intelligence quotient (IQ) in combination with reduced total grey matter and cortex volume in the offspring (Korevaar et al., 2016). On the other hand, the major risk factor for reduced levels of TH in the mother worldwide is iodine deficiency (250 µg/day recommended intake during pregnancy), which is very problematic because the maternal TH production needs to rises nearly 50 % during the first trimester and iodine deficiency not only impairs the maternal but also the foetal TH production during the second half of pregnancy (Alexander et al., 2017). In iodine sufficient areas of the world, maternal hypothyroidism or hypothyroxinaemia (normal TSH and reduced T_4) is mostly elicited by chronic autoimmune thyroid disorder (e.g. Hashimoto's thyroiditis), which is often asymptotic but progressively worsen in the course of pregnancy (Glinoer and Delange, 2000). In this situation, the placenta lacks the ability to compensate the declining maternal TH concentration to ensure an optimal maternal-foetal transfer (Chan 2009).

Untreated maternal hypothyroidism is associated with an increased risk for miscarriage and placental abruption (van den Boogaard et al., 2011), whereas hypothyroid pregnant women receiving T_4 substitution show no association with abortions or premature deliveries compared to controls (Hirsch et al., 2013). Furthermore, children (age 7 - 9) of untreated hypothyroid mothers show reduced IQ and attention as well as delayed language and motor skill development, indicating impaired brain development (Haddow et al., 1999; Man et al., 1991). Therefore, immediate treatment with levothyroxine is recommended by the American Thyroid Association to keep the TSH concentration in the population- and trimester-specific reference range to minimize adverse effects (Alexander et al., 2017). Accordingly, the question arises whether the same impairments were seen in mothers with subclinical or asymptotic thyroid diseases and their children. A Greek study demonstrated that women with thyroid autoantibodies, independent of symptoms, are at a higher risk for spontaneous preterm delivery and the combination with high TSH was associated with gestational diabetes and low birth weight (Karakosta et al., 2012). Also, an inverse association between maternal free T_4 and birth weight z-scores, estimated foetal growth and head and abdominal circumferences at 10, 18 and 26 weeks of gestation was found, indicating interference of TH with soft tissue accretion and bone growth (Johns et al., 2017). Again, by treating women with subclinical hypothyroidism from the first trimester of pregnancy onwards with T_4, a decreased risk of adverse obstetric events was achieved (Zhao et al., 2018). More controversially discussed are the effect of maternal subclinical hypothyroidism and

hypothyroxinaemia on brain development and IQ. Korevaar and colleagues examined children from mothers with low free T_4 levels, showing a reduced IQ at the age of six as well as lower grey matter and cortex volume compared to offspring from healthy mothers (Korevaar et al., 2016). Maternal hypothyroxinaemia during early pregnancy lead to delayed mental and motor function in the offspring (Pop et al., 2003). In contrast, Casey et al. analysed differences in IQ of children at the age of five, from treated and untreated mother with subclinical hypothyroidism or hypothyroxinaemia and found no significant improvements in offspring from mother with treatment onset between 8 - 20 weeks after gestation (Casey et al., 2017). Although the analysis of IQ in children at a young age is a common approach, this allows no predictions about long-term consequences or other TH target tissues besides the brain (Lazarus 2012, Casey 2017). Overall, new clear cut off markers are needed to predict effects of impaired TH signalling on children and ensure optimal treatment of mother and child during pregnancy (Brabant et al., 2015).

1.3.2. Parvalbumin (PV) Neurones and the Hypothalamus

Although the importance of TH for brain development is established for over a century, surprisingly little is known on the precise neuroanatomical and molecular targets of the hormone in the developing brain. Recently, PV neurones emerged as a possible target of TH signalling in mice, which was in line with earlier findings that pre- and postnatal hypothyroidism in rats leads to reduced PV immunoreactivity in the cortex (Berbel et al., 1996; Wallis et al., 2008).

PV is a soluble Ca^{2+} buffer involved in the control of the intracellular concentration of Ca^{2+} and is found in skeletal muscles and the brain. There it is primarily expressed in neurones and homogeneously distributed in soma, dendrites and axons but not nuclei (Celio and Heizmann, 1981; Heizmann, 1984). Most likely the Ca^{2+} binding capacity of PV is involved in shortening of the refractory period in the neurones, which facilitates rapid fire repetition and a quicker recovery from presynaptic excitatory potentials (Celio, 1986). PV was found in a subset of interneurones, classified by their expression of the neurotransmitter gamma-aminobutyric acid (GABA). These interneurones form a very heterogeneous group, however they have in common that they modulate information in local circuits by inhibition. Best studied are GABAergic interneurones in the cortex, which can be categorized in three subpopulations by their expression of PV, somatostatin (SST) or the serotonin receptor 3a ($5HT_{3a}$) (Rudy et al., 2011). During development, the six characteristic layers of the cortex are build up by the migration of neuronal precursor cells from zones of neurogenesis into the

cortex. Early generated excitatory pyramidal neurones accumulate in deeper layers, whereas later ones migrate further to the surface. Within this structure, neuronal precursor cells of GABA interneurones migrate tangentially from the basal forebrain towards the surface of the brain and integrate in their cortical layer of destination (Watson, 2010). The majority of these PV- and SST-interneurones emerge from the medial ganglionic eminence (MGE, ~ 50 – 60 %), whereas the $5HT_{3a}$ interneurones mainly arise from the caudal ganglionic eminence (CGE, ~ 30 – 40 %) (Kelsom and Lu, 2013). The remaining interneurones are attributed to the preoptic area (Gelman et al., 2009). Their role is to control the excitatory action in the cortex to avoid over-excitement accompanied by seizures. Cortical PV interneurones are also involved in gamma oscillation cycles and malformation in this circuit is associated with schizophrenia (Gonzalez-Burgos et al., 2015). Besides the cortex, co-expression of PV and GABA was also detected in other brain regions such as reticular nucleus, thalamus, pars reticulate of the substantia nigra, hippocampus, cerebellum and spinal cord (Celio, 1986).

To be able to manipulate TH mediated TRα1 signalling in the brain, the TRα1R384C (*Thra1*$^{+/m}$) mutant mouse was established. These mice display a 10-fold reduced ligand affinity of the TRα1, leading to aporeceptor activity at physiological T_3 concentrations, whereas an elevated T_3 concentration facilitates the formation of the holoreceptor (Tinnikov et al., 2002). Using this model, reduced numbers of PV neurones in the hippocampus were associated with anxiety and memory deficiencies and a delayed maturation of PV neurones in the motor cortex with locomotor deficiencies. The hippocampal malformations could be corrected by reactivating the TRα1 at the adult stage, whereas populations of PV neurones in the motor cortex were irreversibly changed by the insufficient TRα1 mediated signalling during development (Venero et al., 2005; Wallis et al., 2008). Interestingly, also a previously unknown population of PV neurones in the anterior hypothalamic area (AHA) was identified (Mittag et al., 2013). The hypothalamus is a particularly important area of the brain because of its significance for neuroendocrine function. The AHA lies in the supraoptic zone together with the paraventricular nucleus (PVN), the suprachiasmatic nucleus and the lateral hypothalamic area. There are direct afferent connections to the hypothalamus from various areas such as the cerebral cortex, the hippocampus and the medial, dorsal and anterior nuclei of the thalamus. Well known efferent connections from the hypothalamus project to the median eminence, the posterior pituitary, the thalamus, the brain stem and the spinal cord. Via the posterior pituitary the hypothalamus controls hormone signalling in several regulatory circuits such as vasopressin to regulate water secretion and thereby modulating blood pressure. In addition, the AHA is associated with parasympathetic activation and homeostatic functions (Felten et al., 2016). In line with that, the population of PV neurones in

the AHA was associated with the cardiovascular system. A diminished population size due to insufficient TH signalling via TRα1 led to increased blood pressure and heart rate and remained unchanged by the reactivation of TRα1 signalling in the adult, indicating a prenatal problem in development (Mittag et al., 2013).

1.4. Aim of the Thesis

TH acts via nuclear receptors on almost all tissues in the body, thus exerting a plethora of direct and secondary effects. Moreover, it can be converted to downstream derivatives such as TAMs, which can have additional consequences. In addition to these acute effects in the adult, the hormone is also relevant during development, especially for the brain. The aim of this thesis was to elucidate the role of TH and its metabolites in the control of metabolism, thermoregulation and cardiovascular functions by dissecting central from peripheral and acute from developmental actions, using the mouse as a model system. Specifically, I addressed the questions:

- How does a transient thyrotoxicosis effect metabolism, thermoregulation and cardiovascular function in adult mice?

- Are two weeks sufficient for the body to normalize metabolism, thermoregulation and cardiovascular function after a thyrotoxicosis in adult mice?

- What is the contribution of TH metabolite e.g. T_0AM for metabolism, thermoregulation and cardiovascular function in adult mice?

- How and when does TH influence the development of PV neurones in the AHA of mice?

2. Materials and Methods

2.1. Materials

Standard chemicals were obtained from Sigma-Aldrich (USA) or Carl Roth (Germany) if not stated otherwise. Suppliers of reagents, kits and drugs are listed in Table 1 and recipes for buffers in Table 2. Antibodies for western blot analysis and immunohistochemistry can be found in Table 3 and Table 4 respectively. Non-standard laboratory equipment and consumables are listed in Table 5 and software can be found in Table 6.

Table 1: Reagents, kits and drugs used in this project.

Substance	**Supplier**
3-iodothyroacetic acid (TA_1)	Alinda Chemical Limited, Russia (Wood et al., 2009)
3,3',5-triiodo-L-thyronine (T_3, T6397-MG)	Sigma, Germany
3,3',5,5'-tetraiodo-L-thyronine (T_4, thyroxine, T2376)	Sigma-Aldrich, USA
ABC-Kit	Vector Laboratories, USA
Absolute qPCR SYBR Green Fluorescein Mix	Thermo Fisher Scientific, USA
Aurum Total RNA Kit (Mini, Fatty and Fibrous Tissue)	Bio-Rad Laboratories, Germany
Avidin/Biotin Blocking Kit	Vector Laboratories, USA
Bepanthen Eye Ointment	Bayer, Germany
Breeding Diet (1314)	Altromin, Germany
Bromodeoxyuridine (BrdU)	Sigma, Germany
CL-Xposure X-Ray Films	Thermo Fisher Scientific, USA
Clarity Western ECL Substrate	BioRad, USA
Clozapine-N-oxid (CNO)	Enzo Life Sciences, Germany
Hard Set Antifade Mountain Medium with Dapi	Vector Laboratories, USA
High-Purity Thyronamine (T_0AM)	Chemical synthesis performed by Dr. R. Smits, ABX Advanced Biochemical Compounds, Germany (Rathmann et al., 2015)
Hydrogen Peroxide (H_2O_2)	Fluka, Schwitzerland
iScript cDNA Synthesis Kit	Bio-Rad Laboratories, Germany
Isoflurane	Zoetis, USA
Normal Goat Serum (NGS)	Abcam, UK
Normal Doneky Serum (NDS)	Sigma, Germany
Pertex	Medite GmbH, Germany
ProLong Diamond Antifade Mounting Medium with Dapi	Life Technologies, USA
Restore PLUS Western Blot Stripping Buffer	Thermo Fisher Scientific, USA

Substance	Supplier
Rimadyl (50 mg/mL, 462986)	Pfizer, USA
RNeasy Kits (Mini, Micro, Lipid Tissue Mini)	Qiagen, Germany
Saline Solution (0.9 %)	Berlin-Chemie AG, Germany
Serum Total T_3 ELISA Kit, DNOVO53	NovaTec Immundiagnostic GmbH, Germany
Serum Total T_4 ELISA Kit, EIA 1781	DRG Instruments GmbH, Germany
Standard Diet (1324)	Altromin, Germany
SYBR Green PCR Master Mix	Roche, Switzerland
Transcriptor First-Strand cDNA Synthesis Kit	Roche, Switzerland
Xylocain (10 mg/mL)	AstraZeneca, UK

Table 2: Recipes of buffers used in this project.

Buffer	Composition	
4 % Formaldehyde Solution	12 g	PFA
(PFA, for 300 mL)	30 mL	10x PBS
Cryo-Protection Solution	75 mL	Ethylene Glycol
(CPS, pH = 7.4, for 250 mL)	75 mL	Glycerol (Gerbu, Germany)
	19 mL	NaH_2PO_4 (0.1 M)
	81 mL	Na_2HPO_4 (0.1 M)
Genotyping Buffer (for 100 mL)	1 mL	EDTA (0.5 M)
	4 mL	NaCl (5 M)
	1 mL	20 % v/v SDS
	10 mL	Tris (1 M, pH 8.5)
Lugol Reaction Mix	500 µL	Lugol Reagent (Fluka, Schwitzerland)
	30 mL	KCl (25 % w/v)
	200 µL	HCl
Phosphate Buffered Saline	2 g	KCl
(10x PBS, 0.1 M, pH = 7.4, for 1 L)	2,4 g	KH_2PO_4
	26,8 g	Na_2HPO_4
	80 g	NaCl
Radioimmunoprecipitation Assay	20 µL	EDTA (500 mM)
Buffer (RIPA-Buffer, pH = 7.4, for	90 mg	NaCl
10 mL) with Phenylmethylsulfonyl	0.25 mL	10 % v/v Na-Deoxycholate in H_2O
Fluoride (PMSF)	20 µL	NaF (500 mM)
	1 mL	10 % v/v NP-40 (Tergitol) in H_2O
	100 µL	PMSF (100 mM)
	1 tablet	cOmplete ULTRA, Roche
	50 µL	activated Sodium Orthovanadate (200 mM)
	79 mg	Tris Base

Buffer	Composition	
Resolving Gel 12% in H_2O (for 10 mL)	4.04 mL	Acrylamid (Serva, Germany)
	40 µL	APS
	0.21 mL	SDS
	20 µL	TEMED
	2.53 mL	Tris Base (1.5 M)
Stacking Gel in H_2O (for 10 mL)	1.66 mL	Acrylamid
	40 µL	APS
	0.08 mL	SDS
	20 µL	TEMED
	2.48 mL	Tris Base (0.5 M)
Tris Buffered Saline with Tween 20 (1x TBS-T, pH = 7.4, 1 L)	8.77 g	NaCl
	1.21 g	Tris Base
	1 mL	Tween 20

Table 3: Primary (a) and secondary (b) antibodies for western blot analysis.

	Antibody	Species	Dilution	Catalog #	Supplier
a)					
	anti-Akt	rabbit	1/1000	#9272	Cell Signaling Technology, USA
	anti-GAPDH	rabbit	1/10000	#5174	Cell Signaling Technology, USA
	anti-Phospho-Akt (Ser473)	mouse	1/1000	#4051	Cell Signaling Technology, USA
	anti-UCP1	rabbit	1/20000		Previously used in (Jastroch et al., 2012)
b)					
	anti-mouse IgG	goat	1/10000	A16072	Invitrogen, Novex, Germany
	anti-rabbit IgG	goat	1/5000	P0448	Dako, Denmark
	anti-rabbit IgG	goat	1/10000	A16104	Invitrogen, Novex, Germany

Table 4: Primary (a) and secondary (b) antibodies for immunohistochemistry/immunofluorescence.

	Antibody	Species	Dilution	Catalog #	Supplier
a)					
	anti-BrdU	rat	1/500	NB500-169	Covance, Austria
	anti-GAD67	mouse	1/200	MAB5406	Merck Millipore, Germany
	anti-mCherry	goat	1/1000	AB0040-500	Sicgen Antibodies, Portugal
	anti-PV	rabbit	1/2000	PV-27	Swant, Switzerland
	anti-PV	goat	1/2000	PVG-213	Swant, Switzerland
	anti-VGLUT2	rabbit	1/1000	135403	Synaptic Systems, Germany

	Antibody	Species	Dilution	Catalog #	Supplier
b)					
	anti-goat (Cy3-conjugated)	donkey	1/800 (VGLUT2) 1/400 (GABA) 1/400 (mCherry)	705-165-147	Jackson ImmunoReasearch, USA
	anti-mouse Alexa Fluor 488	donkey	1/800	A-21202	Invitrogen, USA
	anti-rabbit (biotinylated)	goat	1/250	BA-1000	Vector Labs Bionordica, Sweden
	anti-rabbit (Cy3-conjugated)	goat	1/800	111-165-144	Jackson ImmunoReasearch, USA
	anti-rabbit Alexa Fluor 488	donkey	1/800 (VGLUT2) 1/400 (GABA) 1/400 (mCherry)	A-21206	Invitrogen, USA
	anti-rabbit Alexa Fluor 488	goat	1/500	A-11008	Invitrogen, USA
	anti-rabbit Alexa Fluor 568	goat	1/1000	ab175471	Abcam, UK
	anti-rat Alexa Fluor 594	donkey	1/1500	A-21209	Invitrogen, USA

Table 5: Laboratory equipment and consumables used in this project.

Device	Supplier
7300 real-time PCR System Applied Biosystems	Thermo Fisher Scientific, USA
96 Well UV Microplate	Corning, USA
Absorbable Suture: V396H Coated Vicryl (5-0)	Ethicon, Germany
Blaubrand Disposable Micropipettes	Brand, Germany
Blood Pressure Device SC1000	Hatteras Instruments, USA
Clipper (Exacta)	Aesculap, Germany
Cryostat	Leica Biosystems, Germany
DMI6000B Fluorescence Microscope	Leica Biosystems, Germany
Eclipse Ci-E Upright Microscope	Nikon, Germany
Infrared Camera T335	FLIR Systems Termisk Systemteknik, Sweden
Micropipette Puller Model P-2000	Sutter Instrument, USA
Model 900 Small Animal Stereotaxic Instrument	Kopf Instruments, USA
Permanent Suture: 681H Perma-Hand Seide (6-0) or EH7823H Ethilon II (5-0)	Ethicon, Germany
Polyvinyidene Fluorid Membrane	Millipore, Germany
CFX Connect Real-Time PCR Detection System	Bio-Rad Laboratories, Germany
Radio Transmitters (G2-HR) and Receiver Plates	Mini Mitter Respironics, USA
Rectal Thermometer Probe (STI 52-1591)	Harvard Apparatus, USA
SM33 Stereomicroscope	Hund Wetzlar, Germany

Device	Supplier
SpectraMax 340PC384 Microplate Reader	Molecular Device, USA
Suture Clips Michel (7.5 mm x 1.75 mm)	allgaier instrumente GmbH, Germany
TCS SP5 Confocal Microscope	Leica Biosystems, Germany

Table 6: Software used in this project.

Software	Supplier
Flir Tools 5.3.15268.1001	FLIR Systems Termisk Systemteknik, Sweden
GraphPad Prism 5 and 7	GraphPad Software Inc, USA
ImageJ	Open Source (Schneider et al., 2012)
Inkscape 0.92	Open Source
Microsoft Office 2013	Microsoft, USA
VitalView Data Acquisition System	Mini Mitter Respironics, USA

2.2. Animal Husbandry and Experimental Set Ups

The following mouse lines were used for breeding: wild-type (wt) C57BL/6J (The Jackson Laboratory, USA), wt C57BL/6NCr (Charles River Laboratory, USA), B6.129P2-Pvalb$^{tm1(cre)Arbr}$/J (*Parv-Cre*, The Jackson Laboratory, USA) as well as *Thra1*$^{+m}$ mice heterozygous for the dominant-negative R384C mutation in *Thra1* (Tinnikov et al., 2002) and the combination with *Thrb* ko (Forrest et al., 1996), both on a C57Bl/6NCr background. Mice were housed at 21 ± 1°C on a 12-h light /12-h dark cycle in breeding pairs or groups of up to five animals and single-housed prior to the experiment. All animals had *ad libitum* access to standard or breeding diet and tap water, if not stated otherwise. If necessary, genotyping was performed (see 2.4.5 Genotyping). Animal care procedures were in accordance with the guidelines set by the European Community Council Directives (86/609/EEC) and approved by Stockholm's Norra Djurförsöksetiska Nämnd, Sweden, or the MELUR Schleswig-Holstein, Germany.

2.2.1. Study 1: Mouse Model of a Transient Thyrotoxicosis

To investigate the effects of a transient thyrotoxicosis, wt C57BL/6J male mice (3 – 4 month) were randomly assigned to the following three groups: control, T_4 and T_4 recovery (N = 8 per group). T_4 and T_4 recovery animals were treated with T_4 containing drinking water (1 mg/L in 0.01 % bovine serum albumin (BSA) containing tap water) for 14 days, as depicted in the experimental design (Figure 4). Weekly measurements of body weight, food and water intake as well as inner ear (= auditory canal), interscapular brown adipose tissue (iBAT) and

tail base temperature (see 2.3.2 Infrared Thermography) were performed by infrared thermography in the T_4 recovery group. Finally, rectal temperature was determined under anaesthesia, heart weight was measured and organ samples from all three treatment groups were collected and stored at -80°C.

For continuous measurements of heart rate, core body temperature and activity, a separate group (N = 7) was treated identically to the T_4 recovery group and received implantable radio transmitters (see 2.3.1 Radio Transmitter Implantation). Data were recorded on day 0, 14 and 28 for 24 h in 30 sec intervals. The average was calculated for every hour and the area under the curve (AUC) was determined. For statistical analysis, a paired two-tailed Student's t test was used.

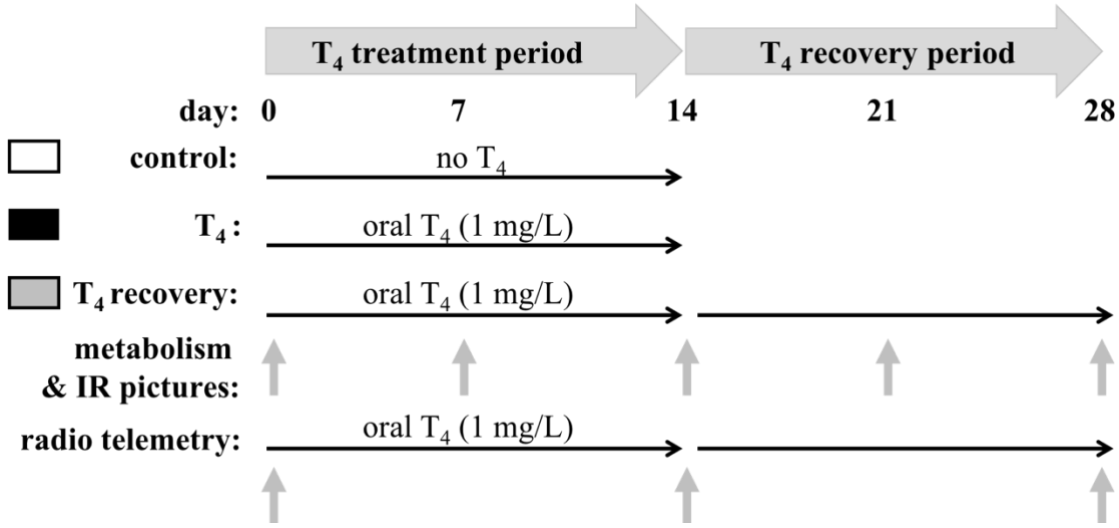

Figure 4: Experimental design of study 1: a wt C57BL/6J mouse model of transient thyrotoxicosis. T_4 treated animal (1 mg/mL, N = 8, black) were compared with untreated controls (N = 8, white) and T_4 recovered animals (two weeks after treatment, N = 8, gray). Metabolic and thermoregulatory parameters were accessed weekly and radio telemetry measurements were performed under each condition in a separate group (modified from (Hoefig et al., 2016a)).

2.2.2. Study 2: Mouse Model for Acute and Chronic T_0AM Effects

Wt C57BL/6J male mice (3 - 4 month) were randomly assigned either to an acute treatment group receiving implantable radio transmitters (N = 9, see 2.3.1 Radio Transmitter Implantation) or to a control and a T_0AM group (N = 6 per group) for chronic treatment. For acute treatment, animals received a single i.p. injection of 50 mg/kg T_0AM (5 µL/g body weight, in 60 % DMSO/40 % 1x PBS), which was compared to an i.p. injection of vehicle

(Figure 5). Parameters were recorded for 24 h every 30 sec and analysed by calculating the average for every 5 min. Furthermore, the AUC of the first 3 h after injection was analysed and heart rate measurement was normalised to a 30 min baseline, prior to the injection. Statistical analysis was performed using a 2-way ANOVA with Bonferroni post-test for temperature and activity and paired, nonparametric two-tailed Student's t test for comparing the AUC of the first 3 h after injection.

For the chronic treatment, the experimental setup involved seven days of baseline measurements followed by seven days of daily i.p. injections with 5 mg/kg T_0AM (5 µL/g body weight in 60 % DMSO/40 % 1x PBS or an equal amount of vehicle) as depicted in the experimental design (Figure 5). Body weight, food and water intake of study animals were measured daily, in parallel to cardiac parameters, which were collected using a tail-cuff system (see 2.3.3 Blood Pressure Determination). Surface temperature of the inner ear, iBAT and tail base was determined using infrared thermography (see 2.3.2 Infrared Thermography). 24 h after the last injection, rectal temperature was taken under anaesthesia, the heart weight was measured and tissue samples were collected from both groups and stored at -80°C.

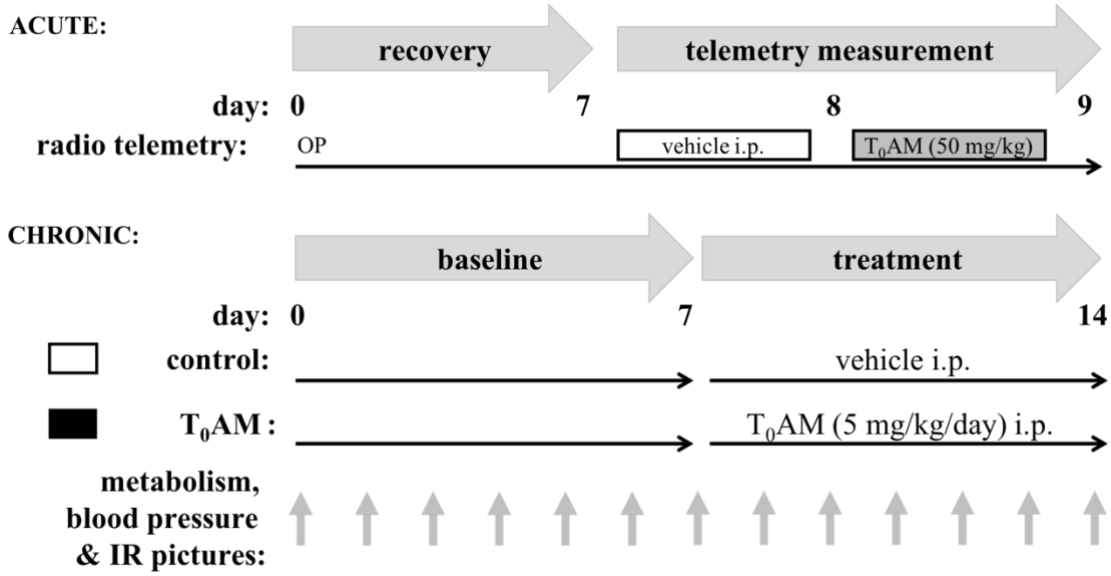

Figure 5: Experimental design of study 2: a wt mouse model for acute and chronic T_0AM effects. Acute T_0AM effects were accessed by radio telemetry measurement after a single i.p. injection of 50 mg/kg (N = 9, gray) compared to a vehicle injection (N = 9, white). Chronic T_0AM treatment (5 mg/kg/day i.p., N = 6, black) was monitored by metabolic, thermoregulatory and cardiovascular parameters und compared with a vehicle treated control group (N = 6, white) (modified from (Harder et al., 2018b)).

2.2.3. Study 3: Characterization of PV Neurones in the AHA

The maturation of PV neurones was addressed by mating wt C57BL/6J mice and separating the females after a positive plug check. Counting from the day of birth (postnatal day 0, P0), male offspring were sacrificed by decapitation at different days ranging from P8 until P14 and brains were processed and stained with 3,3'-diaminobenzidine (DAB, see 2.5 Histological Examination).

To determine the appearance of PV neurones in the embryonic brain, a bromodeoxyuridine (BrdU) birth dating experiment was performed. Wt C57BL/6J mice were mated and females were separated after a positive plug (defined as E0.5). Weight gain was monitored and pregnant females were i.p. injected once with 50 mg/kg BrdU in 0.1 M PBS on different days after conception ranging from E9.5 to E13.5. At 6 weeks of age, brains of male offspring were removed and processed (see 2.5 Histological Examination). Pictures of immunofluorescent sections from the AHA and the motor cortex (M1 and M2 area) of 3 - 6 animals per injection time point were obtained and the total numbers of PV labelled cells as well as the number of BrdU/PV double-labelled cells were counted in the respective areas.

In order to investigate the physiological consequences of PV neuronal activity in the AHA a designer receptor exclusively activated by designer drugs (DREADD) system was used for specific activation of PV neurones in the AHA. *Parv-Cre* mice (N = 12, 3 - 6 month) underwent stereotaxic surgery, receiving a bilateral intracerebral injection of a Cre-dependent recombinant adeno-associated virus (rAAV) rAAV-CAG-flex(hM3Dq-mCherry) vector in the AHA (see 2.3.4 Stereotaxic Injections). The expression of the encoded fusion protein hM3Dq-mCherry is under the control of the Cre-recombinase which is expressed under the control of the PV promoter in the *Parv-Cre* mouse model. A stimulation of hM3Dq in PV neurones is possible by i.p. administration of the pharmacological inert compound clozapine-N-oxide (CNO), which in turn leads to an activation of the $G\alpha_{q/11}$ signalling pathway in the neurones (Armbruster et al., 2007). Within the same surgery, mice were implanted with radio transmitters (see 2.3.1 Radio Transmitter Implantation) to detect potential changes in temperature, heart rate or activity evoked by CNO injection. After recovery, a 24 h untreated baseline was measured (1 min recording, average calculated per hour, Figure 6). Next, mice received a control i.p. injection of vehicle (0.9 % saline solution, 5 µL/g body weight) and 24 h later an i.p. injection of 0.5 mg/kg CNO (5 µL/g body weight). Mice were measured continuously during this time (10 s recording, average calculated per minute, Figure 6). Animals, which had successfully completed the experiment (N = 11), were controlled for the position of the stereotaxic injection by labelling the

membrane-bound fusion protein hM3Dq-mCherry (see 2.5 Histological Examination). Additionally, animals with an unusual low baseline heart rate (more than 5 % </= 250 bpm) due to suboptimal lead placement were excluded from the analysis (3 out of 11). Statistical analyses were performed by multiple t tests comparing each time point of the measurement (40 min bevor until 200 min after the injection) for temperature, heart rate and activity. For detailed heart rate analysis, AUC of 40 min bins from 40 min bevor until 600 min after injection were calculated and analysed by a 2way ANOVA with repeated measures by both factors and controlled for multiple comparisons by Sidak test.

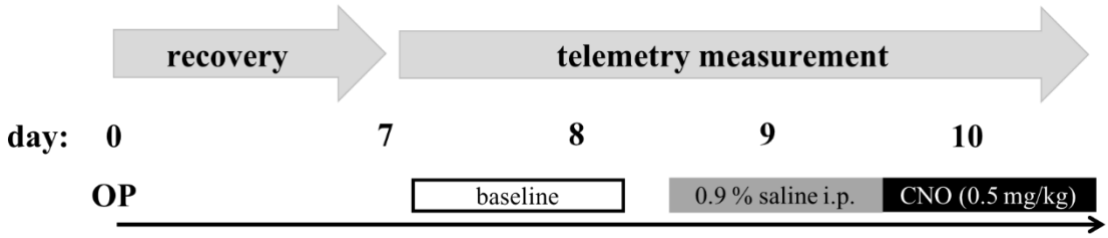

Figure 6: Experimental design for the chemogenetic activation of PV neurones in the AHA by a 'designer receptors exclusively activated by designer drugs' system. *Parv-Cre* mice (N = 12) received in one operation an intracerebral injection (75 nL) of AAV-CAG-flex(hM3Dq-mCherry) in the AHA and a radio transmitter in the abdominal cavity. After seven days of recovery mice were recorded for 24 h untreated (baseline, 1 min interval, white), for 24 h after 0.9 % saline injection (10 sec interval, gray) and for 24 h after CNO injection (0.5 mg/kg, 10 sec intervals, black). CNO, Clozapine-N-oxid.

To modulate maternal TH levels during pregnancy, two strategies were implemented. On the one hand *Thrb* ko dams with endogenously elevated TH levels (Forrest et al., 1996) were breed with male *Thra1*$^{+m}$ or male *Thra1*$^{+m}$/*Thrb* ko mice to achieve high maternal TH levels throughout the entire pregnancy. On the other hand, wt dams were mated with male *Thra1*$^{+m}$ mice and pregnant females were treated orally with T_3-containing drinking water (0.5 mg/L T_3 and 0.01 % BSA) from E12.5 until birth. Brains of male wt, *Thra1*$^{+m}$, *Thrb* ko and *Thra1*$^{+m}$/*Thrb* ko offspring were collected at 3 - 6 weeks of age and DAB staining was performed to determine the number of cells (see 2.5 Histological Examination).

2.3. *In vivo* Methods

2.3.1. Radio Transmitter Implantation

To record core body temperature, heart rate, and activity in conscious and freely moving mice, implantable radio transmitters and receiver plates were used. To implant the transmitter device, mice were anaesthetized with 4 % isoflurane, then placed on a heating pad and kept at approx. 2 % isoflurane at 300 ml/min flow-rate during the surgery. Animals

were i.p. injected with pain medication (5 mg/kg Rimadyl in sterile 1x PBS), eye ointment was applied to prevent eye drying, and the abdomen was shaved to minimize the risk of contamination. Depth of anaesthesia was controlling by toe-pinch reflex and repeatedly tested throughout the surgery, body temperature was monitored using a rectal probe. A vertical incision of 1.5 cm was made in the skin and the abdominal wall and the sterilised transmitter was implanted into the peritoneal cavity, then the abdominal wall was closed with absorbable suture. Next the wires were placed below the skin and the electrodes sutured to the right shoulder and the lower left chest wall using permanent suture (681H Perma-Hand Seide). Finally, the lesion was closed using permanent suture (EH7823H Ethilon II), if needed Michel clips were used to additionally secure the suture and the animals returned to a pre-warmed single cage. At the first day of recovery, animals received another i.p. injection of pain medication and recordings started after seven days.

2.3.2. Infrared Thermography

To measure temperature of inner ear, iBAT and tail base (light phase, room temperature (RT)) non-invasively, in conscious and freely moving animals an infrared camera (± 0.05°C sensitivity) was used. Three images of each region were taken from the same animal per session, and the maximum temperature in the selected area across all images per time point and animal was determined using the infrared analysis software Flir Tools. Statistical analysis was performed using a paired two-tailed Student's t test (study 1) or an unpaired nonparametric two-tailed Mann-Whitney t test (study 2).

2.3.3. Blood Pressure Determination

To access blood pressure parameters in study 2 a tail-cuff system was used which recorded systolic, diastolic and mean arterial pressure and pulse rate. For the measurement, the mouse was restrained on top of a 37°C warm platform, its tail was threaded through the tail-cuff and fixed in the v-notch under the top half of the sensor. Animals ran through two consecutive sessions (15 attempts of measurement each), of which the first was only for adaptation. If no pulse was detected within 30 sec the next attempt started. Mean values of all successful attempts in the second session were analysed, using an unpaired nonparametric two-tailed Mann-Whitney t test.

2.3.4. Stereotaxic Injections of rAAV

To chemogenically activate PV neurones in the AHA, *Parv-Cre* mice were bilateral, intracerebral injected with the Cre-dependent rAAV-CAG-flex(hM3Dq-mCherry). The vector rAAV-CAG-flex(hM3Dq-mCherry) was kindly provided by Dr. Helge Müller-Fielitz (Müller-Fielitz et al., 2017). The rAAV consists of a rAAV2-based expression vector with inverted terminal repeats of serotype 2 (Musatov et al., 2002), a woodchuck posttranscriptional regulatory element (WPRE) and a bovine growth hormone polyadenylation site (bGHpA). The plasmid pAAV-CAG-flex(hM3Dq-mCherry) consists of the CMV enhancer chicken β-actin (CAG) promoter from the pAAV-CAG-BMP2-2A-Tomato (Heinonen et al., 2014), inserted in the Mlu1/Sal1 site of the pAAV-Syn-flex(hM3Dq-mCherry) plasmid (Krashes et al., 2011). Stereotaxic coordinates for the AHA relative to bregma: mediolateral ± 0.3 mm, anteriorposterior -0.6 mm, dorsoventral -5 mm (from the dura mater) were determined from a mouse brain atlas (Paxinos and Franklin, 2004).
Mice were anaesthetized with 4 % isoflurane and placed on a heating pad in a stereotaxic frame. By fixing spout piece and ear bars the skull was positioned horizontally and symmetrically and lateral movement was prevented. Pain medication (5 mg/kg Rimadyl in sterile 1x PBS) was i.p. injected and eye ointment was applied. Depth of anaesthesia was checked by absence of the toe-pinch reflex before and frequently during the surgery, anaesthesia was lowered to 2 % and 300 ml/min during the surgery. The skin of the head was wiped with 70 % EtOH, a 1 cm lesion was cut vertically in the skin and the skull was cleaned and treated with xylocain. Bregma and lambda positions were identified on the skull using a SM33 stereomicroscope and the position of the skull was further adjusted until bregma and lamda were horizontally aligned. AHA coordinates were marked with methylene blue on the skull and holes were drilled using a 23G cannula. Injection was performed using a 5 µL micropipette, pulled apart and cropped to create a long narrow tip and marked with a 1 mm scale (Cetin et al., 2006). 75 nL of vector solution per injection site were delivered at an injection rate of 75 nL/min and the micropipettes were kept in place for 5 min before retraction to minimize backflow. After the injection, the skull was treated with xylocain to loosen the wound margin and prevent scratching of the lesion by the animal and the skin was sutured using permanent suture (681H Perma-Hand Seide). Animals received pain medication again 24 h after surgery and were allowed to recover for at least seven days bevor experiments started, to allow for sufficient hM3Dq-mCherry expression.

2.4. Molecular Methods

2.4.1. RNA Isolation, cDNA Synthesis and Quantitative Real-Time PCR (qPCR)

RNA was isolated from snap-frozen tissues using RNeasy Kits or the Aurum Total RNA Kits according to the manufacturer's protocols. Subsequent cDNA synthesis was performed using anchored-oligo(dT)18 primers and the Transcriptor First-Strand cDNA Synthesis Kit or the iScript cDNA Synthesis Kit. qPCR was performed with the 7300 real-time PCR system or the CFX Connect Real-Time PCR detection system and SYBR Green PCR master mix or Absolute qPCR SYBR Green Fluorescein Mix. A 2-step PCR protocol with 40 cycles and a temperature of 60°C for annealing and extension was used (Table 7). A melting curve was recorded to confirm the specificity of the reaction and standard curves were calculated to correct for PCR efficiency. All primer sequences utilized are listed in Table 8. In Study 1 gene expression was normalised to *hypoxanthine guanine phosphoribosyl transferase* (*Hprt*) as a housekeeping gene. In study 2 four housekeeper genes (*18S ribosomal protein (Rps18)*, *actin beta* (*Actb*), *Hprt*, *peptidylprolyl isomerase a* (*Ppia*)) were measured and the geometric mean was calculated tissue-dependently of a set of non-regulated genes (iBAT: *Actb, Hprt, Ppia;* heart: *Actb, Rps18, Hprt*; kidney: *Hprt*; liver: *Actb, Rps18, Ppia*; lung: *Actb, Rps18, Hprt, Ppia*; pituitary: *Actb, Rps18, Hprt*; thyroid: *Actb, Rps18, Hprt*) and used for target-gene normalisation.

Table 7: 2-step PCR protocol for qPCR measurement.

Temperature (°C)	**Time (min)**	**Replications**
50	2.00	1
95	10.00	1
95	0.15	40
60	1.00	
95	0.15	1
60	0.30	1
95	0:15	1
melting curve program		

Table 8: Sequences of qPCR primers.

Gene	Abbreviation	Primer Sequence 5`-3′ (fw/rev)
3-hydroxy-3-methylglutaryl-CoA lyase	*Hmgcl*	CAGGTGAAGATCGGTGAAGTC
		GGAGCCCTGCTTCGGAAAC
3-hydroxy-3-methylglutaryl-CoA reductase	*Hmgcr*	TGTTCACCGGCAACAACAAGA
		CCGCGTTATCGTCAGGATGA
3-hydroxy-3-methylglutaryl-CoA synthase 2	*Hmgcs2*	GAAGAGAGCGATGCAGGAAAC
		GTCCACATATTGGGCTGGAAA
3-hydroxybutyrate dehydrogenase type 1	*Bdh1*	TTCCCCTTCTCCGAAGAGC
		CCCAGAGGGTGCATCTCATAG
3-oxoacid CoA transferase 1	*Oxct1*	CATAAGGGGTGTGTCTGCTACT
		GCAAGGTTGCACCATTAGGAAT
acetyl-CoA carboxylase 1	*Acaca*	GTCCCCAGGGATGAACCAATA
		GCCATGCTCAACCAAAGTAGC
acetyl-CoA carboxylase 2	*Acacb*	GAATCTCACGCGCCTACTATC
		ACGGTGAAATCTCTGTGCAGG
acetyl-Coenzyme A acyltransferase 2 (mitochondrial 3-oxoacyl-Coenzyme A thiolase)	*Acaa2*	CTGCTACGAGGTGTGTTCATC
		AGCTCTGCATGACATTGCCC
actin, beta	*Actb*	GGCTGTATTCCCCTCCATCG
		CCAGTTGGTAACAATGCCATGT
adrenergic receptor beta 1	*Adrb1*	AGCGCTGATCTGGTCATGG
		CCAGAGCTCGCAGAAGAAGG
adrenergic receptor beta 2	*Adrb2*	GGGAACGACAGCGACTTCTT
		GCCAGGACGATAACCGACAT
adrenergic receptor beta 3	*Adrb3*	AGAAACGGCTCTCTGGCTTTG
		TGGTTATGGTCTGTAGTCTCGG
aldolase b	*Aldob*	GAAACCGCCTGCAAAGGATAA
		GAGGGTCTCGTGGAAAAGGAT
angiotensin I converting enzyme	*Ace1*	TCCAAGCAGGAAGCTAATCC
		CAGCCTACCTGCTTCCTTCC
angiotensinogen	*Agt*	TTCCAAGGAACGATGAGAGG
		ACTCCAGTGCTGGAAGTTGC
ATPase, Ca++ transporting, cardiac muscle, slow twitch 2 (SERCA2a)	*Atp2a2*	TCCGCTACCTCATCTCATCC
		CAGGTCTGGAGGATTGAACC
calsequestrin 2	*Casq2*	TGCTCATGGTGGGGG TTTATC
		AGGTTCGTGGTAATAGAGACAGA
cell death-inducing DNA fragmentation factor alpha subunit-like effector A	*Cidea*	TGACATTCATGGGATTGCAGAC
		GGCCAGTTGTGATGACTAAGAC
cholinergic receptor muscarinic 2	*Chrm2*	CAAGATCCAGAATGGCAAGG
		GACAGACGTGGAGTCATTGG
citrate synthase	*Cs*	GGACAATTTTCCAACCAATCTGC
		TCGGTTCATTCCCTCTGCATA

Gene	Abbreviation	Primer Sequence 5`-3′ (fw/rev)
cytochrome P450 family 11 subfamily b polypeptide 1	*Cyp11b1*	AACCCAAATGTTCTGTCACCAA CAAAGTCCCTTGCTATCCCATC
cytochrome P450 family 11 subfamily b polypeptide 2	*Cyp11b2*	TGGCTGAAGATGATACAGATCCT CACTGTGCCTGAAAATGGGC
iodothyronine deiodinase type I	*Dio1*	GCTGAAGCGGCTTGTGATATT GTTGTCAGGGGCGAATCGG
iodothyronine deiodinase type II	*Dio2*	GATGCTCCCAATTCCAGTGT AGTGAAAGGTGGTCAGGTGG
iodothyronine deiodinase type III	*Dio3*	CTACGTCATCCAGAGTGGCA CTGTTCATCATAGCGCTCCA
dopa decarboxylase	*Ddc*	GACTACAGGCACTGGCAGAT CTGGCGTACCAGTGACTCAA
dopamine beta hydroxylase	*Dbh*	TGGACCCCGAAGGGATTTTAG CCATCTCTCCTCGATCTGACA
fatty acid synthase	*Fasn*	GGAGGTGGTGATAGCCGGTAT TGGGTAATCCATAGAGCCCAG
fibroblast growth factor 21	*Fgf21*	CTGCTGGGGGTCTACCAAG CTGCGCCTACCACTGTTCC
glucokinase	*Gck*	TGAGCCGGATGCAGAAGGA GCAACATCTTTACACTGGCCT
glucose-6-phosphatase	*G6pc*	TCAACCTCGTCTTCAAGTGGATT TGTAGTAGTCGGTGTCCAGGACC
hyperpolarization-activated cyclic nucleotide-gated K+ 2	*Hcn2*	CGAGCTGACACCTACTGTCG CTTGCCTATGCGATCTAGCC
hyperpolarization-activated cyclic nucleotide-gated K+ 4	*Hcn4*	GGAGAGGGTTAAGTCAGCAGG AGGGTGTGGTGTTCTCATCCT
hypoxanthine guanine phosphoribosyl transferase	*Hprt*	GCAGTACAGCCCCAAAATGG AACAAAGTCTGGCCTGTATCCAA
lactate dehydrogenase A	*Ldha*	CATTGTCAAGTACAGTCCACACT TTCCAATTACTCGGTTTTTGGGA
lipase, hormone sensitive	*Lipe*	CACCCATAGTCAAGAACCCCTTC TCTACCACTTTCAGCGTCACCG
malic enzyme 1, NADP(+)-dependent, cytosolic	*Me1*	GAAAGAGGTGTTTGCCCATGA AATTGCAGCAACTCCTATGAGG
malonyl-CoA decarboxylase	*Mlycd*	CTGTCGCCTATCCCTGGATTC CCGGTAACCGCTGAGATTTCT
myosin, heavy polypeptide 6, cardiac muscle, alpha	*Myh6*	GCCCAGTACCTCCGAAAGTC GCCTTAACATACTCCTCCTTGTC
myosin, heavy polypeptide 7, cardiac muscle, beta	*Myh7*	GGAATCCTTTGGAAATGCGAAGA GCCCCAACAATATAGCCAGTTAC
natriuretic peptide type B	*Nppb*	GAGGTCACTCCTATCCTCTGG GCCATTTCCTCCGACTTTTCTC

Gene	Abbreviation	Primer Sequence 5`-3′ (fw/rev)
peptidylprolyl isomerase A	*Ppia*	CATCCTAAAGCATACAGGTCCTG
		TCCATGGCTTCCACAATGTT
peroxisome proliferative activated receptor, gamma coactivator 1 alpha	*Ppargc1a*	TTGTCAGGCTGGAGTGTACC
		CACCATGGTCGTATCAGAGG
phenylethanolamine-N-methyltransferase	*Pnmt*	CAGACCTGAAGCACGCTACAG
		TAGTTGTTGCGGAGATAGGCG
phosphoenolpyruvate carboxykinase 1, cytosolic	*Pck1*	ATCTTTGGTGGCCGTAGACCT
		GCCAGTGGGCCAGGTATTT
phospholamban	*Pln*	ACTGTGACGATCACCGAAGC
		TTCCATTATGCCAGGAAGG
PR domain containing 16	*Prdm16*	CCCCACATTCCGCTGTGAT
		CTCGCAATCCTTGCACTCA
pyruvate kinase liver and red blood cell	*Pklr*	CCGCATCTACATTGACGACG
		CAAGTTCACACCCTTCCTGTT
regulator of G-protein signaling 4	*Rgs4*	GAGTGCAAAGGACATGAAACATC
		TTTTCCAACGATTCAGCCCAT
renin 1	*Ren1*	ACGGGTCCGACTTCACCAT
		TGCCTAGAACACCGTCAAACT
ribosomal protein S18	*Rps18*	TTGACGGAAGGGCACCACCAG
		GCACCACCACCCACGGAATCG
ryanodine receptor 2	*Ryr2*	ACGGCGACCATCCACAAAG
		CGGGGGAACATTCTTGGAATTG
sema domain, immunoglobulin domain (Ig), short basic domain, secreted, (semaphoring) 3A	*Sema3a*	GAGCAGCAACAAGTGGAAGC
		CGCAGCTCAGACACTTCTGG
thyroid hormone responsive (Spot14)	*Thrsp*	AAGGTGGCTGGCAACGAAA
		GGGTCAGGTGGGTAAGGATG
thyroid stimulating hormone beta	*Tshb*	CCG CAC CAT GTT ACT CCT TA
		GTT CTG ACA GCC TCG TGT AT
transmembrane protein 26	*Tmem 26*	TTCCTGTTGCATTCCCTGGTC
		GCCGGAGAAAGCCATTTGT
tumour necrosis factor receptor superfamily, member 9	*Tnfrsf9*	CCTTGCAGGTCCTTACCTTGT
		GTTGCTTGAATATGTGGGGGA
tyrosine hydroxylase	*Th*	GCTGGAGGATGTGTCTCACT
		GACGAGGCATGACGGATGTA
uncoupling protein 1	*Ucp1*	ACTCAGGATTGGCCTCTACG
		CCACACCTCCAGTCATTAAGC

2.4.2. Total T_4 and T_3 ELISA for Mouse Serum Analysis

Serum total T_4 (EIA 1781) and total T_3 (DNOVO53) were determined by commercial ELISA kits according to the manufacturer's protocols.

2.4.3. Glycogen Determination in Liver Tissue

Hepatic glycogen content was determined as described previously (Van Der Vies, 1954) with some modifications. Samples (10 – 20 mg) were homogenized in 1 mL 5 % trichloroacetic acid and incubated for 30 min (RT) before centrifugation (10 min, 20000 g, RT). The supernatant was incubated overnight (4°C) and all subsequent steps were performed in triplicates. A mixture of 50 µL supernatant and 100 µL ethanol (EtOH, 99.5 %) was incubated (30 min, RT) and centrifuged (30 min, 20000 g, RT). The supernatant was discarded and the dry pellet was re-suspended in 75 µL Lugol reaction mix. After incubation (10 min, RT) optic density (OD) was measured at 600 nm. Measurements were normalised against the blank (Lugol reaction mix) and the mean OD of triplicates was calculated and normalised to tissue weight.

2.4.4. Western Blot Analysis

Protein isolation was performed from samples of snap frozen iBAT in 100 µL RIPA-buffer with PMSF and protein concentration was determined by a bicinchoninic acid assay. For immunological detection, 15 µg protein were separated on a 12 % SDS polyacrylamide gel and transferred onto a polyvinyidene fluorid membrane using standard procedures. Blots were blocked in 5 % w/v BSA or 5 % w/v non-fat dry milk (in 1x TBS-T) and probed with primary antibodies for UCP1, GAPDH, Phospho-Akt (Ser473) or Akt (Table 3) overnight (4°C). Subsequently blots were incubated (1 h, RT) with the corresponding peroxidase-conjugated secondary antibody (Table 3) and visualized using Clarity Western ECL Substrate and CL-Xposure x-ray films. After each detection, the blots were stripped with Restore PLUS Western Blot Stripping Buffer for 15 min. Quantification of band intensity was performed by ImageJ. Statistical analysis was performed using an unpaired two-tailed Student's t test.

2.4.5. Genotyping

Tail or ear snips were incubated overnight in genotyping buffer with proteinase K (10 mg/mL) at 55°C. Samples were centrifuged (5 min, 18000 g) and the supernatant was transferred in a new tube. DNA was precipitated by adding 500 µL isopropanol and pelletised (30 min, 18000 g). The supernatant was discarded and the pellet was washed with 80 % EtOH and centrifuged again (30 min, 18000 g). Afterwards, the pellet was dried,

resolved in 100 µL 1/10 TE buffer and used together with the relevant primer pairs (Table 9) for PCR analysis as indicated in Table 10.

Table 9: Primer sequences for genotyping.

Strain	**Primer Sequence 5`-3′ (fw)**	**Primer Sequence 5`-3′ (rev)**
Parv-Cre	GCGGTCTGGCAGTAAAAACTATC	GTGAAACAGCATTGCTGTCACTT
Thra1^{+m}	GGACAAGATCGAGAAGAGTCAGGA	CACTGCATTCTAGTTGTGGTTTGTCC
Thrb wt	GCACAGGGAGGAAGTAGGCTGTCT	CCCTGGAGGCCAAAGGTCAATG
Thrb ko	GCACAGGGAGGAAGTAGGCTGTCT	GTGCCAGCGGGGCTGCTAAAG

Table 10: PCR cycles for genotyping.

Parv-Cre			***Thra1***			***Thrb***		
Temp. (°C)	Time (min)		Temp. (°C)	Time (min)		Temp. (°C)	Time (min)	
94	3.00		95	5.00		94	3.00	
94	0.50		95	0.70	34x	94	0.50	
55	1.00	33x	67	1.33		55	1.00	
72	1.00		74	10.00		72	1.00	32x
72	2.00		4	∞		72	2.00	
4	∞					4	∞	

2.5. Histological Examination

Tissue from the following mouse lines were used to perform immunohistochemistry as described below: C57BL/6J, C57BL/6NCr, *Parv-Cre*, *Pax8* (*Pax8*$^{-/-}$ and *Pax8*$^{+/-}$) (Mansouri et al., 1998), *Mct8* (*Mct8*$^{-/y}$) (Trajkovic et al., 2007), *Mct8/Oatp1c1* (M/O dko; *Mct8*$^{-/y}$/*Oatp1c1*$^{-/-}$) (Mayerl et al., 2014), *Mct10* (*Mct10*$^{-/-}$ and *Mct10*$^{+/-}$) (Mariotta et al., 2012; Müller et al., 2014), *Thra1*$^{+m}$ (Tinnikov et al., 2002) as well as the combination with *Thrb* (*Thrb* $^{-/-}$) (Forrest et al., 1996), *Nkx2-1-Cre*:RFP (Luche et al., 2007) crossed to *5HT$_{3a}$R-BAC*^{EGFP} (Munoz-Manchado et al., 2016) and ObRb.Zsgreen mice (Madisen et al., 2010).

2.5.1. Brain Tissue Processing

Removed brains were directly fixed in 4 % PFA overnight (4°C), followed by incubation in 30 % w/v sucrose in 1x PBS for at least three days. Subsequently, brains were snap-frozen and cut in 20 µm coronal sections using a cryostat and stored in CPS. For immunofluorescence staining protocols, consecutive sections were sampled in 10 tubes per brain, with the sections in one tube covering intervals of 200 µm. For cell counting in the

AHA, consecutive sections were sampled in 5 tubes, covering intervals of 100 µm per section. Up to two tubes per brain of several animals per genotype were analysed by counting PV positive cells bilaterally in the AHA under the microscope and calculating the average per animal and genotype. Throughout, the raw cell count is given, to calculate the true cell number, results need to be multiplied by 2.85 (Guillery and Herrup, 1997; Mittag et al., 2013).

2.5.2. Immunohistochemistry

DAB staining was performed on 4 % PFA fixed, free floating 20 µm cryostat coronal sections and all solutions were prepared with 1x PBS. First, sections were blocked with 1 % H_2O_2 (1 h) followed by 5 % NGS, avidin (avidin/biotin blocking kit) and 0.3 % Triton-X 100 (1 h). Next, sections were incubated in 5 % NGS, biotin (avidin/biotin blocking kit), 0.3 % Triton-X 100 and rabbit anti-PV primary antibody (Table 4) overnight (4°C). The following day, sections were treated with a biotinylated secondary antibody (Table 4, 1 h) in 0.3 % Triton-X 100 followed by ABC-Solution (ABC-Kit, 1 h) and stained in DAB-solution (0.5 mg/mL with 0.15 % H_2O_2, 2 min). Subsequently, sections were mounted and dried overnight at RT, dehydrated and cleared in xylene, and coverslipped using pertex.

2.5.3. Immunofluorescence

Immunofluorescence staining was performed on 4 % PFA fixed, free floating 20 µm cryostat coronal sections and all solutions were prepared with 1x PBS.

Sections from BrdU treated mice offspring were blocked with 5 % NGS and 0.3 % Triton-X 100 (1 h), followed by incubation in rabbit anti-PV primary antibody (Table 4) in blocking solution overnight (RT). Next, sections were incubated in Alexa Fluor 488 labelled secondary antibody (Table 4, 1 h) followed by antigen retrieval (10 min in 1 M HCl on ice, 10 min in 2 M HCl at RT, 20 min in 2 M HCl at 37°C, 10 min in 0.1 M borate buffer at RT). Subsequently sections were incubated in rat anti-BrdU primary antibody (Table 4) in blocking solution overnight (RT) which was followed by an incubation with Alexa Fluor 594 secondary antibody (Table 4, 1 h).

Wt samples were treated with 10 mM Na-Citrate at 80°C for 10 min for antigen retrieval and blocked with 5 % NDS and 0.3 % Triton-X 100. Next, sections were incubated in goat anti-PV primary antibody in combination with rabbit anti-vesicular glutamate transporter 2 (VGLUT2) or rabbit anti-PV primary antibody in combination with mouse anti-glutamate decarboxylase 67 (GAD67, Table 4) in blocking solution overnight (4°C). Subsequently, sections were incubated using the respective secondary antibodies (Table 4, 1 h).

For *Parv-Cre* mouse samples no additional antigen retrieval step was necessary and the protocol was performed as described above using NDS, rabbit anti-PV and goat anti-mCherry primary antibody (Table 4) and the respective secondary antibodies (Table 4).
All slices were mounted on object slides using ProLong Diamond Antifade Mounting Medium with Dapi or Hard Set Antifade Mountain Medium with DAPI. Samples from *Nkx2-1-Cre*:RFP x *5HT$_{3a}$*-EGFP double reporter mice were processed using a rabbit anti-PV primary antibody (Table 4) and an Alexa Fluor 568 labelled secondary antibody (Table 4) as described (in collaboration with Susi Dudazy-Gralla and Jens Hjerling Leffler) (Luche et al., 2007; Munoz-Manchado et al., 2016).

2.6. Statistical Analysis

GraphPad Prism 5 and 7 software was used to analyse the data and all statistic tests are indicated in the figure legends. All data are represented as mean ± standard error of the mean (S.E.M.) and statistical significance was defined as *$p < 0.05$, **$p < 0.01$, ***$p < 0.001$.

3. Results

In order to dissect the interplay of peripheral TH with body thermogenesis and cardiovascular function, this thesis investigated the effects of a transient thyrotoxicosis by systemic T_4 treatments (study 1) and the role of the TH metabolite T_0AM in this context (study 2) as well as the central aspects of TH for brain development and the influence of TH-dependent neurones on thermoregulation and cardiovascular control (study 3). The results will be presented in the following section.

3.1. Study 1: Peripheral Effects of Two Weeks Oral T_4 Treatment Followed by Two Weeks of T_4 Withdrawal in Adult Male Mice

In the first part of the thesis, the focus was on the consequences of a strong short-term increase in TH concentration in the body, called transient thyrotoxicosis. Such an event could be the result of an overproduction of endogenous TH or an excessive intake of exogenous TH. Furthermore, also the ability of the body to recover within two weeks from the thyrotoxicosis was of interest. Therefore, a mouse model for a transient thyrotoxicosis was developed, using male wt C57BL/6J mice, which received T_4 containing drinking water (1 mg/L) for two weeks. The treatment led to a 3-fold increase in serum total T_4 and a 2.5-fold increase in serum total T_3 concentration in the T_4 group compared to the controls (Figure 7A), which indicated a hyperthyroid state in these animals. After two weeks of T_4 recovery, during which animals received untreated drinking water, total T_4 concentration normalised again, whereas total T_3 concentration even went below the baseline (Figure 7A). This was concurrent with a strong reduction of pituitary *Tsh* mRNA expression during T_4 treatment (Figure 7B) and an increase of the TH sensitive *Dio1* in liver and kidney (Figure 7C). Two weeks after T_4 withdrawal, pituitary *Tsh* and hepatic *Dio1* mRNA expression normalised, whereas renal *Dio1* was still increased compared to controls (Figure 7B, C).

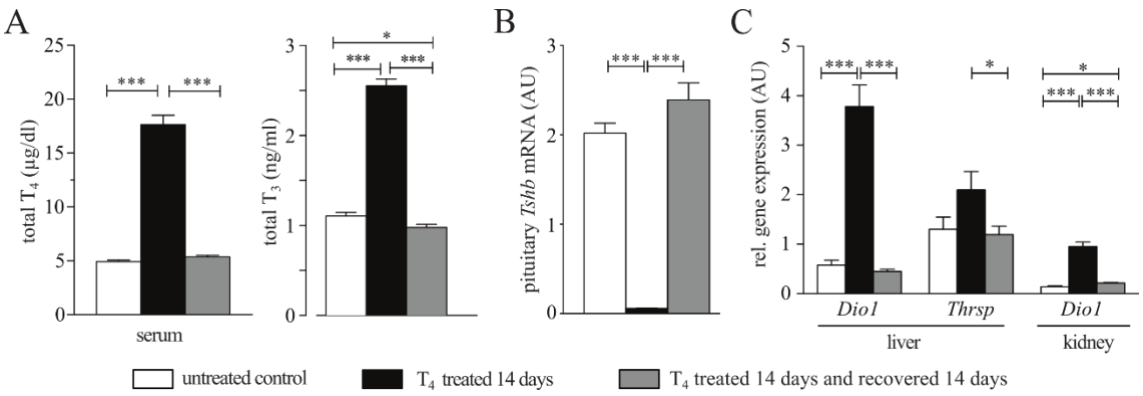

Figure 7: Two weeks of oral T_4 treatment successfully induces a transient thyrotoxicosis in male wt C57BL/6J mice. (A) Total T_4 and total T_3 concentrations in serum of untreated (white), T_4 treated (black) and T_4 recovery (grey) animals. Relative mRNA expression of (B) pituitary *Tsh* as well as (C) thyroid hormone sensitive genes in liver and kidney, normalised to *Hprt*, in untreated (white), T_4 treated (black) and T_4 recovery (grey) animals. All values are mean ± S.E.M. and statistic testing was performed using an unpaired two-tailed student's t test with *p < 0.05, **p < 0.01 or ***p < 0.001. AU, arbitrary unit; *Dio1*, *iodothyronine deiodinase type I*; *Hprt*, *hypoxanthine guanine phosphoribosyl transferase*; *Thrsp*, *thyroid hormone responsive* (*Spot14*); *Tsh*, *thyroid stimulating hormone*; T_3, 3,3',5-triiod-L-thyronine; T_4, thyroxine (modified from (Hoefig et al., 2016a)).

3.1.1. Metabolic Switch in Liver and Adipose Tissue Due to a Transient Thyrotoxicosis and Subsequent Recovery

To evaluate the metabolic consequences of a transient thyrotoxicosis, body weight, food and water intake were monitored in the T_4 recovery group (n = 8) over the experimental course of four weeks (Figure 8A-C). Mice showed an increased body weight gain upon T_4 treatment; however, after recovery all animals were back to a weight appropriate for their age (Figure 8A). Absolut and relative food intake did not change significantly during the rather short T_4 treatment period, but both were significantly diminished after T_4 recovery (Figure 8B). In contrast, absolute water intake increased upon T_4 treatment, but was unaltered when normalised to body weight, whereas absolute and relative water intake were reduced after T_4 recovery (Figure 8C). Examination of liver gene expression revealed a hyperthyroid state of the tissue during thyrotoxicosis, demonstrated by a significant increased mRNA expression of the T_3 sensitive gene *malic enzyme 1* (*Me1*; Figure 9A) as published before for rats and mice (Song et al., 1988; Takeuchi et al., 2002). A significant reduction of the glycogen content in the liver was identified during T_4 treatment (Figure 8D) together with significantly reduced relative mRNA expression of the glycolytic enzyme *aldolase b* (*Aldob*). Other genes, involved in gluconeogenesis e.g. *lactate dehydrogenase* a (*Ldha*), *phosphoenolpyruvate carboxykinase* (*Pck1*) and *glucose-6-phosphatase* (*G6pc*) were unaltered (Figure 9A).

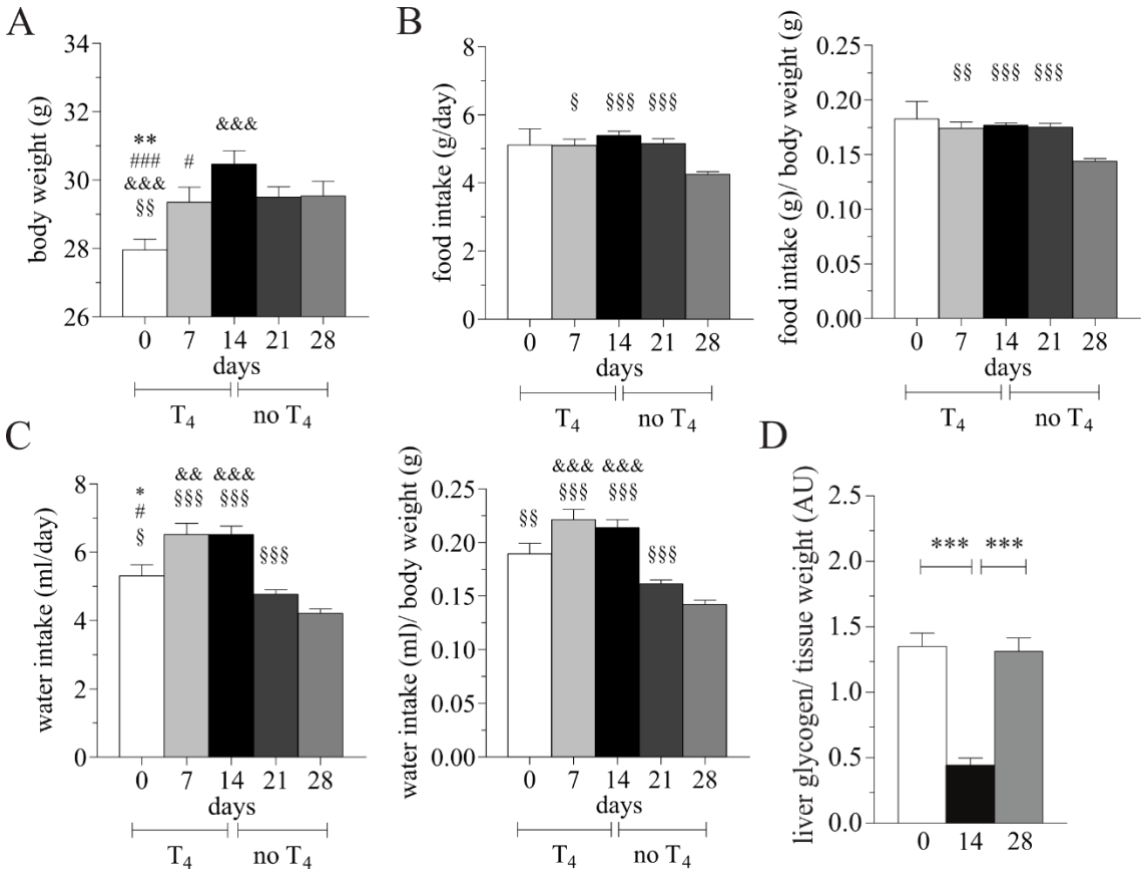

Figure 8: Analysis of metabolic parameters in male wt C57BL/6J mice during two weeks of T_4 treatment and two subsequent weeks of recovery. (A) Body weight, (B) absolute food intake and food intake normalised to body weight and (C) absolute water intake and water intake normalised to body weight of T_4 recovery animals (n = 8) in the course of the experiment. (D) Liver glycogen normalised to tissue weight in control (white), T_4 treated (black) and T_4 recovery (grey) animals (n = 8 per group). All values are mean ± S.E.M. and statistic testing was performed using a paired, two-tailed student's t test (A-C) with $^{*}p < 0.05$, $^{**}p < 0.01$ versus day 7, $^{\#}p < 0.05$, $^{\#\#\#}p < 0.001$ versus day 14, $^{\&\&}p < 0.01$ $^{\&\&\&}p < 0.001$ versus day 21, $^{\S}p < 0.05$, $^{\S\S}p < 0.01$, $^{\S\S\S}p < 0.001$ versus day 28 or an unpaired two-tailed student's t test (D) with $^{***}p < 0.001$. AU, arbitrary units; T_4, thyroxine (modified from (Hoefig et al., 2016a)).

After T_4 recovery, glycogen content (Figure 8D) as well as mRNA expression of *Aldob* returned back to normal and other genes, crucial for glycolysis such as *glucokinase* (*Gck*) and *pyruvate kinase* (*Pklr*) showed significant increased mRNA expression (Figure 9A). The same was observed for genes involved in fatty acid synthesis such as *acetyl-CoA carboxylase 1* (*Acaca*) and *fatty acid synthase* (*Fasn*; Figure 9A). Together with the results of the *Pck1/Pklr* ratio (Figure 9B), these findings indicated a switch from hepatic gluconeogenesis due to limited hepatic glucose availability during thyrotoxicosis to glycolysis and high glucose consumption and fatty acid production upon recovery. At the same time, there was no clear indication for true starvation because relative mRNA expression of genes important for

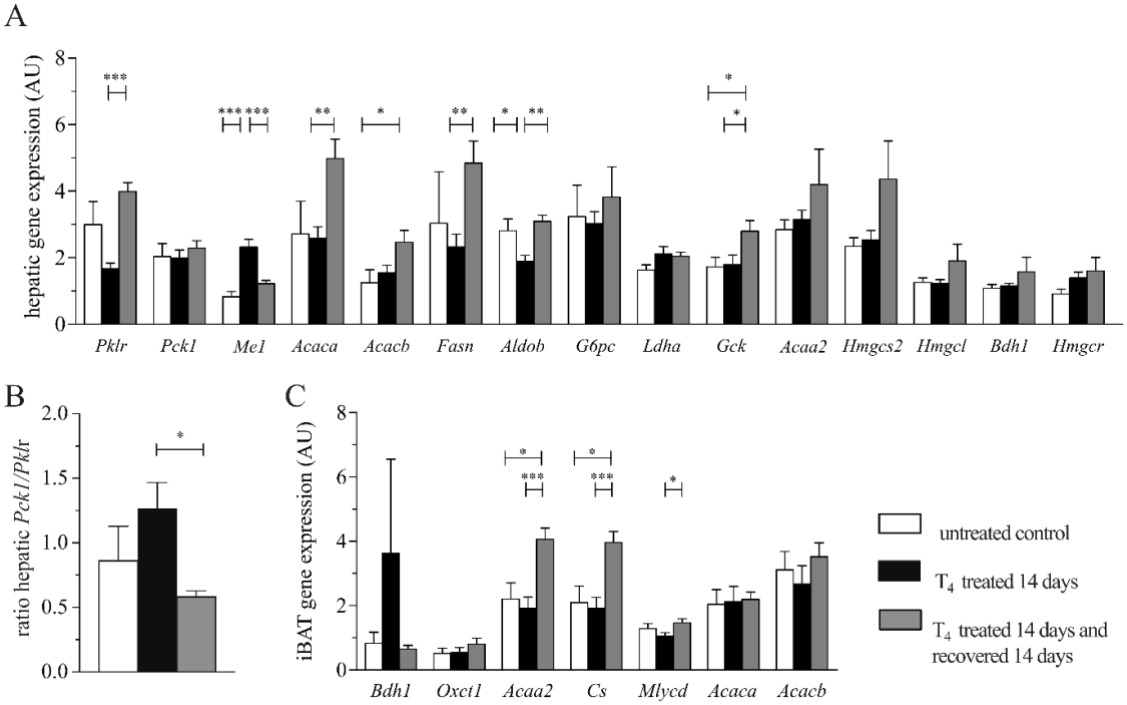

Figure 9: Metabolic switch due to oral T_4 treatment and –recovery in male wt C57BL/6J mice. (A) Relative expression of genes involved in glycolysis, gluconeogenesis and ketogenesis in the liver. (B) Evaluation of the hepatic metabolic state by determining the *Pck1/Pklr* ratio in all three groups. (C) Relative expression of genes involved in metabolism and ketone body oxidation in iBAT. Relative gene expression was measured by qPCR and normalised against *Hprt* in control (white), T_4 treated (black) and T_4 recovery (grey) animals (n = 8 per group). All values are mean ± S.E.M. and statistic testing was performed using an unpaired two-tailed student's t test with *$p < 0.05$, **$p < 0.01$ or ***$p < 0.001$. AU, arbitrary units; *Acaa2*, *acetyl-CoA acetyltransferase 2*; *Acaca*, *acetyl-CoA carboxylase 1*; *Acacb*, *acetyl-CoA carboxylase 2*; *Aldob*, *aldolase b*; *Bdh1*, *3-hydroxybutyrate dehydrogenase type 1*; *Cs*, *citrate synthase*; *Fasn*, *fatty acid synthase*; *G6pc*, *glucose-6-phosphatase*; *Gck*, *glucokinase*; *Hmgcl*, *3-hydroxymethyl-3-methylglutaryl-CoA lyase*; *Hmgcr*, *3-hydroxy-3-methylglutaryl-CoA reductase*; *Hmgcs2*, *3-hydroxy-3-methylglutaryl-CoA synthase 2*; *Hprt*, *hypoxanthine guanine phosphoribosyl transferase*; iBAT, interscapular brown adipose tissue; *Ldha*, *lactate dehydrogenase*; *Mlycd*, *malonyl-CoA decarboxylase*; *Me1*, *malic enzyme 1*; *Oxct1*, *3-oxoacid CoA transferase*; *Pck1*, *phosphoenolpyruvate carboxykinase*; *Pklr*, *pyruvate kinase*; T_4, thyroxine (modified from (Hoefig et al., 2016a)).

ketogenesis including *acetyl-CoA acyltransferase 2* (*Acaa2*), *3-hydroxy-3-methylglutaryl-CoA synthase 2* (*Hmgcs2*), *3-hydroxy-3-methylglutaryl-CoA lyase* (*Hmgcl*), *3-hydroxybutyrate dehydrogenase type 1* (*Bdh1*) and *3-hydroxy-3-methylglutaryl-CoA reductase* (*Hmgcr*) showed no alteration during T_4 treatment or after recovery (Figure 9A). Likewise, there was no alteration in relative mRNA expression of genes necessary for ketone body degradation in iBAT between control and thyrotoxicosis (Figure 9C). Nevertheless, *Acaa2*, *citrate synthase* (*Cs*) and *malonyl-CoA decarboxylase* (*Mlycd*) displayed significant increases in mRNA expression after T_4 recovery (Figure 9C), indicating a somewhat elevated metabolic activity of the tissue.

3.1.2. The Role of iBAT in Thermoregulatory Response to a Transient Thyrotoxicosis and Subsequent Recovery

To evaluate the thermoregulatory consequences of a transient thyrotoxicosis, 24 h radio telemetry profile of body temperature before treatment (day 0), after two weeks T_4 treatment (day 14) and after T_4 recovery (day 28; n = 7) were recorded and analysed (Figure 10A). A significant increase in mean daily body temperature in the light and dark phase due to T_4 treatment was revealed, which normalised after T_4 recovery (Figure 10B). Independent measurements of rectal temperature under anaesthesia in all three treatment groups (n = 8) were in accordance with these findings (Figure 10C). A detailed analysis of iBAT, the primary thermogenic tissue in mice, indicated no changes in thermogenesis upon T_4 treatment, accessed by infrared thermography images (Figure 11 and Figure 12, middle column). Furthermore, relative mRNA expression of *uncoupling protein 1* (*Ucp1*), *cell death-inducing DNA fragmentation factor alpha subunit-like effector A* (*Cidea*) and *fibroblast growth factor 21* (*Fgf21*) was decreased (Figure 10D) and mUCP1 protein level (Figure 10E) as well as phosphorylation of murine thymoma viral proto-oncogene 1 (mAKT1, Figure 10F; unpaired two-tailed student's t test: $p = 0.054$) remained unchanged during T_4 treatment. After T_4 recovery iBAT temperature was significantly reduced (Figure 12, middle column) and mRNA expression of *Ucp1* and *Fgf21* normalised, whereas *Cidea* even exceeded the initial transcript level (Figure 10D). This is most likely owed to the normalisation of the body temperature (Figure 10A). To test whether the increase in core body temperature is caused by a reduced heat loss, surface temperature of the tail base, which provides information about vasoconstriction or vasodilation of the tail vein, was analysed but showed no changes (Figure 12, right column). Analysis of mRNA gene expression in epididymal white adipose tissue (eWAT) showed a strong increase in *Ucp1* mRNA expression and modest increase of *Cidea* and *tumor necrosis factor receptor superfamily member 9* (*Tnfrsf9*) (Figure 10G), all known as markers for browning (Obregon, 2014). However, on protein level no mUCP1 was detectable in eWAT using western blot analysis.

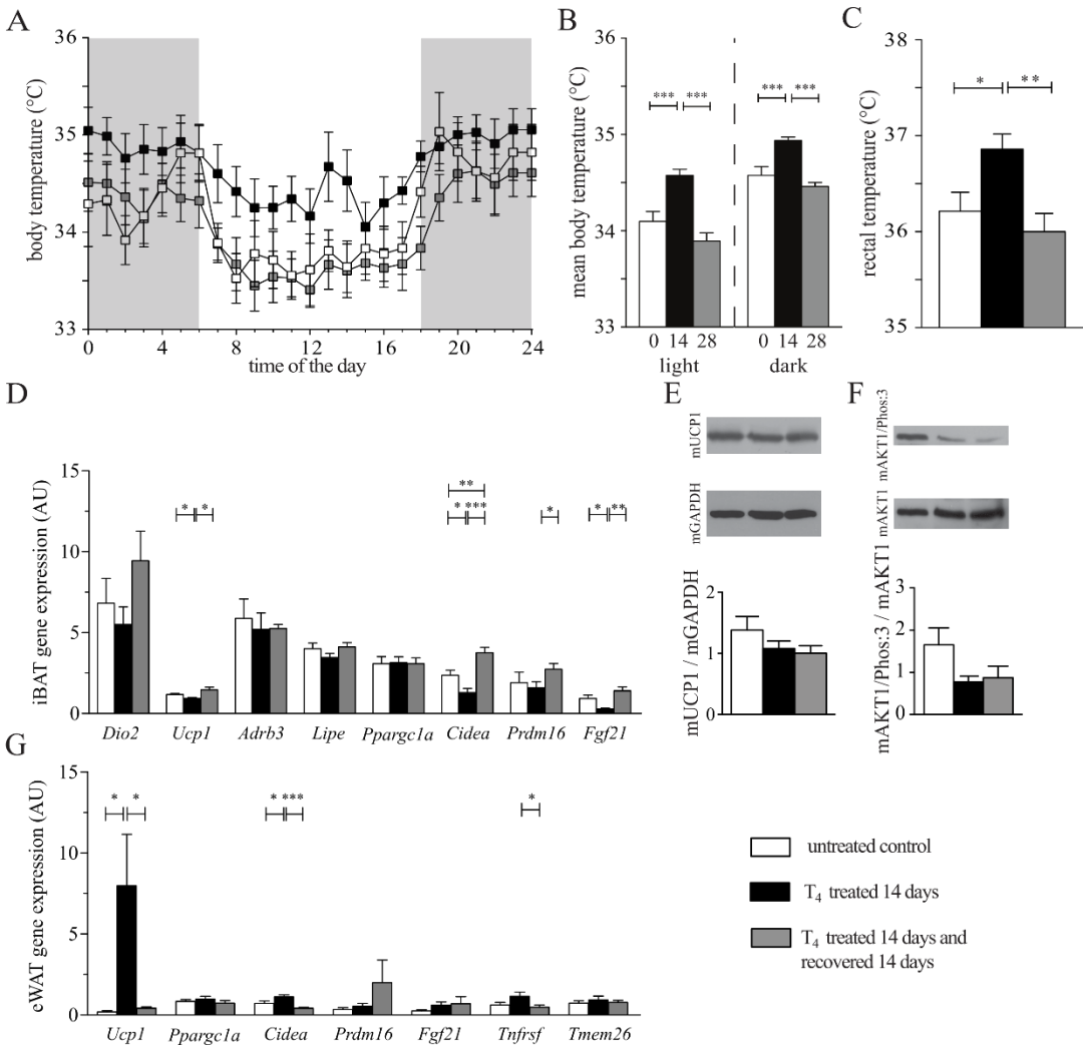

Figure 10: No elevated iBAT activity during oral T_4 treatment in male wt C57BL/6J mice. (A) 24 h profile of body temperature under control (day 0, white), thyrotoxicosis (day 14, black) and T_4 recovery (day 28, grey, n = 7), by radio telemetry. (B) Mean body temperature at each time point and for light and dark phase. (C) Rectal temperature under anaesthesia for control (white), T_4 treated (black) and T_4 recovery (grey) animals (n = 8 per group). (D) Relative mRNA expression of thermoregulatory genes in iBAT. Quantification of (E) mUCP1 protein level normalised to mGAPDH and (F) mAKT1/Phos:3 to AKT1 protein ratio in iBAT by western blot analysis in the three groups (n = 5 – 6). (G) Relative mRNA expression of thermoregulatory genes in eWAT. Relative gene expression (D, G) was measured by qPCR and normalised against *Hprt* for the three groups (n = 8 per group). All values are mean ± S.E.M. and statistical testing was performed using a paired two-tailed student's t test (B) or an unpaired two-tailed student's t test (C, D, E, F, G) with *p < 0.05, **p < 0.01 or ***p < 0.001. *Adrb3*, *adrenergic receptor beta 3*; mAKT1, murin thymoma viral proto-oncogene 1; mAKT1/Phos:3, murine phospho-AKT1 (Ser473); AU, arbitrary units; *Cidea*, *cell death-inducing DNA fragmentation factor alpha subunit-like effector A*; *Dio2*, *deiodinase iodothyronine type II*; eWAT, epididymal white adipose tissue; *Fgf21*, *fibroblast growth factor 21*; mGAPDH, glyceraldehyde-3-phosphate dehydrogenase; *Hprt*, *hypoxanthine guanine phosphoribosyl transferase*; iBAT, interscapular brown adipose tissue; *Lipe*, *lipase hormone sensitive*; *Ppargc1a*, *peroxisome proliferative activated receptor gamma coactivator 1 alpha*; *Prdm16*, *PR domain containing 16*; T_4, thyroxine; *Tmem26*, *transmembrane protein 26*; *Ucp1*, *uncoupling protein 1 Tnfrsf9*, *tumor necrosis factor receptor superfamily member 9*; (modified from (Hoefig et al., 2016a)).

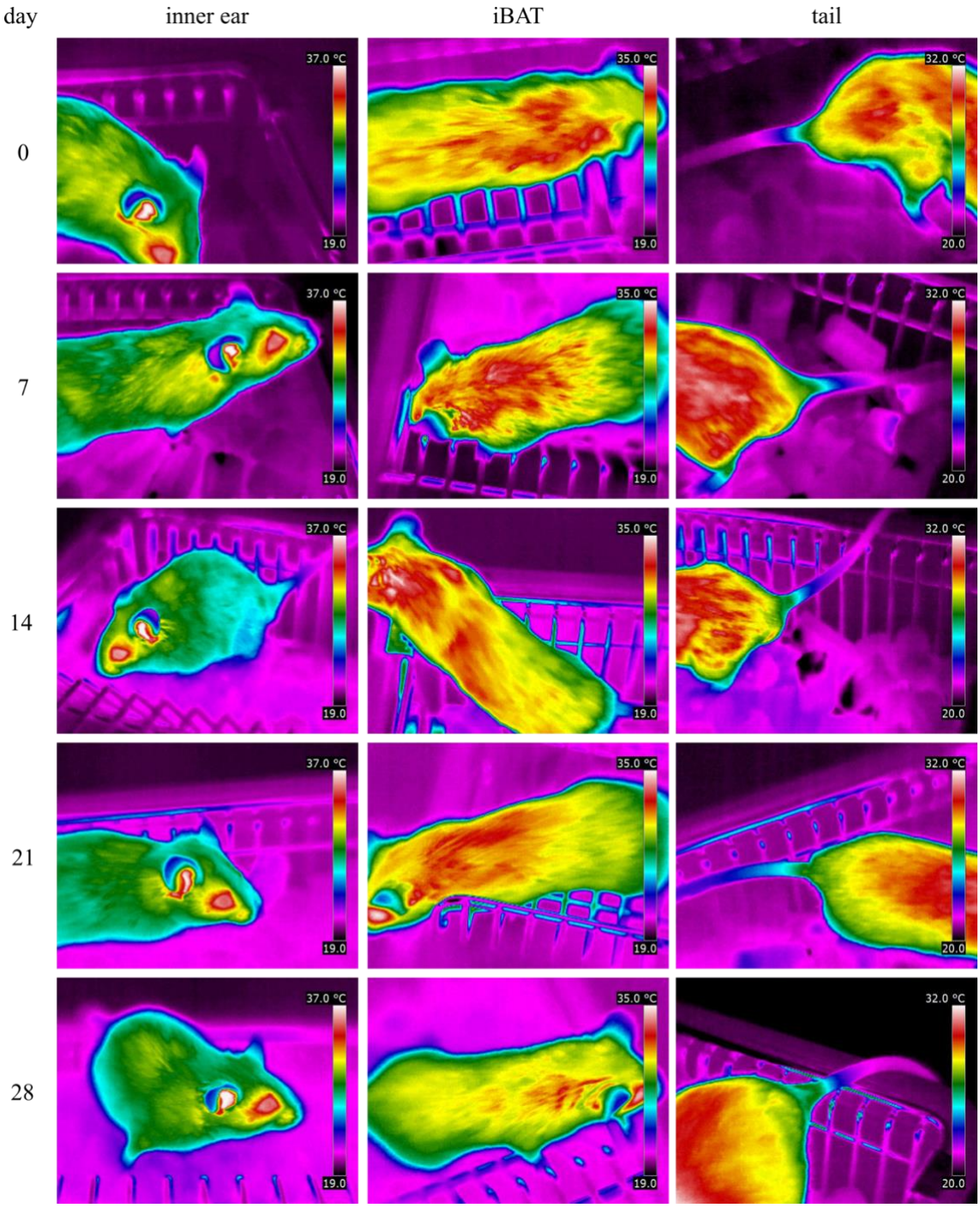

Figure 11: Evaluation of surface temperature changes by infrared thermography in a transient model of thyrotoxicosis using male wt C57BL/6J mice. Representative images of the inner ear (left column), the iBAT (middle column) and the tail base (right column) on day 0 (control), 7 and 14 (T_4 treatment), 21 and 28 (T_4 recovery) of the thyrotoxicosis treatment regime. iBAT, interscapular brown adipose tissue (modified from (Hoefig et al., 2016a)).

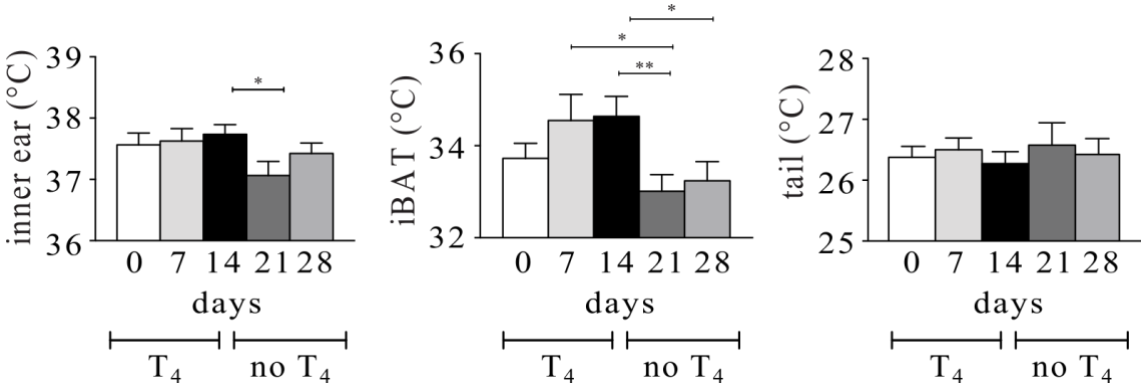

Figure 12: Quantification of surface temperature changes of inner ear (left), iBAT (middle) and tail base (right) temperature on day 0 (control), 7 and 14 (T_4 treatment), 21 and 28 (T_4 recovery) of the thyrotoxicosis treatment regime. All values are mean ± S.E.M. and statistical testing was performed using a paired two-tailed student's t test with *p < 0.05, **p < 0.01 or ***p < 0.001. iBAT, interscapular brown adipose tissue; T_4 thyroxine (modified from (Hoefig et al., 2016a)).

3.1.3. Tachycardia as Response to Oral T_4 Treatment Followed by Surprising Bradycardia after the Subsequent Recovery

The effects on cardiovascular function by a transient thyrotoxicosis were assessed by implantable radio transmitter measurements of the heart rate (Figure 13A). The mean heart rate increased after T_4 treatment (day 14) compared to baseline (day 0) in the light phase as well as the dark phase (Figure 13B).

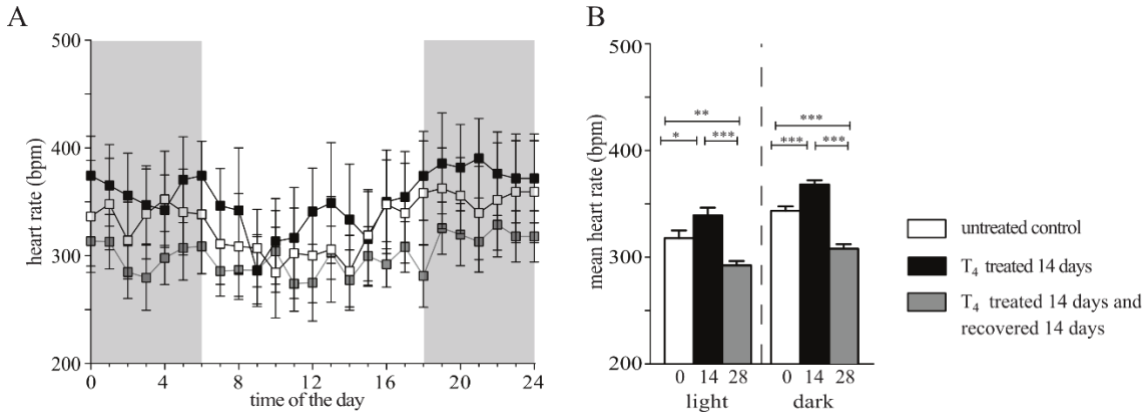

Figure 13: Tachycardia followed by strong bradycardia due to T_4 treatment and –recovery in male wt C57BL/6J mice. (A) 24 h profile of heart rate under control conditions (day 0, white), after 14 days of oral T_4 treatment (day 14, black) and after 14 subsequent days of T_4 recovery (day 28, grey, n = 7), measured by radio telemetry. (B) Analysis of mean heart rate for each time point during the light and the dark phase of the day. All values are mean ± S.E.M. and statistical testing was performed using a paired two-tailed student's t test with *p < 0.05, **p < 0.01 or ***p < 0.001; bpm, beats per minute; T_4, thyroxine (modified from (Hoefig et al., 2016a)).

Comparing the heart weight of all three groups, T_4 treated animals displayed an increase (Figure 14B), which was still true after normalisation to body weight (Figure 14C). Concurringly, the mRNA expression of the cardiac hypertrophy marker *natriuretic peptide type b* (*Nppb*) was increased due to T_4 treatment (Figure 14D). Further analysis of mRNA expression displayed no alteration of genes involved in blood pressure regulation between control and T_4 treated animals, except for a small decrease of *angiotensinogen* (*Agt;* Figure 14A), and a clear elevation of *adrenergic receptor beta 2* (*Adrb2*) and *hyperpolarization-activated cyclic nucleotide-gated K+ 2* (*Hcn2*), genes involved in heartbeat regulation and contractility (Figure 14D). Otherwise *phospholamban* (*Pln*) mRNA expression, regulating the cardiac Ca^{2+} pump, was reduced (Figure 14D) and adrenal genes involved in catecholamine synthesis remained unchanged with the exception of suppressed *tyrosine hydroxylase* (*Th*) and a tendancy of suppressed *dopamine beta hydroxylase* (*Dbh*; unpaired two-tailed student's t test: $p = 0.09$; Figure 14E) by high T_3 and T_4 levels.

Surprisingly, T_4 recovery elicited a strong bradycardia with a mean heart rate even below the initial measurements in the light and in the dark phase (Figure 13B). Furthermore, blood pressure regulating genes such as *angiotensin I converting enzyme* (*Ace1*), *cytochrome P450 family 11 subfamily b polypeptide 1* and *2* (*Cyp11b1* and *2*) were significantly increased compared to control as well as T_4 treated animals (Figure 14A), presumably constituting a compensation to keep blood pressure stable. Relative mRNA expression of cardiac genes disclosed continuously high levels of *Adrb2* and *Hcn2*. *Pln* and *ATPase Ca^{2+} transporting cardiac muscle slow twitch 2* (*Atp2a2*) even increased significantly, indicative of an altered reuptake of Ca^{2+} into the cardiac sarcoplasmic reticulum. Furthermore, *myosin heavy polypeptide 6 cardiac muscle alpha* (*Myh6*), *myosin heavy polypeptide 7 cardiac muscle beta* (*Myh7*), *ryanodine receptor 2* (*Ryr2*) and *regulator of G-protein signalling 4* (*Rgs4*) all decreased significantly below baseline (Figure 14D).

The examination of a 24 h activity profile (Figure 15A) and mean activity during light and dark phase demonstrated no activity changes due to T_4 treatment or T_4 recovery (Figure 15B), clarifying that activity patterns did not evoke the observed changes in the heart rate.

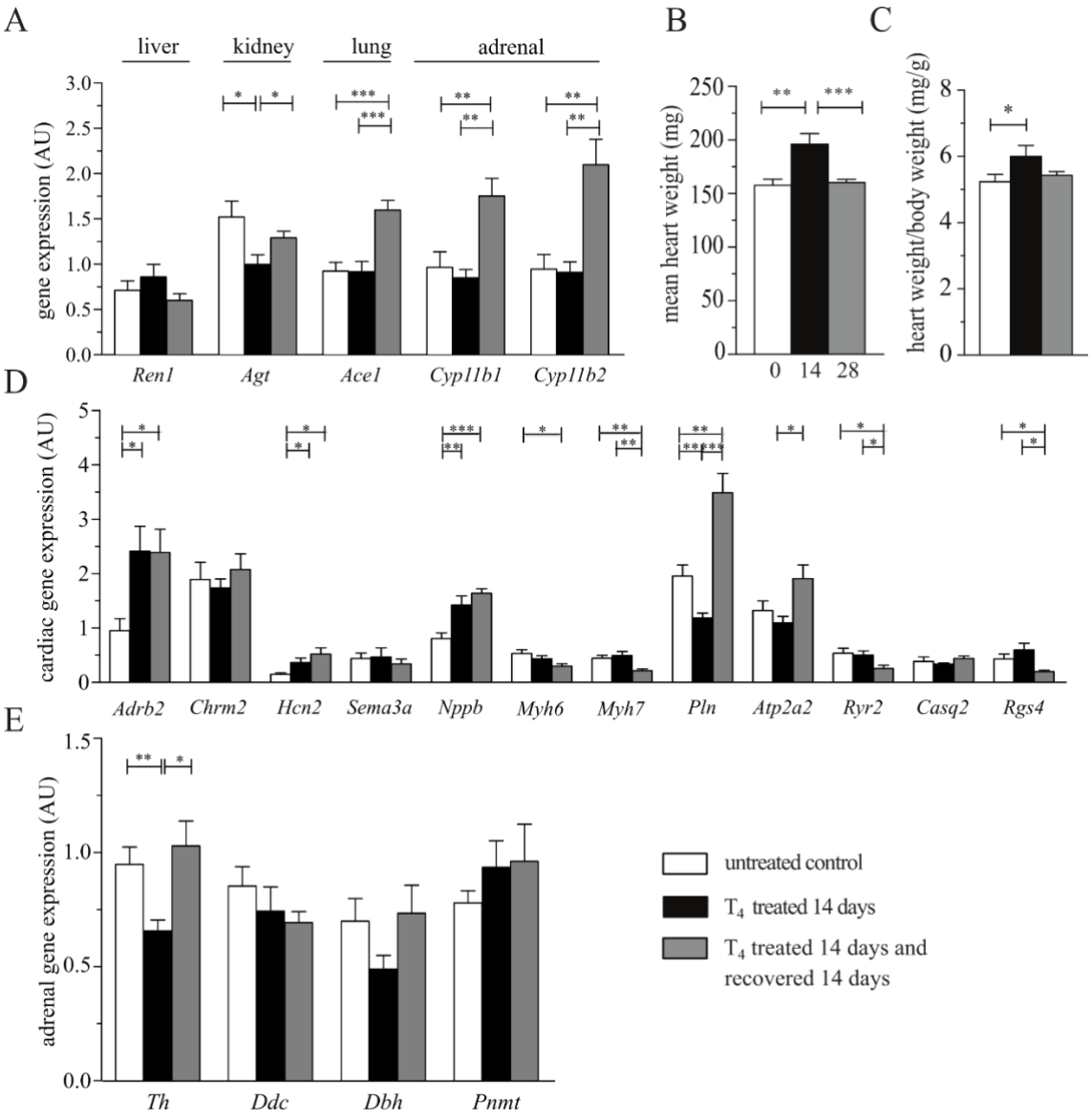

Figure 14: Cardiovascular analysis of male wt C57BL/6J mice under T_4 treatment and –recovery. (A) Relative mRNA expression of genes involved in blood pressure regulation. (B) Heart weight and (C) heart weight normalised to body weight for the three groups. Relative mRNA expression of (D) cardiac and (E) adrenal genes. Relative mRNA expression (A, D, E) was measured by qPCR and normalised against *Hprt* for control (white), T_4 treated (black) and T_4 recovery (grey) animals (n = 8). All values are mean ± S.E.M. and statistical testing was performed using an unpaired two-tailed student's t test with *p < 0.05, **p < 0.01 or ***p < 0.001. *Ace1*, *angiotensin I converting enzyme*; *Adrb2*, *adrenergic receptor beta 2*; *Agt*, *angiotensinogen*; *Atp2a2*, *ATPase C^{2+} transporting cardiac muscle slow twitch 2*; AU, arbitrary units; *Nppb*, *natriuretic peptide type b*; *Casq2*, *calsequestrin 2*; *Chrm2*, *cholinergic receptor muscarinic 2*; *Cyp11b1/2*, *cytochrome P450 family 11 subfamily b polypeptide 1/2*; *Dbh*, *dopamine beta hydroxylase*; *Ddc*, *DOPA decarboxylase*; *Hcn2*, *hyperpolarization-activated cyclic nucleotide-gated K^+ 2*; *Hprt*, *hypoxanthine guanine phosphoribosyl transferase*; *Myh6*, *myosin heavy polypeptide 6 cardiac muscle alpha*; *Myh7*, *myosin heavy polypeptide 7 cardiac muscle beta*; *Pln*, *phospholamban*; *Pnmt*, *phenylethanolamine-N-methyltransferase*; *Ren1*, *renin 1*; *Rgs4*, *regulator of G-protein signalling 4*; *Ryr2*, *ryanodine receptor 2*; *Sema3a*, *semaphoring 3A* , thyroxine; *Th*, *tyrosine hydroxylase* (modified from (Hoefig et al., 2016a)).

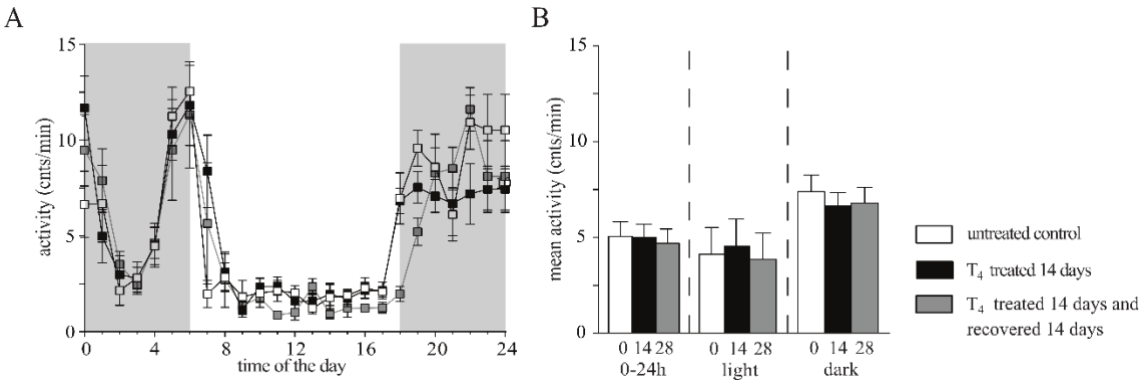

Figure 15: No abnormalities in the activity profiles throughout the experimental thyrotoxicosis treatment regime. (A) 24 h profile of activity under control conditions (day 0, white), after 14 days of oral T_4 treatment (day 14, black) and after 14 subsequent days of T_4 recovery (day 28, grey, n = 7), measured by radio telemetry. (B) Analysis of mean activity for each time point over 24 h as well as divided in the light and the dark phase of the day. All values are mean ± S.E.M. and statistical testing was performed using a paired two-tailed student's t test. cnts, counts; T_4, thyroxine (modified from (Hoefig et al., 2016a)).

3.2. Study 2: Peripheral Effects of TH Downstream Metabolites

In the following part of the thesis the focus shifts from THs to a group of metabolites derived from TH by deiodination and/or decarboxylation, called TAMs. Their most prominent representative, the 3-T_1AM, shows opposite properties compared to THs, namely inducing hypothermia and bradycardia (Scanlan et al., 2004). However, 3-T_1AM is rapidly converted to downstream metabolites *in vivo*, and it remains unknown whether these compounds also contribute to observed effects after 3-T_1AM administration. Therefore, the acute and chronic effects of TA_1, the major degradation product of 3-T_1AM, on metabolism, thermogenesis and cardiovascular function have been investigated in a previous study (Hoefig et al., 2015a). The data revealed no effect of an acute pharmacological dose of TA_1 (50 mg/kg, i.p.) on body temperature, heart rate and activity assessed by radio telemetry measurement. In line with these results, also a chronic TA_1 treatment (5 mg/kg/day) for 7 days failed to affect metabolic parameters, thermoregulation or heart rate, blood pressure and cardiac gene expression in male wt C57BL/6J mice. This suggests, that the degradation of 3-T_1AM by oxidative deamination to TA_1 might be an important inactivation path for 3-T_1AM functions (Hoefig et al., 2015a). Notably, 3-T_1AM is also converted to T_0AM by deiodination (Piehl et al., 2008); thus an analysis of the acute and chronic effects of T_0AM in vivo in male wt C57BL/6J mice was performed (Harder et al., 2018b), using in the same experimental paradigm as in the TA_1 study (Hoefig et al., 2015a).

3.2.1. No Acute Effects of T_0AM Addressed by Radio Telemetry Measurements

To investigate the consequences of a single dose of T_0AM (50 mg/kg, i.p.) in male wt C57BL/6J mice, animals were implanted with radio telemetry transmitters and body temperature, heart rate and activity were determined in conscious and freely moving mice. The body temperature data set displayed no T_0AM effects (Figure 16A; repeated measurement 2-way ANOVA for T_0AM effect; $p = 0.3225$; Figure 16B, paired, nonparametric, two-tailed Wilcoxon t test; $p = 0.195$). Likewise, the analysis of the heart rate change revealed no significant differences between sham and T_0AM treatment neither during the first three hours after injection (Figure 16C), nor for the mean change of heart rate during the first 60 min (Figure 16D; paired, nonparametric, two-tailed Wilcoxon t test; $p = 0.844$). In addition, there was no alteration in locomotor activity during the first three hours after injection (Figure 16E) and for the AUC during the first 60 min (Figure 16F; paired, nonparametric, two-tailed Wilcoxon t test; $p = 0.9453$).

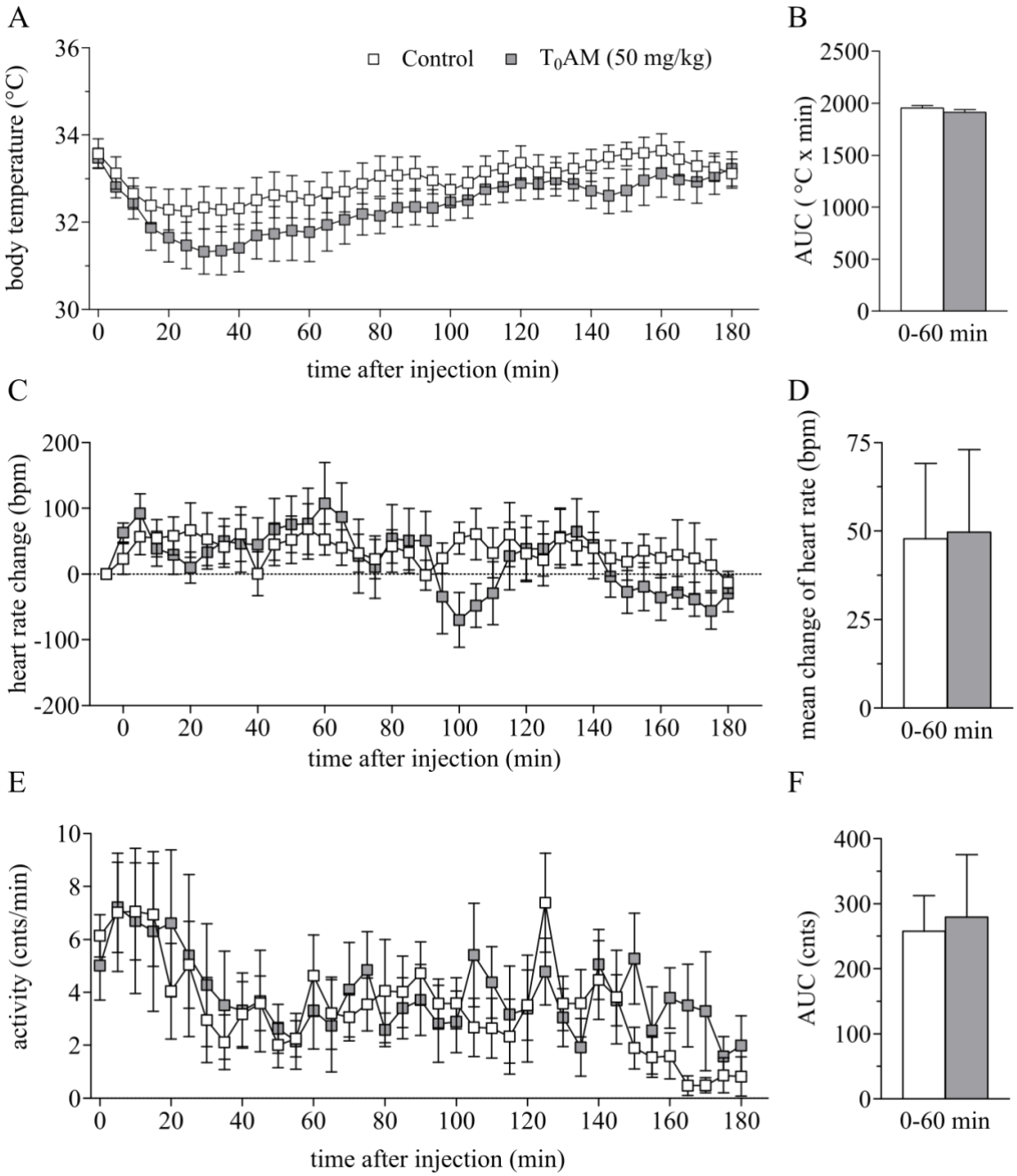

Figure 16: Acute treatment with 50 mg/kg T_0AM had no effect on temperature, heart rate or activity in male wt C57BL/6J mice. Three hours radio telemetry profile of (A) body temperature (p = 0.3225 for T_0AM effect), (C) heart rate change (normalised to 30 min baseline measurement prior to the injection) and (E) locomotor activity in control (white) and T_0AM treated (grey, 50 mg/kg, i.p.) animals (n = 8 - 9). (B) Calculated mean AUC of body temperature (p = 0.195) over 60 min post injection. (D) Calculated mean change of heart rate over 60 min post injection in both groups (p = 0.844). (F) Calculated mean AUC of locomotor activity (p = 0.9453) in the control (white) and the T_0AM (grey) treatment group. All values are mean ± S.E.M. and statistical testing was performed using a repeated measurement 2-way ANOVA (A) or a paired, nonparametric, two-tailed Wilcoxon t test (B, D, F). AUC, area under the curve; bpm, beats per minute; cnts, counts; T_0AM, thyronamine (modified from (Harder et al., 2018b)).

3.2.2. No Metabolic, Thermoregulatory or Cardiovascular Effects of a Chronic Treatment with T_0AM

To analyse the effects of a chronic treatment with T_0AM in male wt C57BL/6J mice, animals were injected for seven consecutive days with T_0AM (5 mg/kg) and compared with a sham injected (60 % DMSO/40 % 1x PBS) control group. No significant changes in body weight (control: 28.5 ± 0.99 g vs. T_0AM: 27.83 ± 0.89 g), mean daily food (control: 4.45 ± 0.18 g vs. T_0AM: 4.20 ± 0.10 g) and water intake (control: 7.58 ± 0.42 mL vs. T_0AM: 7.35 ± 0.35 mL) were observed between the groups after 7 days of treatment (Harder et al., 2018b). To monitor changes in the peripheral TH metabolism, serum total T_3 (control: 0.99 ± 0.03 ng/mL vs. T_0AM: 0.99 ± 0.04 ng/mL) and total T_4 concentrations (control: 4.43 ± 0.16 µg/dL vs. T_0AM: 4.32 ± 0.29 µg/dL) were determined 24 h after the last injection, revealing no changes upon treatment (Harder et al., 2018b). This was also true for the hepatic concentration of total T_3 (control: 8.32 ± 0.65 pmol/mg vs. T_0AM: 7.13 ± 0.85 pmol/mg) and total T_4 (control: 52.92 ± 10.94 pmol/mg vs. 59.59 ± 14.29 pmol/mg), assessed by LC-MS/MS measurements (in collaboration with Carolin S. Hoefig, Charité Berlin; (Harder et al., 2018b)).

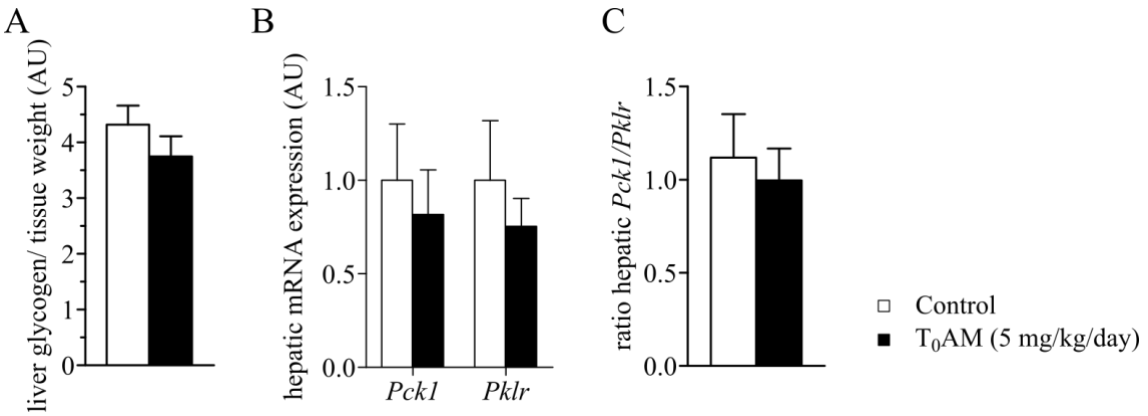

Figure 17: Chronic T_0AM treatment (5 mg/kg/day for seven days) did not change hepatic metabolism. Hepatic (A) glycogen in control (white) and T_0AM treated animals (black, n = 6 per group) and (B) relative mRNA expression of *Pck1* and *Pklr* measured by qPCR and normalised against a set of unregulated housekeeping genes (*Rps18*, *Actb*, *Hprt*) in control (white, n = 6) and T_0AM treated animals (black, n = 5). (C) Evaluation of the hepatic metabolic state assessed by the ratio of *Pck1* and *Pklr* gene expression. All values are mean ± S.E.M. and statistical testing was performed using an unpaired, nonparametric, two-tailed Mann-Whitney t test (A, C) or a multiple t test controlled with the Sidak-Bonferroni correction for multiple comparisons (B). *Actb*, *actin beta*; AU, arbitrary units; *Hprt*, *Hypoxanthine guanine phosphoribosyl transferase*; *Pck1*, *phosphoenolpyruvate carboxykinase*; *Pklr*, *pyruvate kinase* (modified from (Harder et al., 2018b)).

Taking together these findings indicate that both groups are euthyroid. Likewise, hepatic glycogen (Figure 17A) as well as relative mRNA expression of hepatic *Pklr* and *Pck1* remained constant between control and T_0AM-treated animals (Figure 17B).

To address the glucose utilization of the liver, the ratio between *Pck1*, the rate-limiting enzyme for gluconeogenesis, and *Pklr*, the rate-limiting enzyme for glycolysis, was calculated; however, no differences were detected between the two groups (Figure 17C).

Nevertheless, the T_0AM treatment was methodologically successful as demonstrated by the high amount of hepatic T_0AM (19.29 ± 9.66 pmol/mg) detectable by LC-MS/MS measurements, 24 h after the last injection, whereas endogenous T_0AM was too low to be detected in the control group (in collaboration with Carolin S. Hoefig, Charité Berlin; (Harder et al., 2018b)).

To confirm that thermoregulatory functions were also unaffected by chronic T_0AM treatment, infrared pictures of the inner ear (Figure 18A), the iBAT (Figure 18B) and the tail base (Figure 18C) were taken and quantified, demonstrating similar temperatures in both groups (Figure 18D - F). This was also true for the rectal temperature measurement on the last day of experiment (Figure 18G). Additionally, relative mRNA expression of genes important for thermoregulation in iBAT were checked but were unaltered as well (Figure 18H).

Next, cardiovascular effects of chronic T_0AM administration were addressed by determining relative mRNA expression of several genes involved in the regulation of cardiovascular function and the renin-angiotensin system. Only pulmonary *Ace1* was significantly regulated between control and T_0AM-treated animals (unpaired, nonparametric, two-tailed Mann-Whitney t test; $p = 0.0173$), all other genes were unaltered (Figure 19A). However, the increased relative mRNA level of pulmonary *Ace1* did not result in altered cardiac output, given that no difference in pulse rate (Figure 19B) or systolic, diastolic and mean arterial blood pressure (Figure 19C) were detected.

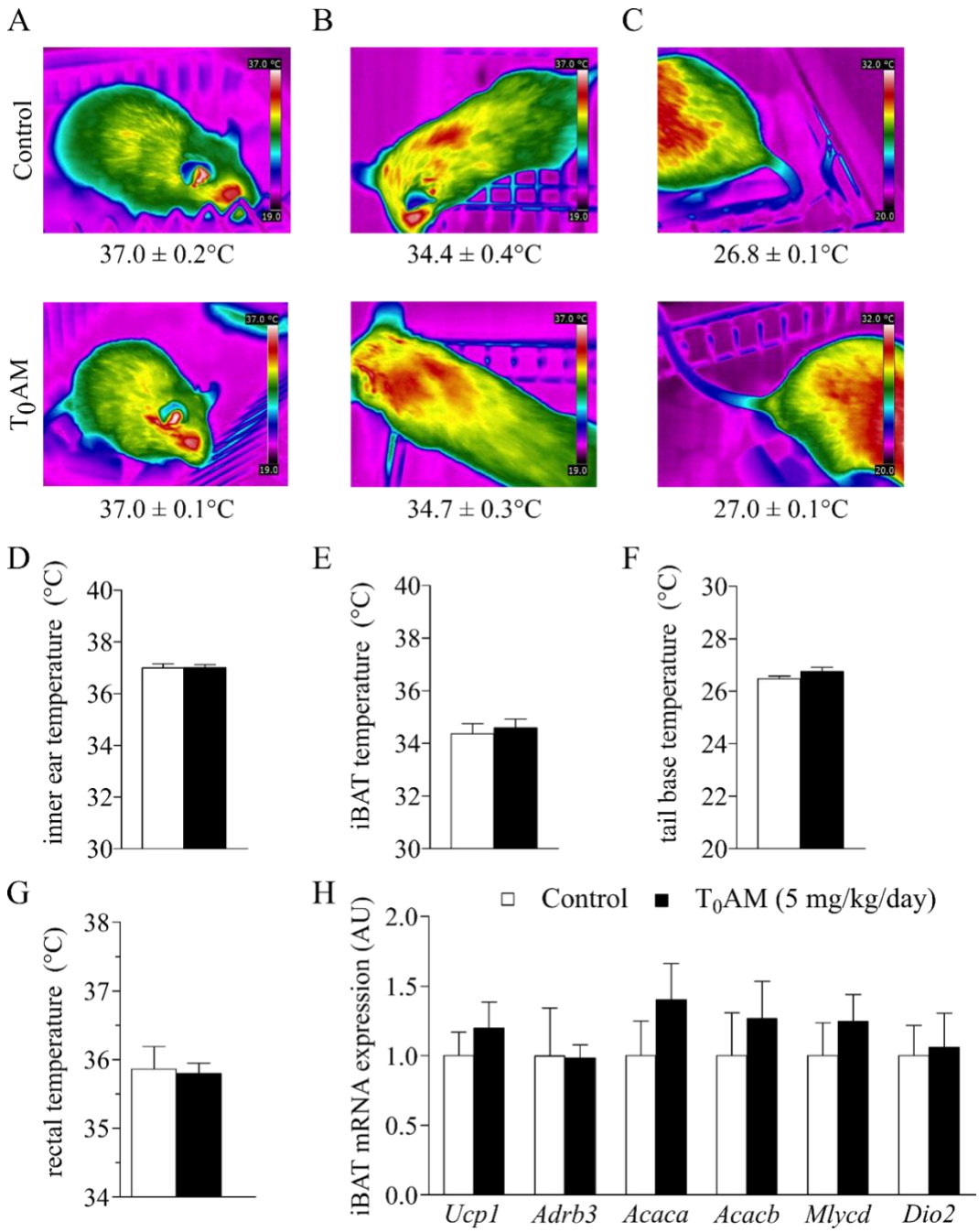

Figure 18: Chronic T_0AM treatment (5 mg/kg, daily for seven days) of wt C57BL/6J male mice had no influence on their thermoregulation. Representative infrared pictures and quantification of (A, D) inner ear, (B, E) iBAT and (C, F) tail base of control (white) and T_0AM treated mice (black, n = 6 per group). (G) Rectal temperature, 24 h after the last injection (n = 6 per group, under anaesthesia). (H) mRNA expression of thermoregulatory genes in iBAT, assessed by qPCR normalised against a set of unregulated housekeeper genes (*Actb*, *Hprt*, *Ppia*) in both groups (n = 6 per group). All values are mean ± S.E.M. and statistical testing was performed using an unpaired, nonparametric, two-tailed Mann-Whitney t test (D - G), or a multiple t test controlled with the Sidak-Bonferroni correction for multiple comparisons (H). *Acaca*, *acetyl-CoA carboxylase 1*; *Acacb*, *acetyl-CoA carboxylase 2*; *Actb*, *actin beta*; *Adrb3*, *adrenergic receptor beta 3*; *Dio2*, *iodothyronine deiodinase type II*; *Hprt*, *hypoxanthine guanine phosphoribosyl transferase*; iBAT, interscapular brown adipose tissue; *Mlycd*, *malonyl-CoA decarboxylase*; *Ppia*, *peptidylprolyl isomerase a*; T_0AM, thyronamine; *Ucp1*, *uncoupling protein 1* (modified from (Harder et al., 2018b)).

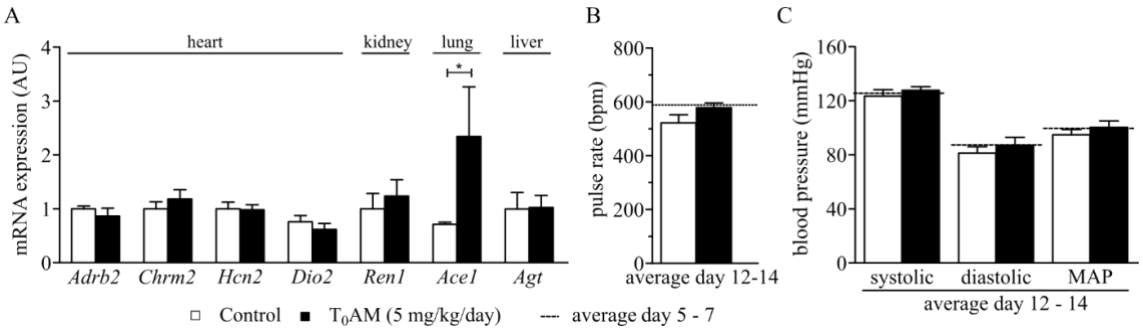

Figure 19: Increases in relative mRNA expression of pulmonary angiotensin 1 converting enzyme due to chronic T_0AM treatment (5 mg/kg/day for seven days) did not result in altered cardiac output. (A) Analysis of mRNA expression of genes involved in cardiovascular function and the renin-angiotensin system using qPCR normalised to a set of unregulated housekeeping genes (heart: *Rps18*, *Actb*, *Hprt*; kidney: *Hprt*; lung: *Rps18*, *Actb*, *Hprt*, *Ppia*; liver: *Rps18*, *Actb*, *Ppia*) comparing control (white, = 5 - 6) and T_0AM treated (black, n = 5 - 6) mice. (B) Pulse rate and (C) systolic, diastolic and mean arterial blood pressure of both groups (dashed lines indicate the baseline measurements before treatment). All values are mean ± S.E.M. and statistical testing was performed using an unpaired, nonparametric, two-tailed Mann-Whitney t test (A (lung *Ace1*; p = 0.0173), B, C) or a multiple t test controlled with the Sidak-Bonferroni correction for multiple comparisons for each tissue (A). *Ace1*, *angiotensin I converting enzyme*; *Actb*, *actin beta*; *Adrb2*, *adrenergic receptor beta 2*; *Agt*, *angiotensinogen*; bpm, beats per minute; *Chrm2*, *cholinergic receptor muscarinic 2*; *Dio2*, *iodothyronine deiodinase type II*; *Hcn2*, *hyperpolarization-activated cyclic nucleotide-gated K+ 2*; *Hprt*, *hypoxanthine guanine phosphoribosyl transferase*; MAP, mean arterial blood pressure; *Ppia*, *peptidylprolyl isomerase a* (modified from (Harder et al., 2018b)).

3.3. Study 3: Central Effects of TH on PV Neurones in the AHA of Male Mice

In addition to the classical view of TH and their metabolites, which concentrates on the direct action in target tissues, the central control of peripheral tissues by TH via the brain has moved into focus recently (Lopez et al., 2013; Mittag et al., 2013). In this regard, not only the influence of acute TH signalling on neuronal activity is of interest but also the role of TH signalling for proper neuronal development. The third part of this thesis therefore deals with the characterization of a recently described population of PV expressing neurones in the AHA of mice (Mittag et al., 2013).

3.3.1. Basic Characteristics of PV Neurones in the AHA

PV neurones in the AHA of male wt C57BL/6J mice are not detectable on P7 but were all present on P14 (Mittag et al., 2013). To pinpoint the precise date when they appear, brain slices from P8 until P14 were analysed using immunohistochemistry. PV immunoreactivity was first detectable at P8 (Figure 20A), and the population size gradually increased until P13,

at which the number of PV neurones was equivalent to the number of PV neurones found in the AHA of adult wt mice (Figure 20B). In order to determine the neurotransmitter repertoire of PV neurones, immunofluorescent labelling was performed, confirming that PV neurones in the AHA were positive for GAD67 (Figure 21A), the essential enzyme for GABA synthesis. The neurones were also positive for GABA itself (Figure 21B), which was observed in PV neurones in the cortex as well (Figure 21A, B). Both populations of PV neurones did neither express VGLUT2 (Figure 22A) nor tyrosine hydroxylase (Figure 23A), the rate-limiting enzyme for dopamine synthesis. Although PV neurones in the AHA were not VGLUT2 positive, several VGLUT2 positive bouts were detected on the cell surface of them (Figure 22B).

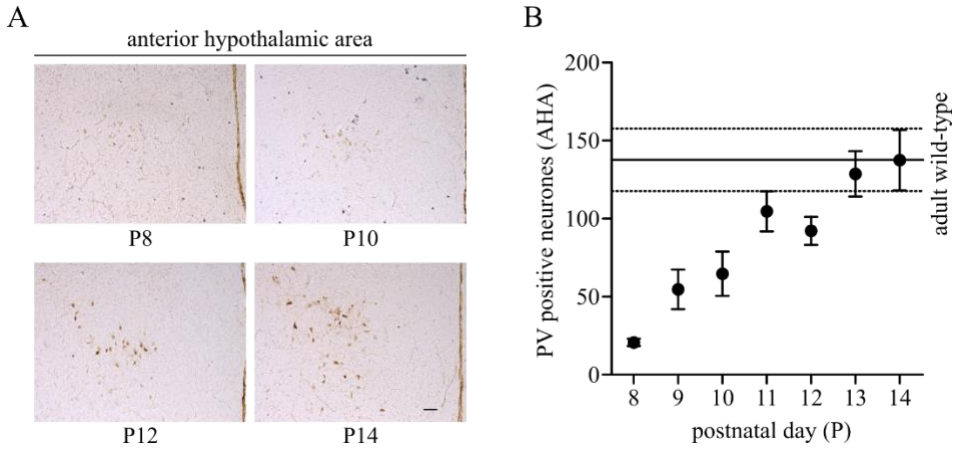

Figure 20: PV neurones arise in the anterior hypothalamic area between P8 and 13. (A) Representative picture of the anterior hypothalamic area on P8, 10, 12 and 14 (Scale bar = 50 µm) in wt C57BL/6J male mice. (B) Quantification of PV neurones in the anterior hypothalamic area between day 8 and 14 of postnatal development (n = 4 per time point), horizontal lines indicate the mean number of PV neurones ± S.E.M. in the anterior hypothalamic area of adult wt C57BL/6J male mice. All values are mean ± S.E.M.; AHA, anterior hypothalamic area; P, postnatal day; PV, parvalbumin (modified from (Harder et al., 2018a)).

PV neurones in the AHA are associated with the control of blood pressure (Mittag et al., 2013), which raised the question whether this neuronal population is also involved in obesity associated hypertension. Recent investigations in mouse models suggested leptin as a possible link between hypertension and obesity, because obesity is connected to high leptin levels (Simonds et al., 2014). Therefore, AHA sections of ObRb.Zsgreen mice (Madisen et al., 2010), which express the fluorescent protein Zsgreen in leptin receptor (ObRb) positive cells, were examined. Immunohistochemistry revealed no expression of ObRb in PV neurones (Figure 24; in collaboration with Jana-Thabea Kiehn and Henrik Oster), indicating no direct regulation of PV neurones via leptin.

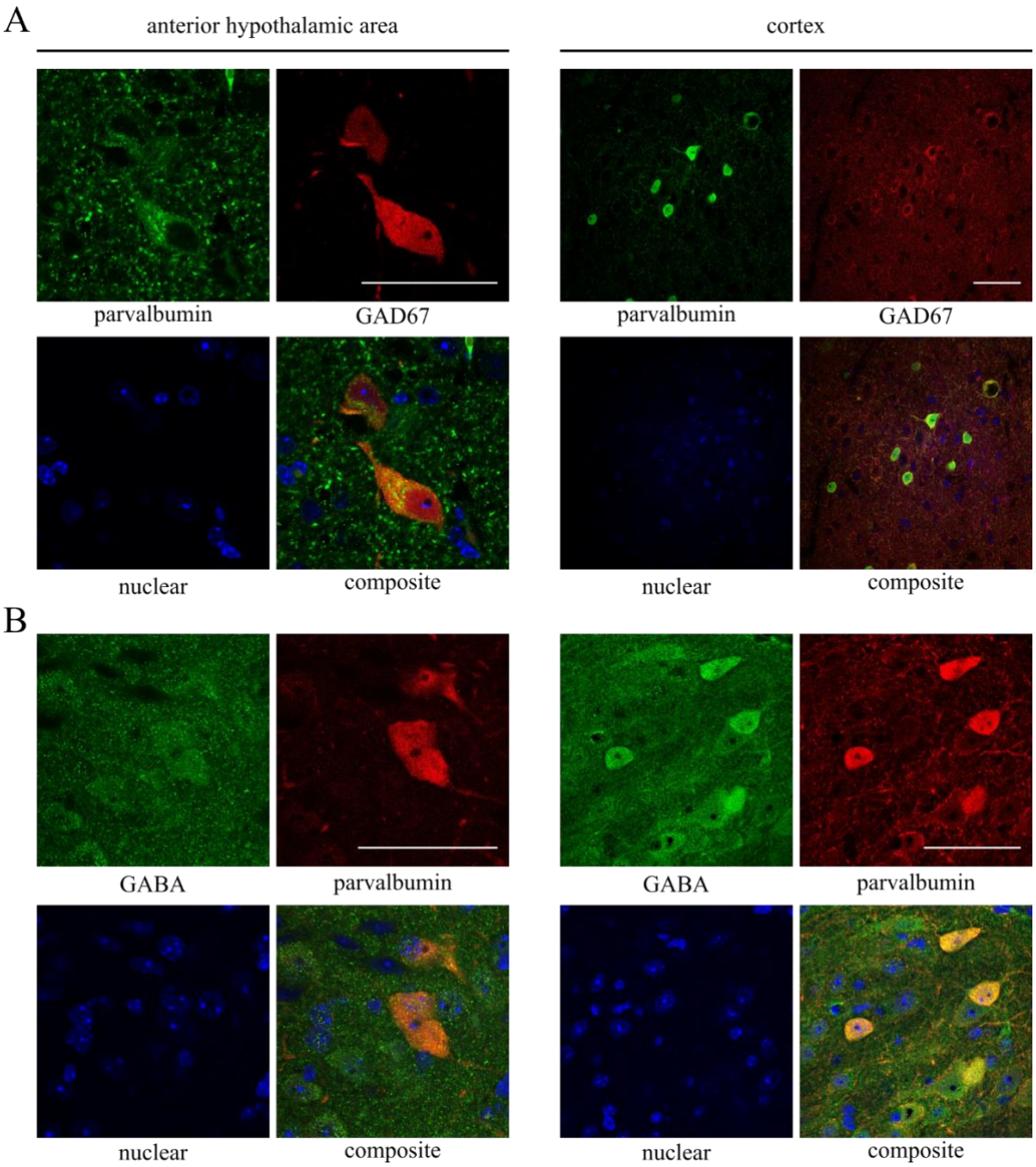

Figure 21: Parvalbumin neurones in the anterior hypothalamic area express the same set of neurotransmitters as cortical parvalbumin neurones. Representative pictures of (A) GAD67 (red) and parvalbumin (green) and (B) GABA (green) and parvalbumin (red) positive neurones in the anterior hypothalamic area (left panels) and the cortex (right panels) of wt C57BL/6J male mice. Scale bars = 50 µm; GABA, gamma-aminobutyric acid; GAD67, glutamate decarboxylase 67 (modified from (Harder et al., 2018a)).

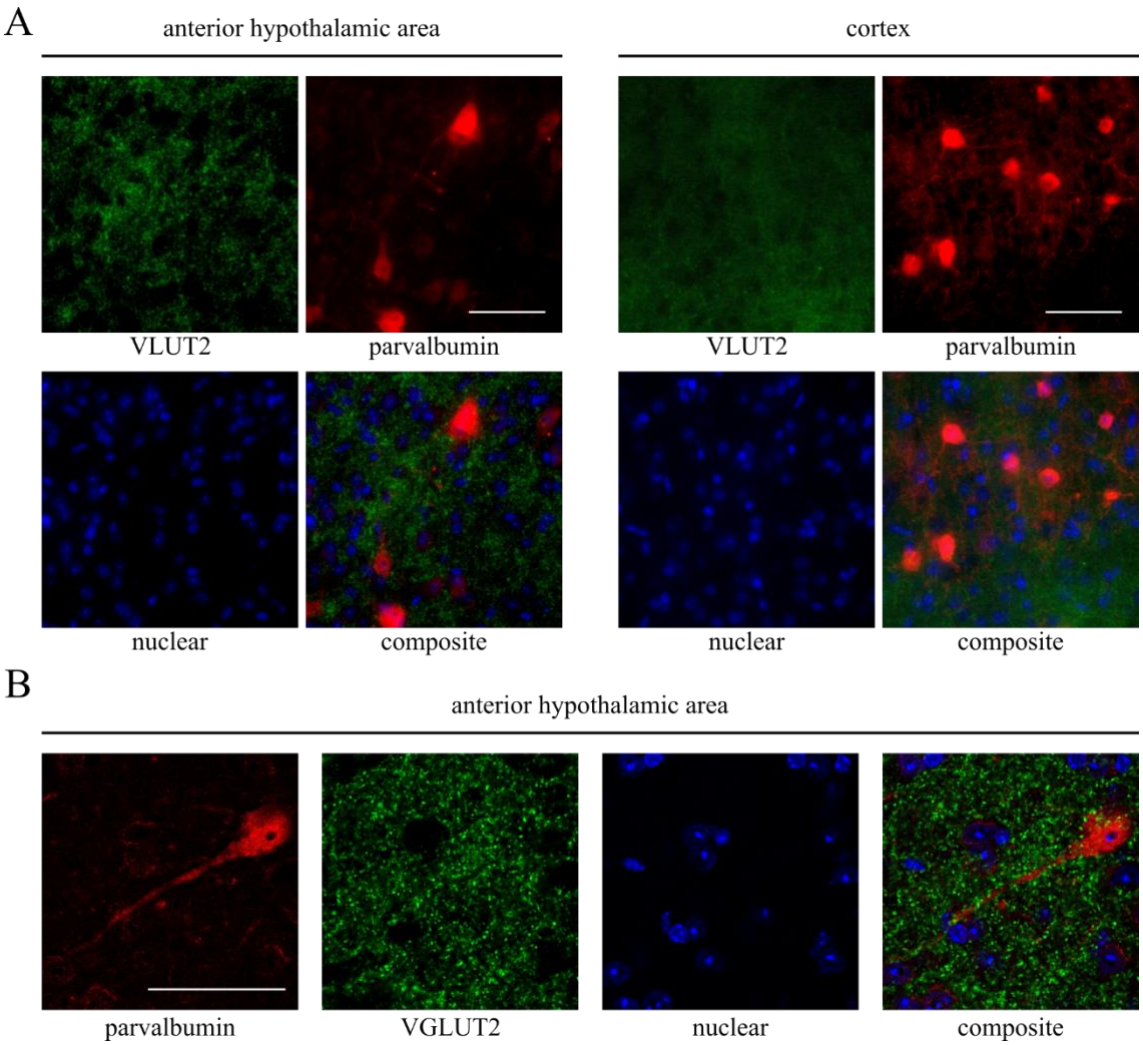

Figure 22: Parvalbumin neurones in the anterior hypothalamic area and the cortex show no expression of the VGLUT2. (A) VGLUT 2 (green) and parvalbumin (red) in the anterior hypothalamic area (left panel) and the cortex (right panel). (B) High magnification of a parvalbumin positive neurone (red) with VGLUT2 positive bouts (green) on its surface, might indicate glutamatergic input. Scale bars = 50 µm; VGLUT2, vesicular glutamate transporter 2 (modified from (Harder et al., 2018a)).

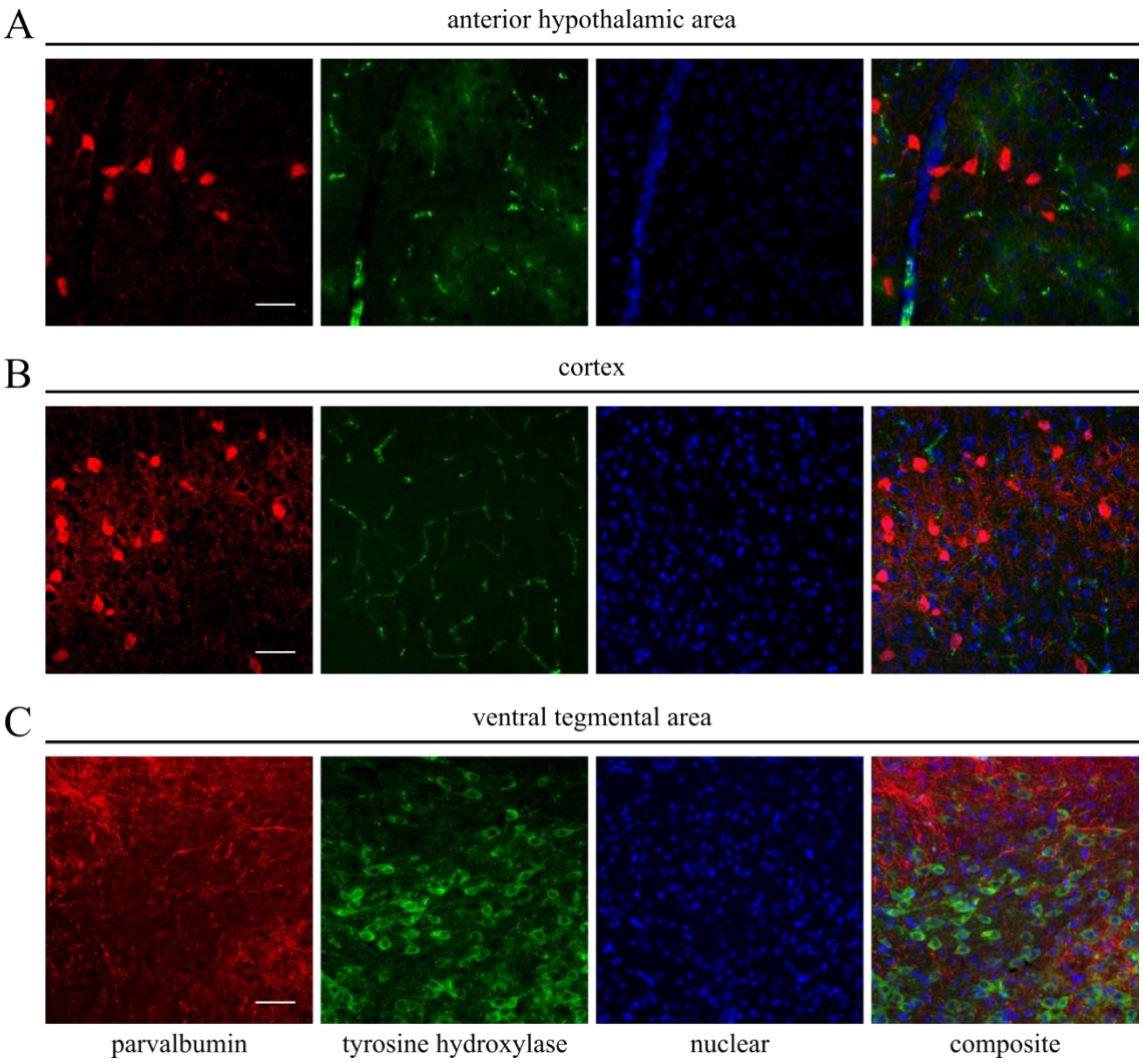

Figure 23: Parvalbumin neurones in the anterior hypothalamic area and the cortex do not express tyrosine hydroxylase. Representative pictures of parvalbumin (red) and tyrosine hydroxylase (green) expressing neurones in (A) the anterior hypothalamic area, (B) the cortex and (C) the ventral tegmental area of wt C57BL/6J male mice. Scale bar = 50 µm.

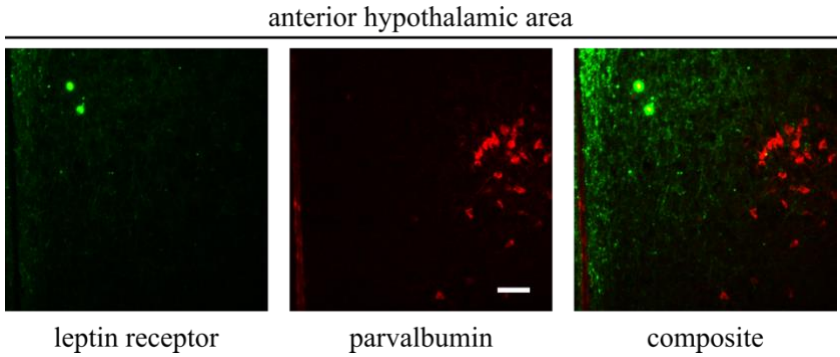

Figure 24: Representative pictures of a co-localization of leptin receptor positive cells (green) and parvalbumin neurones (red, scale bar = 100 µm) in the anterior hypothalamic area of ObRb.Zsgreen mice ((Madisen et al., 2010); in collaboration with Jana-Thabea Kiehn and Henrik Oster).

Specific labelling of PV neurones in the AHA by the stereotaxic administration of a rAAV that mediates cre-depending mCherry expression in *Parv-Cre* mice revealed no long-distance projections to other brain areas, but several short projections in parallel to the coronal sectioning plane, probably forming a network between several PV neurones (Figure 25A, B). In line with this synaptotagmin 2 (SYT2) positive bouts were found on the cell surface of PV neurones (Figure 25C) in the AHA.

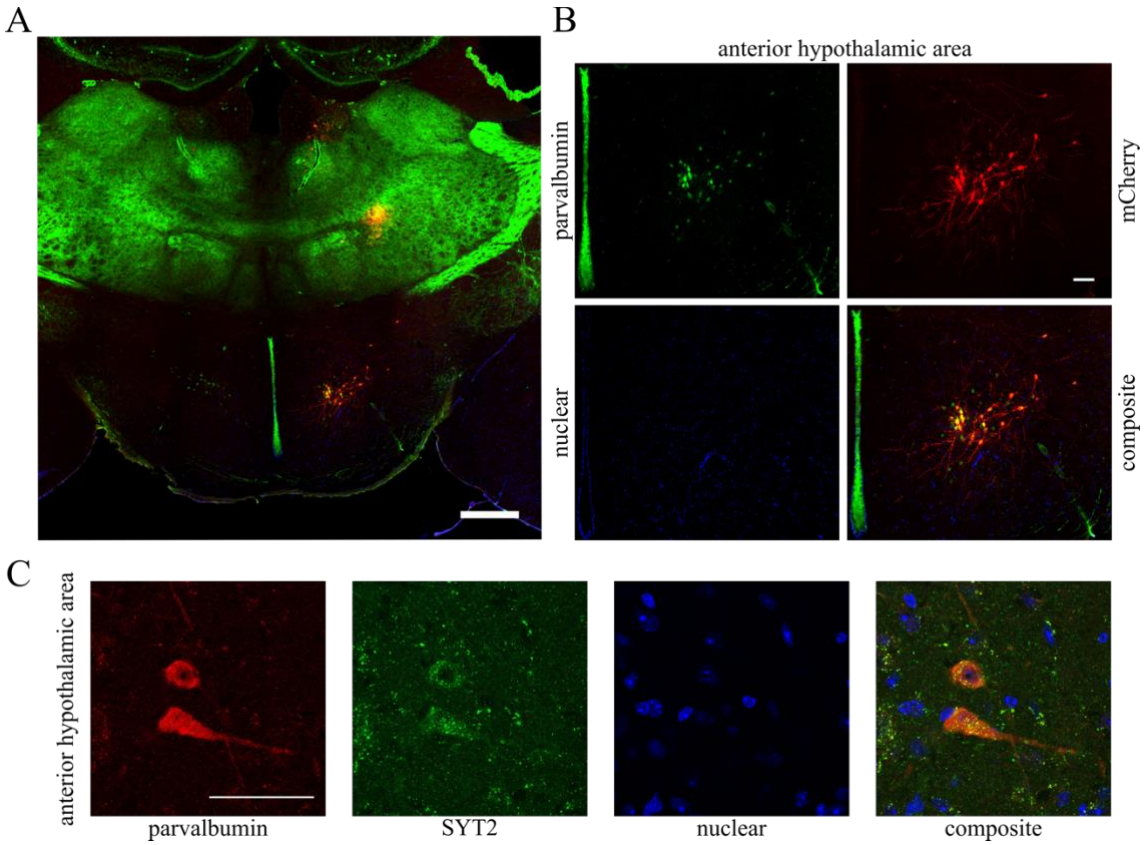

Figure 25: Projections and connections between parvalbumin neurones in the anterior hypothalamic area. (A) Representative picture of a rAAV-CAG-flex(hM3Dq-mCherry) (red) infected population of parvalbumin (green) neurones in the anterior hypothalamic area (scale bar = 500 µm) and (B) a higher magnification of this population depicting short projections between different parvalbumin neurones (scale bar = 50 µm). (C) Representative pictures of parvalbumin (red) and synaptotagmin2 (green) positive neurones in the anterior hypothalamic area, depicting synaptotagmin2 positive bouts on the surface of a parvalbumin positive neurone (scale bar = 50 µm). SYT2, synaptotagmin2.

3.3.2. PV Neurones in the AHA and in the Cortex Arise from Different Origins

To determine the origin of the PV populations from the AHA and the cortex, brain tissue from *Nkx2-1-Cre*:RFP x $5HT_{3a}$-EGFP double reporter mice (Luche et al., 2007; Munoz-

Manchado et al., 2016) was analysed. In these animals, all neurones which arise from the MGE, and therefore express the MGE marker protein Nkx2-1 at any point during their development, are permanently labelled with a red fluorescent protein (RFP). In addition, all cells expressing $5HT_{3a}$, a marker for cells originating from the CGE, express a green fluorescent protein (EGFP) (Fogarty et al., 2007; Luche et al., 2007; Munoz-Manchado et al., 2016). An immunofluorescence co-staining for PV on the tissue revealed that PV neurones in the AHA show no co-staining with RFP and only occasionally overlap with EGFP, indicating that only a subpopulation might arise from the CGE, but none of the neurones originate from the MGE (Figure 26A; in collaboration with Susi Dudazy-Gralla and Jens Hjerling Leffler). In contrast, PV neurones in the cortex were predominantly positive for RFP, demonstrating their origin from the MGE, as expected (Figure 26B in collaboration with Susi Dudazy-Gralla and Jens Hjerling Leffler).

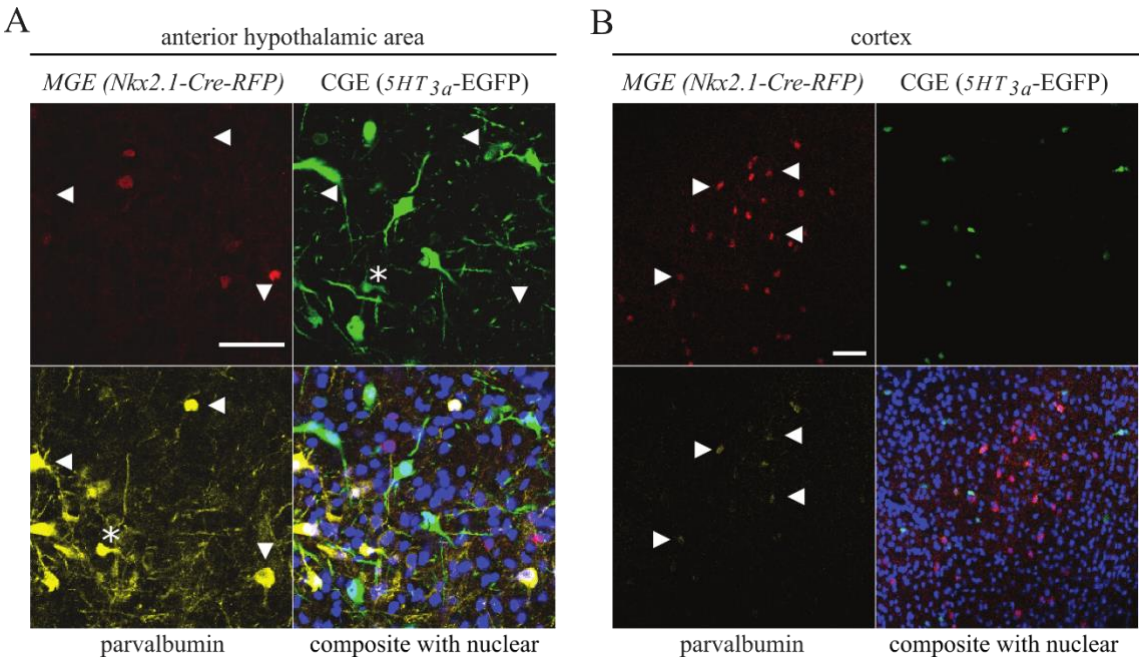

Figure 26: Parvalbumin neurones in the anterior hypothalamic area do not arise from the same origin as cortical parvalbumin neurones. Co-staining of brain tissue from *Nkx2-1-Cre*:RFP x $5HT_{3a}$-EGFP double reporter mice (Luche et al., 2007; Munoz-Manchado et al., 2016) with parvalbumin (yellow) in (A) the anterior hypothalamic area revealed no overlap with red labelled cells, originating from the MGE (white arrow heads) and only one overlay with a green labelled cell, originating from the CGE (white asterisk). (B) In contrast, cortical parvalbumin neurones show a clear overlap with red labelled cells. $5HT_{3a}$, serotonin receptor 3a CGE, caudal ganglionic eminence; EGFP, enhanced green fluorescent protein; MGE, medial ganglionic eminence; RFP, red fluorescent protein (modified from (Harder et al., 2018a); in collaboration with Susi Dudazy-Gralla and Jens Hjerling Leffler).

3.3.3. PV Neurones in the AHA Are Born around E12 during Development

To determine the transition from proliferation to migration and differentiation in PV neurones of the AHA and the motor cortex (M1 and M2), a birth dating experiment was

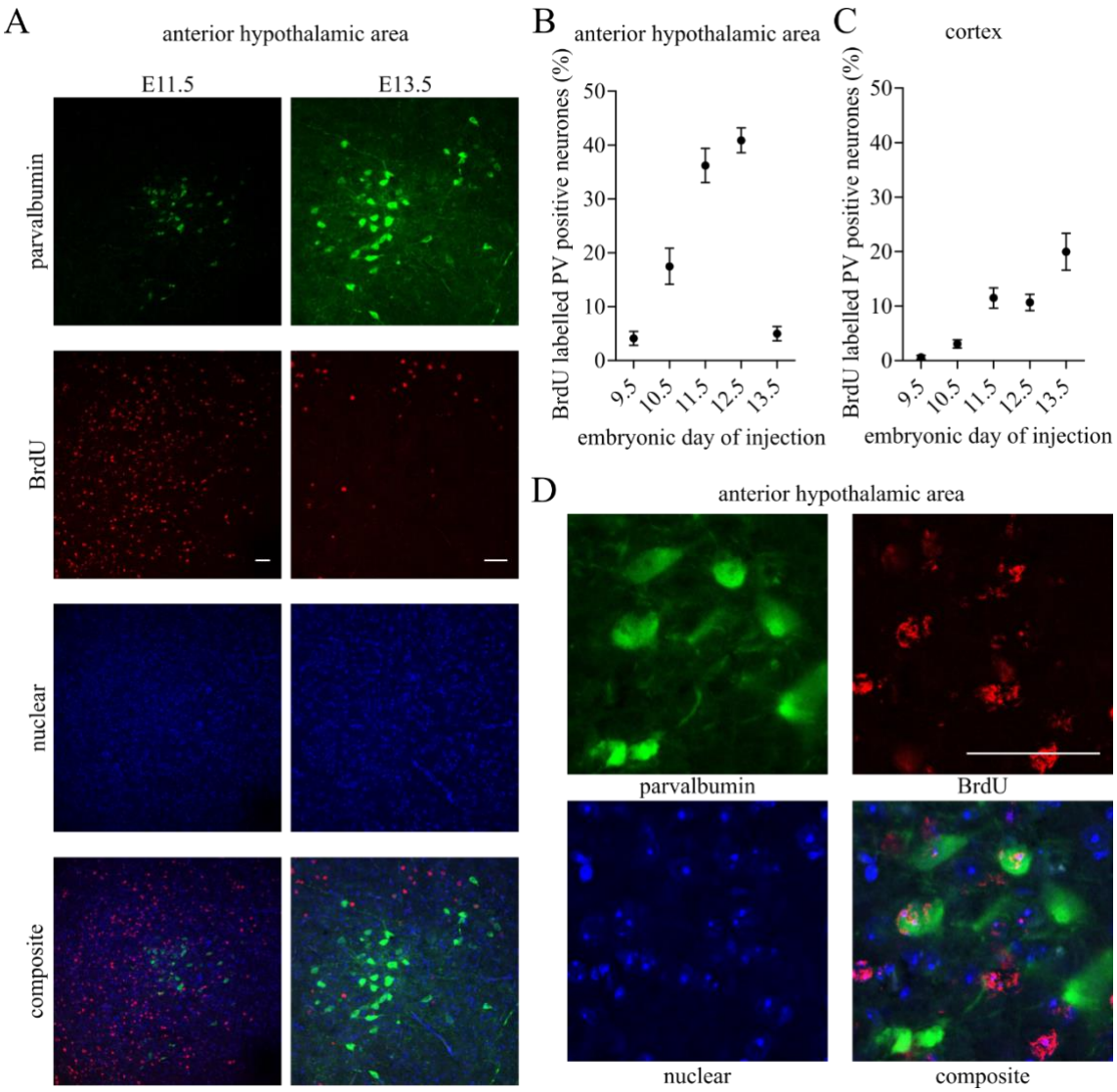

Figure 27: PV neurones in the anterior hypothalamic area arise 1 - 2 days earlier than cortical PV neurones. Representative pictures of (A) PV (green) and BrdU (red) double labelled cells injected at E11.5 (left column) and E13.5 (right column) in the anterior hypothalamic area. Quantitative analysis of PV and BrdU double labelled cells (n = 3 - 6 animals per time point) in (B) the anterior hypothalamic area (total number of PV neurones analysed: 174 (E9.5), 403 (E10.5), 410 (E11.5), 256 (E12.5) and 330 (E13.5)) and (C) the motor cortex (total number of PV neurones analysed: 480 (E9.5), 1027 (E10.5), 1198 (E11.5), 664 (E12.5) and 608 (E13.5)). (D) High magnification of PV (green) and BrdU (red) double labelled cells in the anterior hypothalamic area labelled at E11.5 (maximal projection of z-stack). Scale bars = 50 µm; all values are mean ± S.E.M.; BrdU, bromodeoxyuridine; E, embryonic day; PV, parvalbumin (modified from (Harder et al., 2018a)).

performed by injecting the proliferation marker BrdU in pregnant wt C57BL/6J mice at different time points after conception. Quantification of PV and BrdU double labelled neurones in the adult male offspring revealed that the majority of PV neurones in the AHA switch from proliferation to differentiation between E11.5 and E12.5 (Figure 27A, B) whereas the PV neurones in the cortex undergo this transition 1 to 2 days later, around E13.5 (Figure 27C).

3.3.4. Thermogenic and Cardiovascular Effects Mediated by PV Neurones in the AHA after DREADD Activation

Given the role of PV neurones in the AHA for the control of the cardiac system (Mittag et al., 2013) we aimed to specifically activate them using a DREADD system. *Parv-Cre* mice were injected in the AHA with a rAAV-CAG-flex(hM3Dq-mCherry) vector, which led to the expression of a hM3Dq-mCherry fusion protein solely in PV neurones at the site of injection. Using CNO as designer drug, an activation of the $G\alpha_{q/11}$ signalling pathway via hM3Dq in these neurones is possible. By radio telemetry, 24 h baseline measurements were recorded one week after surgery, confirming normal body temperature (Figure 28A), heart rate (Figure 28B) and activity (Figure 28C) of mice injected with the virus. As expected all three parameters were increased during the dark phase, the active phase of mice, indicating normal behaviour rhythms even after the surgical intervention in the AHA. For DREADD activation, a sham injection (0.9 % saline) was compared to a CNO injection (0.5 mg/kg), which was applied 24 h later. Comparing the measurements, after the initial stress reaction of the animal, no significant differences for temperature (Figure 28D; multiple t tests corrected for multiple comparisons using the Holm-Sidak method), heart rate (Figure 28E; multiple t tests corrected for multiple comparisons using the Holm-Sidak method) and activity (Figure 28G; 2-way ANOVA with repeated measures for both factors and a Sidak test to control for multiple comparisons, $p = 0.0105$ for time effect) were detected from minute 20 till 200 after injection. To ensure that no slower long-term effect or endocrine reaction was missed, the heart rate measurements were further analysed for 5 h after injection by calculating the AUC for 40 min sections (Figure 28E; 2-way ANOVA with repeated measures for both factors and a Sidak test to control for multiple comparisons, $p = 0.0007$ for time effect), which also revealed no differences between the two treatments.

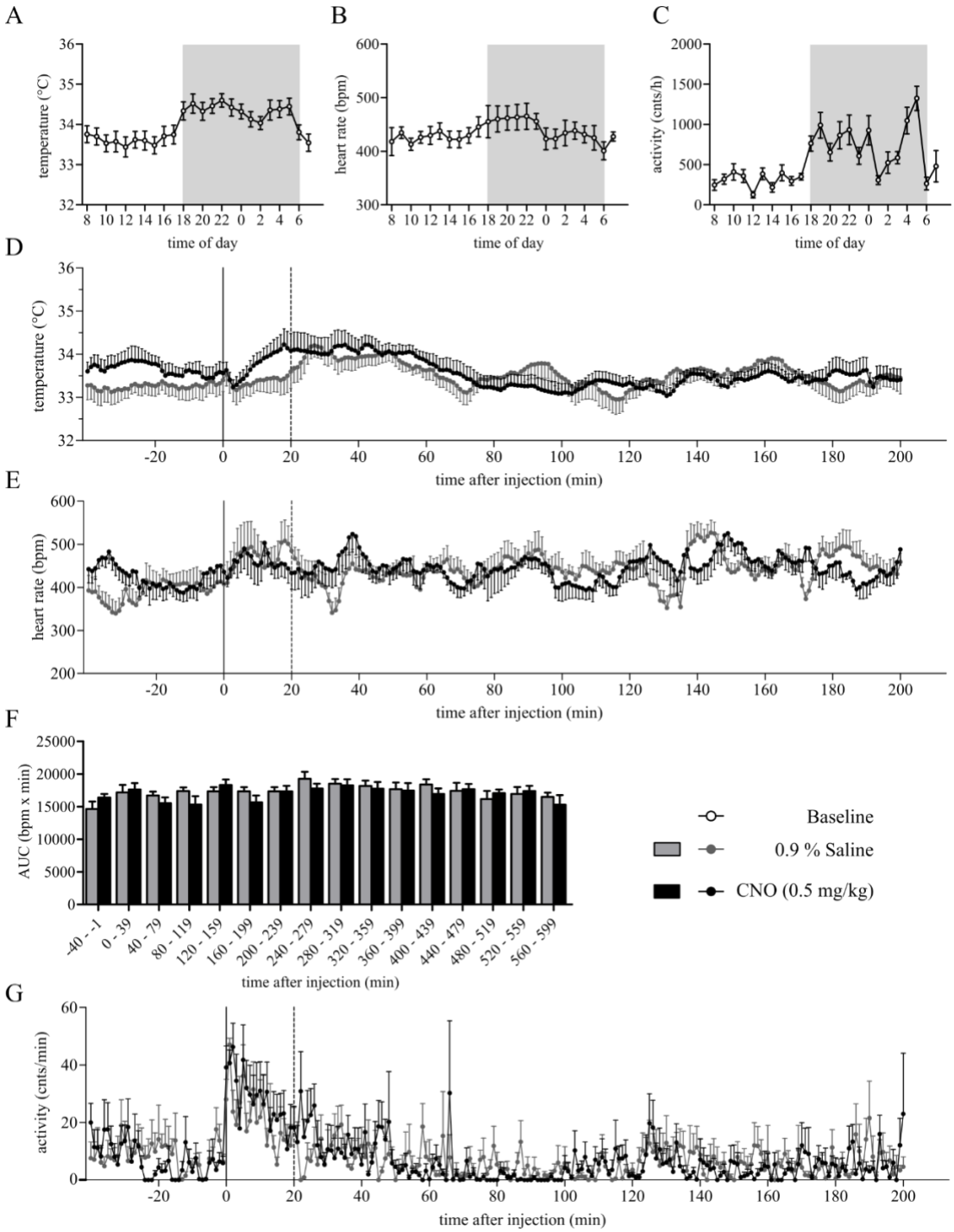

Figure 28: Specific activation of parvalbumin neurones in the anterior hypothalamic area, causes no short-term changes in body temperature or heart rate. 24 h untreated baseline of (A) temperature, (B) heart rate and (C) activity of male *Parv-Cre* mice, one week after intracranial injection of a rAAV-CAG-flex(hM3Dq-mCherry) vector in the anterior hypothalamic area (grey background indicates dark phase, N = 8). Four hours measurement of 0.9 % saline (N = 8, grey) and CNO (0.5 mg/kg, N = 8, black) i.p. injections for (D) temperature, (E) heart rate and (G) activity (black line = time of injection, dotted line = end of stress response). (F) Calculation of the AUC of the heart rate for 40 min sections under both conditions. All values are mean ± S.E.M. and statistical testing was performed using a multiple t test corrected for multiple comparisons using the Holm-Sidak method (D, E) or a 2-way ANOVA with repeated measures for both factors and a Sidak test to control for multiple comparisons (F, G); AUC, area under the curve; bpm, beats per minute; CNO, clozapine-N-oxide; cnts, counts.

3.3.5. Impaired Postnatal TH Signalling Does Not Affect the Development of PV Neurones in the AHA

To identify the crucial time frame of TH signalling for proper development of PV neurones in the AHA, different mouse models for impaired postnatal TH signalling were analysed:

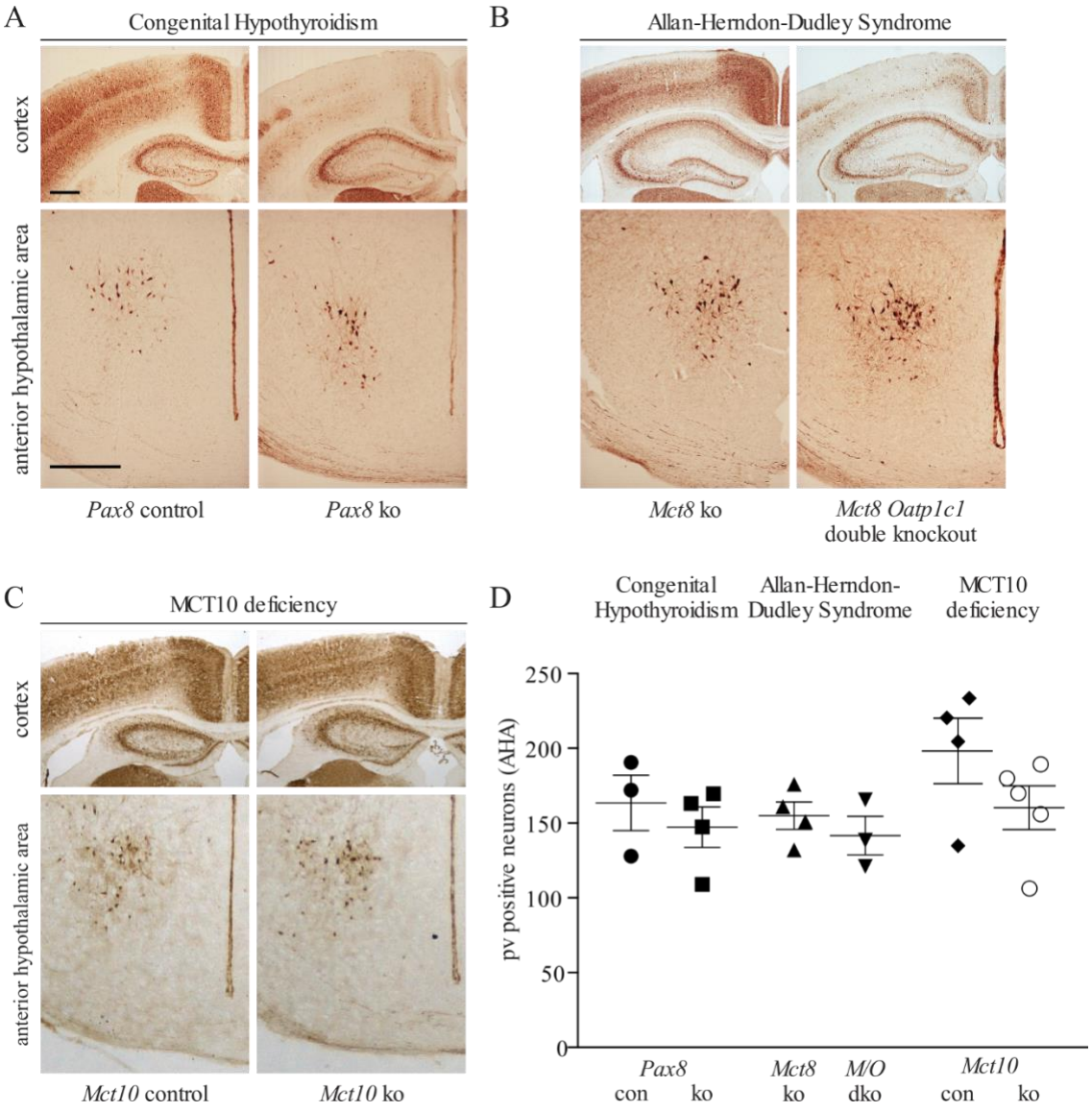

Figure 29: Impaired postnatal thyroid hormone signalling had no influence on the development of parvalbumin neurones in the AHA. Representative immunohistochemistry pictures of motor cortex and AHA of a mouse model for (A) congenital hypothyroidism (*Pax8* ko), (B) Allan-Herndon-Dudley Syndrome (*Mct8/Oatp1c1* dko) and (C) MCT10 transporter deficiency (*Mct10* ko) and their respective controls. (D) Quantitative analysis of parvalbumin neurones in the AHA of all three mouse models. Scale bars = 250 µm; values are mean ± S.E.M. and statistical testing was performed using an unpaired 2-tailed Student's t test. AHA, anterior hypothalamic area; con, control; ko, knock out; MCT8/10, Monocarboxylate transporter 8/10; *Oatp1c1*, *organic anion transporter family member 1c1*; PV parvalbumin; *M/O* dko, *Mct8/Oatp1c1* double knockout. (modified from (Harder et al., 2018a); in collaboration with Heike Heuer).

Pax8 ko mice, a model for CH, do not produce TH postnatally because they lack a functional thyroid gland (Mansouri et al., 1998). *M/O* dko mice, a model for Allan-Herndon-Dudley Syndrome, lack the MCT8 and OATP1C1 transporter and show no uptake of TH into the brain after tightening of the blood-brain-barrier around E16 (Mayerl et al., 2014). Both models showed reduced numbers of immunoreactive PV neurones in the motor cortex (Figure 29A, B) underlining that postnatal TH signalling is crucial for the development of cortical PV neurones. In contrast, the number of immunoreactive PV neurones in the AHA was unchanged in both models compared to the respective controls (Figure 29A, B, D; *Pax8* ko to wt control $p = 0.50$ and $t = 0.73$; *Mct8/Oatp1c1* dko to *Mct8* ko $p = 0.43$ and $t = 0.87$). Mice lacking only the MCT10 transporter showed no differences in population size of PV neurones neither in the cortex nor in the AHA compared to control mice (Figure 29C, D; *Mct10* ko to wt control $p = 0.18$ and $t = 1.50$), most likely indicating a compensation of MCT10 mediated TH transport by other TH transporters.

3.3.6. Effects of Maternal TH Treatment on PV Neurones in the AHA

To investigate whether the reduced number of PV neurones in the AHA in *Thra1*$^{+m}$ mice (Mittag et al., 2013) can be rescued by reactivating the mutant receptor with an increased T_3 concentration during embryonic development (Tinnikov et al., 2002; Wallis et al., 2008), two different treatment approaches were performed. First, *Thrb* ko dams (*Thrb*$^{-/-}$) with high endogenous TH concentrations (Forrest et al., 1996) were breed with *Thra1*$^{+m}$ males. Thereby the high endogenous TH concentration was used to reactivate the embryonic mutant TRα1 throughout the entire pregnancy. The possible offspring, *Thra1*$^{+m}$ and control (*Thrb*$^{+/-}$ with normal TH concentrations (Forrest et al., 1996)) were then compared to *Thra1*$^{+m}$ and control offspring from wt dams with normal maternal TH concentration. This revealed a significant interaction between treatment and TRα1 mutation (Figure 30A, B, E left; 2-way ANOVA effect of *Thra1* genotype $p < 0.0001$ (###), effect of maternal TH $p = 0.048$ (&)). This indicates that PV neurones in the AHA may be differently affected by TH depending on the presence of the *Thra1* mutation: TH may exert a rescuing effect in *Thra1*$^{+m}$ mice but may impair development in control mice. However, no significance was reached, testing this effect in separate posthoc tests (Figure 30E, left; Holm-Sidak posthoc *Thra1*$^{+m}$ normal maternal to *Thra1*$^{+m}$ high maternal $p = 0.35$ and $t = 0.97$ and control normal maternal to high maternal $p = 0.11$ and $t = 2.02$).

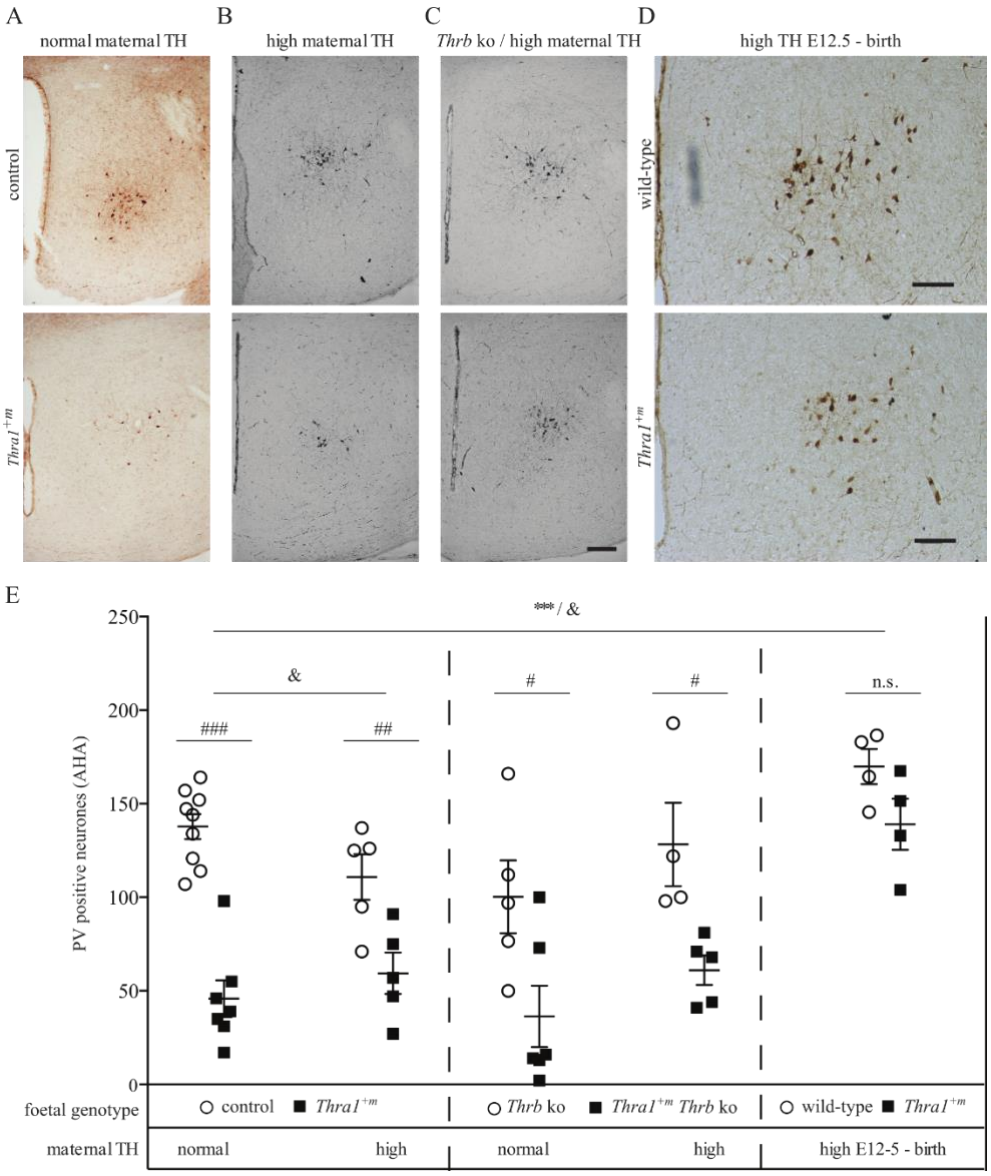

Figure 30: PV neurones in the AHA are a primary target for maternal TH. Representative pictures of the AHA of (A) control (wt, top) and *Thra1*$^{+m}$ (*Thra1*$^{+/m}$, bottom) offspring born from euthyroid mothers (wt), (B) control (*Thrb*$^{+/-}$, top) and *Thra1*$^{+m}$ (*Thra1*$^{+/m}$/*Thrb*$^{+/-}$, bottom) offspring born from hyperthyroid mothers (*Thrb*$^{-/-}$) and (C) control (Thrb$^{-/-}$, top) and *Thra1*$^{+m}$/*Thrb* ko (*Thra1*$^{+/m}$/*Thrb*$^{-/-}$, bottom) offspring born from hyperthyroid mothers (*Thrb*$^{-/-}$). (D) Representative pictures of the AHA of control (wt, top) and *Thra1*$^{+m}$ (*Thra1*$^{+/m}$, bottom) offspring born from euthyroid mothers (wt), treated orally with T_3 (0.5 µg/mL) from E12.5 until birth. (E) Quantification of PV neurones in the AHA of *Thra1*$^{+m}$ mice (black) and control littermates (white) from wt (normal maternal TH) or *Thrb* ko mothers (high maternal TH, left panel), *Thra1*$^{+m}$/*Thrb* ko mice (black) and *Thrb* ko littermates (white) from *Thrb*$^{+/-}$ (normal maternal TH) or *Thrb* ko mothers (high maternal TH, middle panel) and *Thra1*$^{+m}$ mice (black) and wt littermates (white) from wt mothers treated orally with T_3 (0.5 µg/mL) from E12.5 until birth (right panel). Horizontal lines indicate mean ± S.E.M. and statistical testing was performed using a 2-way-ANOVA ($^{\&}p < 0.05$ for interaction of maternal TH and *Thra1*; $^{***}p < 0.001$ for effect of maternal TH) with Holm-Sidak posthoc test corrected for multiple comparison for the respective conditions ($^{n.s.}p > 0.05$; $^{\#}p < 0.05$; $^{\#\#}p < 0.01$; $^{\#\#\#}p < 0.001$ for effect of *Thra1*). All scale bars 100 µm. AHA, anterior hypothalamic area; E, embryonic day; ko, knockout; PV, parvalbumin; TH, thyroid hormone; *Thra/b*, *thyroid hormone receptor alpha/beta* (modified from (Harder et al., 2018a)).

To analyse TRβ as a possible mediator of the observed negative effects of high maternal TH, the experiment was repeated using offspring with a *Thrb* ko background, again under normal (*Thrb*$^{+/-}$ mothers with normal TH concentration) and high maternal (*Thrb* ko mothers with high endogenous TH concentrations) TH conditions (Figure 30C, E middle; 2-way ANOVA effect of *Thra1* genotype $p = 0.014$ (#), effect of maternal thyroid hormone $p = 0.142$, interaction $p = 0.924$). This suggested a role of TRβ for the development of PV cells in the AHA, however, a direct comparison of control and *Thra1*$^{+m}$ mice with and without *Thrb* from euthyroid mothers showed only a tendency for a reduced number of PV neurones in the absence of TRβ (Figure 30E, left and middle; 2-way ANOVA effect of *Thra1* genotype $p < 0.0001$, effect of *Thrb* genotype $p = 0.071$, interaction $p = 0.272$).

We thus hypothesised, based on the rather mild benefits of TRα1 reactivation in *Thra1*$^{+m}$ mice, that a reactivation of the TRα1 mutant receptor only during the post-mitotic period of PV neurones in the AHA might avoid some possible negative effects of hyperthyroidism on the proliferating precursor cells. Indeed, after a specific increase of maternal TH concentration (pregnant mice treated with 0.5 mg/L T_3 and 0.01 % BSA in the drinking water) only from day 12.5 after conception until the birth of the offspring, a significant increase in PV neurones in the AHA of *Thra1*$^{+m}$ animals compared to control offspring (wt) from untreated mothers (wt) was observed (Figure 30D, E, left and right; effect of genotype $p < 0.0001$, effect of maternal thyroid hormone ***$p < 0.0001$, interaction &$p = 0.006$, Holm-Sidak posthoc test control to control TH E12.5 - birth $p = 0.031$ and $t = 2.32$, Holm-Sidak posthoc test *Thra1*$^{+m}$ to *Thra1*$^{+m}$ TH E12.5 - birth $p < 0.0001$ and $t = 6.48$). Comparing directly *Thra1*$^{+m}$ and control (wt) offspring from mothers treated with T_3 between E12.5 and birth, the number of PV neurones in *Thra1*$^{+m}$ mice was fully rescued (Figure 30E, right; Holm-Sidak posthoc test control TH E12.5-birth to *Thra1*$^{+m}$ TH E12.5-birth $p = 0.072$ and $t = 1.903$). Taken together the experiment demonstrated a crucial role of maternal TH for the development of PV neurones in the AHA solely in the second half of pregnancy via TRα1.

4. Discussion

The scope of this doctoral thesis was to further decipher the central and peripheral as well as acute and developmental actions of TH in the mouse regarding metabolism, thermoregulatory and cardiovascular aspects. To initially characterize the systemic effects provoked by excessive T_4 *in vivo*, mice were treated with TH for two weeks and subsequently recovered from this treatment for another two weeks. This first part of the thesis established the basic consequences of a transient thyrotoxicosis. To determine a possible contribution of downstream TH metabolites, similar paradigms were conducted with e.g. the deiodinated and decarboxylated form T_0AM, and compared to the basic effects of TH. In the final part, the focus was shifted on the role of TH for brain development, namely TH sensitive PV neurones in the AHA and their impact on cardiovascular control.

4.1. Study 1: Peripheral Effects Provoked by a Transient Thyrotoxicosis and Body's Ability to Recover

The following part of the thesis discusses the consequences of a short-term transient thyrotoxicosis and the ability of the body to recover from it within two weeks (Hoefig et al., 2016a). From the clinical point of view this is highly interesting, because it mimics the situation of a T_4 overtreatment after thyroidectomy or the decline of TH levels during thyrostatic drug treatment in hyperthyroid patients as well as in short-time abuse of TH preparations for e.g. for body building competitions. Due to its stimulating influence on the basal metabolic rate (Kim, 2008), TH still gains popularity among fitness centre visitors of all age groups and overweight people as an easy way to lose fat mass, disregarding possible side effects. This is especially problematic because non-professionals easily get access to the substances over the internet and there is no control of the ingredients of the products (Siegmund-Schultze, 2013). In single cases, clinical consequences have been observed as a result of uncontrolled intake of excessive amounts of TH, such as sweating, palpitation and confusion but in severe cases also sudden death (Bhasin et al., 1981; Braunstein et al., 1986; Ioos et al., 2008; McKillop, 1987). In the case of bodybuilders, cardiomyopathy and hypokalemic paralysis were described in the context of TH abuse (Mark et al., 2005; Mayr et al., 2012). While the long-term consequences of TH excess such as a hypermetabolic state, heat intolerance, elevated heart rate, cardiac hypertrophy and an increased risk for atrial fibrillation are well established (De Leo et al., 2016; Kim, 2008), little is known about basic metabolic, thermoregulatory and cardiac changes due to a transient thyrotoxicosis. To mimic

this situation, mice underwent a T_4 treatment which was comparable to the intake of a 2- to 3-fold full substitution dose of T_4 in humans.

4.1.1. Metabolic Effects of Thyrotoxicosis and Recovery

Serum total T_3 and T_4 measurement in the mouse model demonstrated that the oral T_4 treatment was sufficient to produce a thyrotoxicosis after two weeks. qPCR results of *Me1* and *Dio1*, demonstrating a hyperthyroid state of the liver during thyrotoxicosis (Song et al., 1988; Takeuchi et al., 2002), further underlined that. Within two weeks of recovery, total T_4 and mRNA expression of TH sensitive genes in liver and kidney had returned to a euthyroid status. Surprisingly, however, total T_3 level fell below baseline, which could be explained by the different speed of normalisation for the involved players. After the end of the T_4 treatment, T_4 concentration declines slower than T_3 concentration, because of its longer half-life (Nicoloff et al., 1972). In parallel, the TSH secretion by the pituitary, which was oppressed by the feet-back loop during the thyrotoxicosis, rises and restimulates the endogenous TH production by the thyroid gland. The pituitary has a very high expression level of DIO2 (Mittag et al., 2009), indicating dependence on T_4 rather than T_3. The consequence is, that the hypothalamus-pituitary-thyroid-axis follows the T_4 concentration rather than the T_3 concentration and therefore the thyroid stimulation is only sufficient to make up for the slowly sinking T_4 but not for the rapidly sinking T_3 concentration. The result is a transient hypothyroid state in all T_3 dependent tissues right after T_4 withdrawal, such as the heart which has very low DIO2 levels and shows almost no T_4 uptake (Everts et al., 1996; Wagner et al., 2003). In contrast, tissues with DIO2 expression such as the iBAT are not affected by the low T_3. Similar alterations from thyrotoxicosis to a transient relative hypothyroidism have been described in humans as well (Distiller and Joffe, 1975).

Even though increased TH concentration in humans leads to weight reduction (Allolio and Schulte, 2011), neither this nor elevated food intake were observed in the mouse model. The increase in body weight of mice during thyrotoxicosis could have two reasons. First, in contrast to humans, mice grow continuously throughout their entire life which could mask an actual reduction in fat mass during the treatment. Secondly, TH stimulates growth hormone synthesis and secretion in mice, and could therefore evoke an increased growth rate during thyrotoxicosis (Cabello and Wrutniak, 1989). The absent of increased food intake could be related to the relatively short treatment period and the moderate level of thyrotoxicosis of the model. The expected increased demand for energy of the body due to the TH-dependent elevated energy expenditure (Kim, 2008), was evidenced by depleted

hepatic glycogen store. After recovery, the liver was again sufficiently supplied with glucose from the circulation, as demonstrated by increased expression of *Pklr*, the rate limiting enzyme of glycolysis, the increase in fatty acid synthesis (*Acaca* and *Fasn*) and the completely refilled glycogen stores. At the same time, no clear indication for true starvation were found, because relative mRNA expression of genes important for ketogenesis showed no alteration during T_4 treatment or after recovery. Taken together, these findings indicated a switch from hepatic gluconeogenesis due to limited hepatic glucose availability during thyrotoxicosis to glycolysis and high glucose consumption and fatty acid production upon recovery.

4.1.2. Consequences of a Thyrotoxicosis on Body's Thermoregulation

It is well established, that TH is involved in facultative thermogenesis such as shivering and non-shivering thermogenesis (Silva, 2003), central control of thermogenesis (Lopez et al., 2010) and peripheral heat loss (Warner et al., 2013). However, the system is further complicated by the fact that TH also influences the basal metabolic rate and with this the obligatory thermogenesis (Silva, 2003). The data of the introduced mouse model showed an increase in body temperature during thyrotoxicosis, but its origin is neither a reduced heat loss over the tail nor an increased activity of the iBAT based on the analysis of IR pictures and UCP1 content. Furthermore, no changes in relative mRNA expression of genes crucial for sympathetic stimulation, lipid depletion or TH activation were detected during thyrotoxicosis, which indicates an unchanged iBAT activity. A possible explanation of this unexpected lack of iBAT stimulation is the general increase of body temperature due to the higher metabolic rate, which prevents an additional increase in facultative thermogenesis (Cannon and Nedergaard, 2004; Lopez et al., 2010; Silva, 2006). In line with that, recent studies demonstrate that a TR mediated thermogenic action of TH is independent from iBAT activity and is rather connected to UCP1 induction in WAT, a process called browning (Lin et al., 2015). Indeed, *Ucp1* mRNA in eWAT was strongly elevated but on protein level UCP1 was not altered. However, eWAT, in contrast to iWAT, is not the classical fat depot associated with browning (Okamatsu-Ogura et al., 2013). Interestingly, after recovery the metabolic activity of the iBAT is slightly increased based on the mRNA expression profile, indicating an attempt to antagonize the sudden drop in temperature, observable during recovery. These findings add on to the growing body of evidence, that increased concentrations of T_4 in the periphery have a repressive effect on iBAT thermogenesis (Solmonson and Mills, 2016). This leads to the conclusion that although T_4 is necessary for

iBAT thermogenesis, it is by itself not sufficient. Even though the findings of the thyrotoxicosis study exclude iBAT as the primary source for the elevated body temperature, they cannot approve whether browning of WAT depots is the source. Another hypothesis would be that elevation in body temperature is the consequence of an increased metabolic rate of other tissues such as the skeletal muscles (Astrup et al., 1989; Gong et al., 1997; Solmonson and Mills, 2016).

4.1.3. The Cardiovascular System under Thyrotoxicosis and after Recovery

The thyrotoxicosis paradigm leads to hypertrophy and tachycardia in the heart which is a primary target of TH action, as described before (Coleman et al., 1989; Klein and Ojamaa, 2001). mRNA levels displayed an increase in *Hcn2*, indicating a change in cardiac pacemaker activity (Ludwig et al., 2003) and *Adrb2*, leading to increased cardiac sympathetic signalling. However, blood pressure parameters were not affected besides elevated renal *Agt*. Surprisingly, after two weeks of recovery the heart rate dropped significantly below the baseline despite normalised T_4 concentration. This was unexpected because mRNA expression of *Hcn2, Adrb2* and *Nppb*, a TH depending marker of ventricular hypertrophy, were still elevated (Liang et al., 2003; Nakagawa et al., 1995). Simultaneously, genes involved in blood pressure regulation increased, most likely to compensate for the reduced heart rate. It is possible that these findings are due to the transient hypothyroid state of the heart, based on the reduced T_3 concentration during recovery in combination with the lack of Dio2 in the tissue. The pacemaker activity of the heart relies mainly on T_3, which is involved in the regulation of the intracellular calcium signalling (Sun et al., 2001). Therefore, already a small reduction in the serum T_3 concentration could result in bradycardia. In line with this, mRNA expression of *Pln,* which is involved in the regulation of cardiac calcium levels, was reduced during thyrotoxicosis and then rose almost 2-fold over baseline upon recovery (Dillmann, 2010). Unexpectedly, at the same time mRNA of *Atp2a2* increased significantly upon recovery compared to thyrotoxicosis. High levels of PLN normally reduce contractility and heart rate by inhibiting SERCA2A production (Frank et al., 2003). The contrary observation could indicate an attempted of the body to overcome the inhibition by *Pln*, which suggest that *Pln* is of higher importance then *Hcn2*.

Further studies of genetic gain- and loss- of function will be necessary to completely understand the regulation of gene expression by changes in T_3 or T_4 concentrations, however, the data support the idea that the heart mainly relies on T_3, leading to a

bradycardia right after the withdrawal of excessive T_4. The important conclusion for the clinical daily routine is that patients, which recover from thyrotoxicosis after thyroidectomy or thyrostatic drug treatment, need close monitoring to avoid cardiac events. Also, people abusing TH could face severe cardiovascular problems, even some time after the substance withdrawal.

4.2. Study 2: Participation of TAMs in Body's Classical Response to TH

The finding that the TH metabolite 3-T_1AM can induce a strong hypothermia and bradycardia in mice and with this acts contrary to classical THs, might allocate 3-T_1AM to a fine-tuning role within the TH signalling cascade (Liggett, 2004; Scanlan et al., 2004). This raised the question to which extent TH metabolites are involved in physiological processes as seen in thyrotoxicosis, which were former only attributed to THs. Based on *in vitro* and *in vivo* demonstration that 3-T_1AM can be metabolised to TA_1 and T_0AM, these two derivatives moved into focus (Piehl et al., 2008; Schanze et al., 2017; Wood et al., 2009). *In vivo* analysis of TA_1 demonstrated that the ethylamine side chain is essential for the thermogenic and cardiac properties of 3-T_1AM because without, none of the expected effects were seen (Hoefig et al., 2015a). This was surprising because the closely related TH derivative triiodothyroacetic acid (Triac) does show cardiac and thermogenic effects (Symons et al., 1975). However, Triac binds and acts specifically via the TRβ (Messier et al., 2001), whereas the target structures for 3-T_1AM and other potential downstream metabolites are still unknown. To resolve the contributions of the other 3-T_1AM downstream metabolite, T_0AM, to cardiac and thermoregulatory actions, the following part of the thesis focused on the effects of an acute or chronic treatment of T_0AM in male wt mice (Harder et al., 2018b).

The data revealed no metabolic or thermoregulatory effects in the *in vivo* mouse model upon treatment with T_0AM, acute or chronic for seven days. Furthermore, no changes in TH homeostasis were observed in the animals. Solely *Ace1* in the lung was moderately increased upon chronic T_0AM treatment, which however did not result in a change in blood pressure. In contrast to 3-T_1AM, neither bradycardia nor anapyrexia were observed in mice due to T_0AM treatment, although older studies described some cardiac and thermoregulatory effects of T_0AM (Scanlan et al., 2004).

It can be concluded that tissue-specific deiodination of 3-T_1AM as well as oxidation of the ethylamine side chain are important deactivation mechanisms of the body. This suggests a novel gate-keeper function of Dio1 and Dio3 in addition to their classical role in TH

metabolism, namely to inactivate the potent precursor 3-T_1AM to T_0AM (Piehl et al., 2008). Based on the findings discussed above, one could hypothesise the reaction to high levels of TH in the body, as in thyrotoxicosis, is a conversion of T_3 to 3-T_1AM. Accordingly, TSH-suppressed and T_4 substituted patients, with normal to high serum T_4 concentrations also display normal to high 3-T_1AM concentrations compared with controls (Hoefig et al., 2011). This conversion would have two beneficial effects. First, the stimulation of hyperthermia and tachycardia by TH is not only reduced but counter steered the effects of 3-T_1AM. Second, 3-T_1AM can be rapidly degraded to TA_1 and T_0AM and by this terminate the effects on thermoregulation and the cardiovascular system.

4.3. Study 3: Importance of TH for Brain Development

In addition to the direct effects of TH in the adult animal, as tested above, TH is also highly important during foetal development. This is best illustrated in CH, in which neonates suffer from a lack of endogenous TH leading to irreversible mental retardation, if not treated with T_4 from birth onwards. Likewise, maternal hypothyroidism and hypothyroxinaemia during pregnancy are linked with neurological dysfunctions such as autism (Andersen et al., 2014). In addition, several studies of women with subclinical hypothyroidism during pregnancy showed adverse effects for their offspring, such as mental and motor dysfunction, altered brain morphology and impaired foetal growth (Johns et al., 2017; Korevaar et al., 2016; Pop et al., 2003). Despite this clinical relevance, so far there is no recommendation for a universal screening of thyroid function during pregnancy (Lazarus et al., 2014). This discrepancy is mainly based on a lack of conclusive population studies on the subject. Two recent publications, with high case numbers, failed to show improvements in IQ of children from treated women with subclinical hypothyroidism compared to children from untreated mothers (Casey et al., 2017; Lazarus et al., 2012). However, it should be taken into account that both studies rely only on cognitive test in young children as readout parameter, which is neither a useful marker to monitor foetal development under TH treatment nor allows any assumptions about consequences of maternal subclinical hypothyroidism in other tissues or its general long-term effects. To overcome this limitation, it is fundamental to better understand the function of TH for cerebral development and to identify time frames for TH action. A promising neuroanatomical readout in this context could be a recently identified population of TH sensitive PV neurones in the AHA. Their ablation can cause hypertension, suggesting an important role in the control of cardiovascular function, which makes blood pressure an important readout parameter in studies focussing on the offspring generation of

hypothyroxinaemic mothers (Mittag et al., 2013). Therefore, the last part of my thesis focused on the characterisation of PV neurones in the AHA and their TH dependency during development (Harder et al., 2018a).

4.3.1. Properties of PV Neurones in the AHA

Neurones expressing the Ca^{2+} binding protein PV can be found in several areas of the brain e.g. the cortex, the hippocampus and the hypothalamus, as demonstrated in rats (Celio, 1990). The recently described population of PV neurones in the AHA (Mittag et al., 2013) were identified as GABAergic interneurones. This was expected, because GABA negative PV neurones have been described only for afferents from the retina and the organ of Corti so far (Celio, 1986). VGLUT2 positive boutons on the surface of the PV neurones in the AHA indicated glutamatergic input into their inhibitory system. From inhibitory PV interneurones of the cortex it is known, that they interact with excitatory pyramidal neurones, leading to gamma-oscillation. The glutamatergic input activates the interneurones, which in turn leads to inhibition of further excitation until the inhibition fades away. By this interaction, excitatory information can be transmitted during recurrent windows without inhibition into other brain areas (Rotaru et al., 2012). It would be possible that the PV neurones in the AHA are integrated in a comparable way in processing information for the control of cardiovascular function. This hypothesis is strengthened by the description of a sympatico-inhibitory centre in the anterior hypothalamus of cats. Electrical stimulation of this area leads to inhibition of the sympathetic tone and by this the blood pressure was manipulated (Folkow et al., 1959). Generally, the regulation of cardiorespiratory functions is attributed to the PVN (Duan et al., 1997), a hypothalamic area next to the AHA, with direct and indirect projections to the brain steam to convey cardiovascular function (Ferguson et al., 2008; Pyner, 2009). However, signals from the PVN are modulated by inhibitory GABAergic input and the AHA was identified as one of four areas in the hypothalamus from which GABAergic projections enter the PVN in the rat (Roland and Sawchenko, 1993). In line with that, immunofluorescence labelling in *Parv-Cre* mice revealed no long-distance projections to other brain regions but suggests tight interconnections within the AHA population based on the detection of SYT2 positive boutons on the surface of PV neurones (Sommeijer and Levelt, 2012).

Despite these analogies between PV neurones in the cortex and the AHA, the data also strongly indicate that PV neurones in the AHA represent a separate population with different properties. In terms of neurogenesis, three main zones, from which cortical

GABAergic neurones can originate, are described: the MGE, the CGE and the preoptic area (Gelman et al., 2009; Miyoshi et al., 2007; Xu et al., 2004). Neurones can be allocated to originate from the MGE or the preoptic area by their developmental expression of Nkx2-1 (Flames et al., 2007; Sussel et al., 1999), whereas neurones derived from the CGE express $5HT_{3a}$ (Rudy et al., 2011). Surprisingly, the analysis of the double reporter mice showed that PV neurones from the AHA do not originate from the MGE or the preoptic area due to the lack of overlay between PV and Nkx2-1 and only very minor overlay was found with $5HT_{3a}$ in the neurones. This also implies that the developmental program of PV neurones in the AHA does not rely on the transcription factor Nkx2-1 at any time during their development. Accordingly, Nkx2-1 null mice show only slightly impaired hypothalamic development (Kimura et al., 1996). A further area not explicitly checked by the double reporter mouse but known to contribute to embryonic neurogenesis is the lateral ganglionic eminence (LGE). It can be subdivided into the ventral pallidum, expressing Trb2, Ngn2 and Dbx1 but no Dlx2, and the remaining LGE, expressing Dlx2, Gsh2 and Pax6 but no Nkx2-1 (Flames et al., 2007). It mainly gives rise to striatal GABAergic projection neurones and a subset of interneurones in the olfactory bulb and the amygdala (Corbin and Butt, 2011). Moreover, a new proliferative zone in the median eminence of the hypothalamus was described, but in the context of hypothalamic neurogenesis in adult mice (Lee et al., 2012). Still it is possible that PV neurones dedicated to the AHA arise from one of these areas.

Further differences between AHA and cortical PV neurones concern the timing of birth and subsequent maturation. PV neurones dedicated to the AHA complete their mitosis around E12, concordant with the birth of the majority of AHA neurones between E10 and E16, peaking at E11 - E14 (Shimada and Nakamura, 1973), and are first detectable in the AHA on P8. In contrast, only a small amount of cortical PV neurones switch from proliferation to differentiation before E13 and they are classically not detectable before P10 in the cortex (de Lecea et al., 1995). A neighbouring population of PV neurones from the parvafox-nucleus of the ventrolateral hypothalamus are born between E9 and E13 with a peak at E12 as well (Bilella et al., 2016). The close relation of birth with the PV population in the AHA could also indicate a common origin (Alvarez-Bolado et al., 2000; Meszar et al., 2012). However, these neurones are not affected by TH during development (Mittag et al., 2013; Wallis et al., 2008), indicating a different developmental path compared to the PV populations in the cortex or the AHA.

4.3.2. Physiological Effects of Chemogenetic Activation of PV Neurones in the AHA

Based on earlier findings, showing that a reduced number of PV neurones in the AHA leads to a significant increase in systolic blood pressure, diastolic blood pressure and mean arterial pressure as well as a significant increase in heart rate at 4°C (Mittag et al., 2013), PV neurones in the AHA were specifically activated using an activating DREADD system with the hypothesis, that it would reduce heart rate in the animal. To this end, a stereotaxic injection of a Cre-dependent rAAV vector in the AHA of *Parv-Cre* mice was performed, to evoke specific hM3Dq-mCherry expression in PV neurones. hM3Dq is a DREADD based on the Gq-coupled human M3 muscarinic receptor and can only be activated by CNO leading to an increase in intracellular Ca^{2+} level which in turn leads to neuronal firing (Armbruster et al., 2007).

The activation of PV neurones in the AHA by CNO induced no changes in body temperature and activity. Surprisingly, also on heart rate were no effects detectable. One possible explanation could be that the PV neurones are not directly but indirectly involved in the cardiovascular control e.g. by an unknown endocrine mechanism. However, ablation of PV neurones in the AHA did not result in changes of adrenal mRNA expression and aldosterone serum levels, serum angiotensin II levels or total T_3 and T_4, making it unlikely but not impossible that PV neurones in the AHA act by endocrine alterations on the cardiovascular system (Mittag et al., 2013). Still, it would be possible that PV neurones in the AHA act via endocrine pathways on the autonomic nerve system and by this influence the control of cardiovascular functions. A more likely interpretation would be that the PV circuit in the AHA is mainly necessary for homeostasis of the cardiac system and therefore very robust against acute changes. In favour of this hypothesis is the observation of short projections and interconnections within the population of PV neurones. A non-directional activation of the system via hM3Dq could elicit an initial activation of PV neurones at the target sites but at the same time self-inhibition would prevent a strong and long-lasting inhibition of the downstream target structures. Immunofluorescent stainings confirmed that hM3Dq solely was expressed in PV neurones but due to the challenging stereotaxic injections in deep brain regions, some animals showed only unilateral infections and none of the analysed AHAs showed a 100% infection of all neurones in the PV population. Therefore, the stimulation of the system by CNO could simply be too weak to evoke a measurable change in the heart rate. Generally, the control of the cardiovascular system is an orchestration of many central and peripheral players, some of them might compensate for the activity changes in the PV

population even before changes in the heart rate are measurable. Still, these findings are not conflicting with the observations of Mittag and colleagues on the role of PV neurones (Mittag 2013), because chronic manipulation of a system by viral ablation is a much stronger intervention than acute manipulations by DREADD (Südhof, 2015). In fact, the observation that within the population of PV neurones in the AHA some cells where activated by increased temperature or TRH and some were inhibited rather indicate that several subpopulations of PV neurones in the AHA exist (Mittag et al., 2013). Therefore, it is conceivable that an activation of all sorts of PV neurones in the AHA at the same time leads to reactions in the circuit that could cancel each other.

On the other hand, there are also some methodical issues which need to be addressed in the context of the DREADD experiment. For example, recent studies challenged the postulation that CNO is an inert compound in mice, that it can cross the blood brain barrier and preferentially acts on DREADDs. They rather claim that the DREADD system requires the conversion of CNO to clozapine, which is able to cross the blood brain barrier and binds with high affinity to DREADDs (Gomez et al., 2017; Manvich et al., 2018). This brings up two main problem for the system. First, due to the conversion step DREADD activation might not peak 30 min after i.p. CNO injection but substantially later, leading to a delay in physiological reaction. However, up to 18 h after injection no unusual events were observed in the heart rate data. Secondly, clozapine is not specific for DREADDs and therefore evokes considerable side effects at higher doses (> 1 mg/kg) such as hypotension and decreased locomotor activity (Roth, 2016). Still the conversion rate of CNO to clozapine is estimated to 2 % (Gomez et al., 2017), which makes it more likely that the applied stimulation with 0.5 mg/kg CNO was too weak than that side effects interfere with the output of the cardiovascular system.

4.3.3. TH Sensitivity of PV Neurones in the AHA during Development

The general importance of TH for proper development of PV neurones in several brain areas is well described in animal models (Venero et al., 2005; Wallis et al., 2008), still research primarily focussed on the cortical population. Human data described cortical changes upon prenatal TH impairments e.g. variation in the thickness of different cortical areas in children (age 10 - 12) exposed to maternal hypothyroidism during pregnancy (Lischinsky et al., 2016). In rats was observed that a lack of TH from E14 onwards led to a reduction of PV expression and axonal development in the neocortex (Berbel et al., 1996). To test whether PV neurones

in the AHA are comparably affected, mouse models of postnatal impaired TH signalling were analysed. Surprisingly, there were no changes observed in the AHA, whereas a strong reduction in the amount of PV neurones in the cortex were visible. This could be due to the advanced developmental stage of PV neurones in the AHA, as described above, leading to postnatal TH independency, compared to cortical PV neurones. Furthermore, the data indicated that neither prenatal nor postnatal TH produced by the foetus was necessary for the development of PV neurones in the AHA, based on the results seen in the *Pax8*$^{-/-}$ model with no endogenous TH (Mansouri et al., 1998).

Since it was already demonstrated that PV neurones in the AHA rely on TH for their development (Mittag et al., 2013), the previous findings suggest that they need prenatal maternal TH. Based on this, the *Thra1*$^{+m}$ mouse model was used, depicting a situation of no TRα1 mediated TH signalling, which can be temporary restored by TH treatment (Tinnikov et al., 2002). The aim was to rescue the PV neurones in the AHA of *Thra1*$^{+m}$ embryos by transiently increasing the maternal TH levels. Raising the TH levels throughout the entire pregnancy using *Thrb* ko mothers with high endogenous TH levels (Forrest et al., 1996; Tinnikov et al., 2002) had only minor effect of the PV population in the AHA of offspring with *Thra1*$^{+m}$ genotype. Interestingly, the treatment showed also a tendency of a negative effect on the PV population size in the wt control offspring. One possible explanation is that this negative effect of high TH is mediated by TRβ, especially because basic neuroanatomical data in the rat indicated that TRβ is highly expressed in proliferative zones during development (Bradley et al., 1992). However, repeating the experiments with *Thra1*$^{+m}$/*Thrb*$^{-/-}$ offspring and *Thrb*$^{-/-}$ controls (Forrest et al., 1996) indicated that TRβ plays only a minor role in the system. Since TRα1 was described to be expressed from E13.5 onwards in post-mitotic neurones (Wallis et al., 2010) and PV neurones in the AHA switch from proliferation to differentiation around E12, the experiment was repeated with wt mothers, treated with T_3 only during the critical TRα1 target period from E12 until birth. This avoids high levels of TH at earlier phases of development. The approach successfully rescued the neuronal population in *Thra1*$^{+m}$ offspring, demonstrating that the liganded TRα1 is crucial for PV neuronal development in the AHA in the second half of murine pregnancy, which is before the onset of foetal TH production (Nilsson and Fagman, 2017). The unfavourable role of TH for proliferation in early development has also been described for other systems, e.g. cone photoreceptor development. Here, high level of DIO3 ensure low TH activity during prenatal development, which reverse during retina differentiation after birth. In line with that, *Dio3* ko mice display an 80 % reduction in M and S cones due to TH induced apoptosis. This is most likely mediated by TRβ, because in contrast to our model,

the cone photoreceptor phenotype can be rescued by TRβ deletion (Ng et al., 2010). Taken together, one can hypothesise that high TH levels have an adverse effect before E12.5 for the development of PV neurones in the AHA; however, the role of TRβ in this context is unknown because there is still not enough information about the expression of TRβ at cellular level in the brain. The findings are also important for mothers with TRβ resistance, who carry an unaffected foetus. Their offspring are exposed to very high TH concentrations during pregnancy, leading to a higher rate of miscarriage, lower birth weight and central resistance to TH throughout life (Anselmo et al., 2004; Srichomkwun et al., 2017). It is likely that these children also display morphological changes in the brain. Generally, the data do not allow any conclusions about the neuroanatomical fate of the PV neurones in the AHA in the situation of restricted TH signalling. The lack of TH signalling could interfere with migration, which is why the neurones do not reach the AHA, or it could lead to increased cell death in the population at any point of their development.

In summary, the data demonstrate that correct development of PV neurones in the AHA is not possible without a tight regulation of TH action, and that the timing of TH sensitivity varies for different PV populations in the brain. When transferring the findings to the human condition, it has to be considered that mice are born at an earlier time point during development. Thereby, the second half of pregnancy in mice is most comparable with the second trimester in humans (Richard and Flamant, 2018). Again, this is a time frame in humans when the foetal thyroid gland is not yet producing TH on its own (Shepard, 1967), linking for the first-time maternal endocrinology to a defined neuroanatomical substrate in the offspring. Considering that the PV neurones in the AHA are involved in the central control of the cardiovascular system, these findings provide further evidence, that maternal TH concentration during pregnancy and control of blood pressure in the offspring are connected. Similar observations were made in humans, when a Danish study found an association between subclinical maternal hypothyroidism during pregnancy and increased systolic blood pressure in the offspring at an age of 20. Interestingly, hypertension was also found in children from mothers with subclinical hyperthyroidism during pregnancy (Rytter et al., 2016). In the ongoing discussion about treatment of TH diseases during pregnancy this clearly advocates for routine maternal thyroid screening in pregnancy and the inclusion of cardiovascular parameters in studies aiming to assess maternal thyroid status. Furthermore, these findings could also be used to establish a testing system for endocrine disrupting compounds during pregnancy (Gore et al., 2015). Still, further investigations are necessary to identify how PV neurones from the AHA are involved in the process of central cardiovascular control.

5. References

Abel, E.D., Ahima, R.S., Boers, M.E., Elmquist, J.K., and Wondisford, F.E. (2001). Critical role for thyroid hormone receptor beta2 in the regulation of paraventricular thyrotropin-releasing hormone neurons. J Clin Invest *107*, 1017-1023.

Ackermans, M.T., Klieverik, L.P., Ringeling, P., Endert, E., Kalsbeek, A., and Fliers, E. (2010). An online solid-phase extraction-liquid chromatography-tandem mass spectrometry method to study the presence of thyronamines in plasma and tissue and their putative conversion from 13C6-thyroxine. J Endocrinol *206*, 327-334.

Alexander, E.K., Pearce, E.N., Brent, G.A., Brown, R.S., Chen, H., Dosiou, C., Grobman, W.A., Laurberg, P., Lazarus, J.H., Mandel, S.J., *et al.* (2017). 2017 Guidelines of the American Thyroid Association for the Diagnosis and Management of Thyroid Disease During Pregnancy and the Postpartum. Thyroid *27*, 315-389.

Allolio, B., and Schulte, H.M. (2011). Praktische Endokrinologie, 2 edn ([s.l.]: Urban Fischer Verlag - Nachschlagewerke).

Alvarez-Bolado, G., Zhou, X., Cecconi, F., and Gruss, P. (2000). Expression of Foxb1 reveals two strategies for the formation of nuclei in the developing ventral diencephalon. Dev Neurosci *22*, 197-206.

Andersen, S.L., Laurberg, P., Wu, C.S., and Olsen, J. (2014). Attention deficit hyperactivity disorder and autism spectrum disorder in children born to mothers with thyroid dysfunction: a Danish nationwide cohort study. BJOG *121*, 1365-1374.

Aniello, F., Couchie, D., Gripois, D., and Nunez, J. (1991). Regulation of five tubulin isotypes by thyroid hormone during brain development. J Neurochem *57*, 1781-1786.

Anselmo, J., Cao, D., Karrison, T., Weiss, R.E., and Refetoff, S. (2004). Fetal loss associated with excess thyroid hormone exposure. JAMA *292*, 691-695.

Armbruster, B.N., Li, X., Pausch, M.H., Herlitze, S., and Roth, B.L. (2007). Evolving the lock to fit the key to create a family of G protein-coupled receptors potently activated by an inert ligand. Proc Natl Acad Sci U S A *104*, 5163-5168.

Astrup, A., Simonsen, L., Bulow, J., Madsen, J., and Christensen, N.J. (1989). Epinephrine mediates facultative carbohydrate-induced thermogenesis in human skeletal muscle. Am J Physiol *257*, E340-345.

Balazs, R., Brooksbank, B.W., Davison, A.N., Eayrs, J.T., and Wilson, D.A. (1969). The effect of neonatal thyroidectomy on myelination in the rat brain. Brain Res *15*, 219-232.

Berbel, P., Marco, P., Cerezo, J.R., and DeFelipe, J. (1996). Distribution of parvalbumin immunoreactivity in the neocortex of hypothyroid adult rats. Neurosci Lett *204*, 65-68.

Bernal, J. (2015). Thyroid Hormones in Brain Development and Function BTI - Endotext.

Bernal, J., and Morte, B. (2013). Thyroid hormone receptor activity in the absence of ligand: physiological and developmental implications. Biochim Biophys Acta *1830*, 3893-3899.

Bhasin, S., Wallace, W., Lawrence, J.B., and Lesch, M. (1981). Sudden death associated with thyroid hormone abuse. Am J Med *71*, 887-890.

Bilella, A., Alvarez-Bolado, G., and Celio, M.R. (2016). Birthdate of parvalbumin-neurons in the Parvafox-nucleus of the lateral hypothalamus. Brain Res *1633*, 111-114.

Bochukova, E., Schoenmakers, N., Agostini, M., Schoenmakers, E., Rajanayagam, O., Keogh, J.M., Henning, E., Reinemund, J., Gevers, E., Sarri, M., *et al.* (2012). A mutation in the thyroid hormone receptor alpha gene. N Engl J Med *366*, 243-249.

Bookout, A.L., Jeong, Y., Downes, M., Yu, R.T., Evans, R.M., and Mangelsdorf, D.J. (2006). Anatomical profiling of nuclear receptor expression reveals a hierarchical transcriptional network. Cell *126*, 789-799.

Brabant, G., Peeters, R.P., Chan, S.Y., Bernal, J., Bouchard, P., Salvatore, D., Boelaert, K., and Laurberg, P. (2015). Management of subclinical hypothyroidism in pregnancy: are we too simplistic? Eur J Endocrinol *173*, P1-P11.

Bradley, D.J., Towle, H.C., and Young, W.S., 3rd (1992). Spatial and temporal expression of alpha- and beta-thyroid hormone receptor mRNAs, including the beta 2-subtype, in the developing mammalian nervous system. J Neurosci *12*, 2288-2302.

Braulke, L.J., Klingenspor, M., DeBarber, A., Tobias, S.C., Grandy, D.K., Scanlan, T.S., and Heldmaier, G. (2008). 3-Iodothyronamine: a novel hormone controlling the balance between glucose and lipid utilisation. J Comp Physiol B *178*, 167-177.

Braunstein, G.D., Koblin, R., Sugawara, M., Pekary, A.E., and Hershman, J.M. (1986). Unintentional thyrotoxicosis factitia due to a diet pill. West J Med *145*, 388-391.

Braverman, L.E., Ingbar, S.H., and Sterling, K. (1970). Conversion of thyroxine (T4) to triiodothyronine (T3) in athyreotic human subjects. J Clin Invest *49*, 855-864.

Cabello, G., and Wrutniak, C. (1989). Thyroid hormone and growth: relationships with growth hormone effects and regulation. Reprod Nutr Dev *29*, 387-402.

Calvo, R.M., Jauniaux, E., Gulbis, B., Asuncion, M., Gervy, C., Contempre, B., and Morreale de Escobar, G. (2002). Fetal tissues are exposed to biologically relevant free thyroxine concentrations during early phases of development. J Clin Endocrinol Metab *87*, 1768-1777.

Cannon, B., and Nedergaard, J. (2004). Brown adipose tissue: function and physiological significance. Physiol Rev *84*, 277-359.

Carle, A., Pedersen, I.B., Knudsen, N., Perrild, H., Ovesen, L., Rasmussen, L.B., and Laurberg, P. (2011). Epidemiology of subtypes of hyperthyroidism in Denmark: a population-based study. Eur J Endocrinol *164*, 801-809.

Casey, B.M., Thom, E.A., Peaceman, A.M., Varner, M.W., Sorokin, Y., Hirtz, D.G., Reddy, U.M., Wapner, R.J., Thorp, J.M., Jr., Saade, G., *et al.* (2017). Treatment of Subclinical Hypothyroidism or Hypothyroxinemia in Pregnancy. N Engl J Med *376*, 815-825.

Celio, M.R. (1986). Parvalbumin in most gamma-aminobutyric acid-containing neurons of the rat cerebral cortex. Science *231*, 995-997.

Celio, M.R. (1990). Calbindin D-28k and parvalbumin in the rat nervous system. Neuroscience *35*, 375-475.

Celio, M.R., and Heizmann, C.W. (1981). Calcium-binding protein parvalbumin as a neuronal marker. Nature *293*, 300-302.

Cetin, A., Komai, S., Eliava, M., Seeburg, P.H., and Osten, P. (2006). Stereotaxic gene delivery in the rodent brain. Nat Protoc *1*, 3166-3173.

Chambard, M., Mauchamp, J., and Chabaud, O. (1987). Synthesis and apical and basolateral secretion of thyroglobulin by thyroid cell monolayers on permeable substrate: modulation by thyrotropin. J Cell Physiol *133*, 37-45.

Chan, S., Kachilele, S., McCabe, C.J., Tannahill, L.A., Boelaert, K., Gittoes, N.J., Visser, T.J., Franklyn, J.A., and Kilby, M.D. (2002). Early expression of thyroid hormone deiodinases and receptors in human fetal cerebral cortex. Brain Res Dev Brain Res *138*, 109-116.

Chan, S.Y., Vasilopoulou, E., and Kilby, M.D. (2009). The role of the placenta in thyroid hormone delivery to the fetus. Nat Clin Pract Endocrinol Metab *5*, 45-54.

Clements, F.W., de Moerloose, J., de Smet, M.P., Holman, J.C.M., Kelly, F.C., Langer, P., Lissitzky, S., Lowenstein, F.W., McCartney, W., Matovinović, J., *et al.* (1961). Endemic goitre. world health organization monograph series no. 44. Annals of Internal Medicine *54*, 171-171.

Coleman, P.S., Parmacek, M.S., Lesch, M., and Samarel, A.M. (1989). Protein synthesis and degradation during regression of thyroxine-induced cardiac hypertrophy. J Mol Cell Cardiol *21*, 911-925.

Contempre, B., Jauniaux, E., Calvo, R., Jurkovic, D., Campbell, S., and de Escobar, G.M. (1993). Detection of thyroid hormones in human embryonic cavities during the first trimester of pregnancy. J Clin Endocrinol Metab *77*, 1719-1722.

Corbin, J.G., and Butt, S.J. (2011). Developmental mechanisms for the generation of telencephalic interneurons. Dev Neurobiol *71*, 710-732.

Cukier, P., Santini, F.C., Scaranti, M., and Hoff, A.O. (2017). Endocrine side effects of cancer immunotherapy. Endocr Relat Cancer *24*, T331-T347.

Dai, G., Levy, O., and Carrasco, N. (1996). Cloning and characterization of the thyroid iodide transporter. Nature *379*, 458-460.

de Escobar, G.M., Ares, S., Berbel, P., Obregon, M.J., and del Rey, F.E. (2008). The changing role of maternal thyroid hormone in fetal brain development. Semin Perinatol *32*, 380-386.

De Felice, M., and Di Lauro, R. (2004). Thyroid development and its disorders: genetics and molecular mechanisms. Endocr Rev *25*, 722-746.

de Lecea, L., del Rio, J.A., and Soriano, E. (1995). Developmental expression of parvalbumin mRNA in the cerebral cortex and hippocampus of the rat. Brain Res Mol Brain Res *32*, 1-13.

De Leo, S., Lee, S.Y., and Braverman, L.E. (2016). Hyperthyroidism. Lancet *388*, 906-918.

Di Cosmo, C., Liao, X.H., Dumitrescu, A.M., Philp, N.J., Weiss, R.E., and Refetoff, S. (2010). Mice deficient in MCT8 reveal a mechanism regulating thyroid hormone secretion. J Clin Invest *120*, 3377-3388.

Dillmann, W. (2010). Cardiac hypertrophy and thyroid hormone signaling. Heart Fail Rev *15*, 125-132.

Distiller, L.A., and Joffe, B.I. (1975). Transient hypothyroidism after withdrawal of thyroxin therapy. Postgrad Med J *51*, 665-666.

Duan, Y.F., Winters, R., McCabe, P.M., Green, E.J., Huang, Y., and Schneiderman, N. (1997). Cardiorespiratory components of defense reaction elicited from paraventricular nucleus. Physiol Behav *61*, 325-330.

Everts, M.E., Verhoeven, F.A., Bezstarosti, K., Moerings, E.P., Hennemann, G., Visser, T.J., and Lamers, J.M. (1996). Uptake of thyroid hormones in neonatal rat cardiac myocytes. Endocrinology *137*, 4235-4242.

Falcone, M., Miyamoto, T., Fierro-Renoy, F., Macchia, E., and DeGroot, L.J. (1992). Antipeptide polyclonal antibodies specifically recognize each human thyroid hormone receptor isoform. Endocrinology *131*, 2419-2429.

Felten, D.L., O'Banion, M.K., and Summo Maida, M. (2016). Netter's Atlas of Neuroscience, Third Edition edn (Philadelphia, PA: Elsevier).

Ferguson, A.V., Latchford, K.J., and Samson, W.K. (2008). The paraventricular nucleus of the hypothalamus - a potential target for integrative treatment of autonomic dysfunction. Expert Opin Ther Targets *12*, 717-727.

Ferreiro, B., Bernal, J., Goodyer, C.G., and Branchard, C.L. (1988). Estimation of nuclear thyroid hormone receptor saturation in human fetal brain and lung during early gestation. J Clin Endocrinol Metab *67*, 853-856.

Flamant, F., Gauthier, K., and Richard, S. (2017). Genetic Investigation of Thyroid Hormone Receptor Function in the Developing and Adult Brain. Curr Top Dev Biol *125*, 303-335.

Flames, N., Pla, R., Gelman, D.M., Rubenstein, J.L., Puelles, L., and Marin, O. (2007). Delineation of multiple subpallial progenitor domains by the combinatorial expression of transcriptional codes. J Neurosci *27*, 9682-9695.

Flores-Morales, A., Gullberg, H., Fernandez, L., Stahlberg, N., Lee, N.H., Vennström, B., and Norstedt, G. (2002). Patterns of liver gene expression governed by TRbeta. Mol Endocrinol *16*, 1257-1268.

Fogarty, M., Grist, M., Gelman, D., Marin, O., Pachnis, V., and Kessaris, N. (2007). Spatial genetic patterning of the embryonic neuroepithelium generates GABAergic interneuron diversity in the adult cortex. J Neurosci *27*, 10935-10946.

Folkow, B., Johansson, B., and Oberg, B. (1959). A hypothalamic structure with a marked inhibitory effect on tonic sympathetic activity. Acta Physiol Scand *47*, 262-270.

Ford, G., and LaFranchi, S.H. (2014). Screening for congenital hypothyroidism: a worldwide view of strategies. Best Pract Res Clin Endocrinol Metab *28*, 175-187.

Forrest, D., Hanebuth, E., Smeyne, R.J., Everds, N., Stewart, C.L., Wehner, J.M., and Curran, T. (1996). Recessive resistance to thyroid hormone in mice lacking thyroid hormone receptor beta: evidence for tissue-specific modulation of receptor function. EMBO J *15*, 3006-3015.

Frank, K.F., Bolck B Fau - Erdmann, E., Erdmann E Fau - Schwinger, R.H.G., and Schwinger, R.H. (2003). Sarcoplasmic reticulum Ca2+-ATPase modulates cardiac contraction and relaxation.

Friedrichs, B., Tepel, C., Reinheckel, T., Deussing, J., von Figura, K., Herzog, V., Peters, C., Saftig, P., and Brix, K. (2003). Thyroid functions of mouse cathepsins B, K, and L. J Clin Invest *111*, 1733-1745.

Friesema, E.C., Docter, R., Moerings, E.P., Verrey, F., Krenning, E.P., Hennemann, G., and Visser, T.J. (2001). Thyroid hormone transport by the heterodimeric human system L amino acid transporter. Endocrinology *142*, 4339-4348.

Friesema, E.C., Ganguly, S., Abdalla, A., Manning Fox, J.E., Halestrap, A.P., and Visser, T.J. (2003). Identification of monocarboxylate transporter 8 as a specific thyroid hormone transporter. J Biol Chem *278*, 40128-40135.

Friesema, E.C., Grueters, A., Biebermann, H., Krude, H., von Moers, A., Reeser, M., Barrett, T.G., Mancilla, E.E., Svensson, J., Kester, M.H., *et al.* (2004). Association between mutations in a thyroid hormone transporter and severe X-linked psychomotor retardation. Lancet *364*, 1435-1437.

Friesema, E.C., Jansen, J., Jachtenberg, J.W., Visser, W.E., Kester, M.H., and Visser, T.J. (2008). Effective cellular uptake and efflux of thyroid hormone by human monocarboxylate transporter 10. Mol Endocrinol *22*, 1357-1369.

Gelman, D.M., Martini, F.J., Nobrega-Pereira, S., Pierani, A., Kessaris, N., and Marin, O. (2009). The embryonic preoptic area is a novel source of cortical GABAergic interneurons. J Neurosci *29*, 9380-9389.

Geraci, T., Fjeld, C., Coasurdo, V., Samuels, M., Schuff, K., and Scanlan, T.S. (2008). 3-Iodothyronamine (T1AM) levels in human serum and tissue. In 79th Annual Meeting of the American Thyroid Association (Chicago, IL).

Glinoer, D. (2001). Potential consequences of maternal hypothyroidism on the offspring: evidence and implications. Horm Res *55*, 109-114.

Glinoer, D., and Delange, F. (2000). The potential repercussions of maternal, fetal, and neonatal hypothyroxinemia on the progeny. Thyroid *10*, 871-887.

Gomez, J.L., Bonaventura, J., Lesniak, W., Mathews, W.B., Sysa-Shah, P., Rodriguez, L.A., Ellis, R.J., Richie, C.T., Harvey, B.K., Dannals, R.F., *et al.* (2017). Chemogenetics revealed: DREADD occupancy and activation via converted clozapine. Science *357*, 503-507.

Gong, D.W., He, Y., Karas, M., and Reitman, M. (1997). Uncoupling protein-3 is a mediator of thermogenesis regulated by thyroid hormone, beta3-adrenergic agonists, and leptin. J Biol Chem *272*, 24129-24132.

Gonzalez-Burgos, G., Cho, R.Y., and Lewis, D.A. (2015). Alterations in cortical network oscillations and parvalbumin neurons in schizophrenia. Biol Psychiatry *77*, 1031-1040.

Gore, A.C., Chappell, V.A., Fenton, S.E., Flaws, J.A., Nadal, A., Prins, G.S., Toppari, J., and Zoeller, R.T. (2015). EDC-2: The Endocrine Society's Second Scientific Statement on Endocrine-Disrupting Chemicals. Endocr Rev *36*, E1-E150.

Göthe, S., Wang, Z., Ng, L., Kindblom, J.M., Barros, A.C., Ohlsson, C., Vennström, B., and Forrest, D. (1999). Mice devoid of all known thyroid hormone receptors are viable but exhibit disorders of the pituitary-thyroid axis, growth, and bone maturation. Genes Dev *13*, 1329-1341.

Grüters, A., and Krude, H. (2011). Detection and treatment of congenital hypothyroidism. Nat Rev Endocrinol *8*, 104-113.

Guadano-Ferraz, A., Obregon, M.J., St Germain, D.L., and Bernal, J. (1997). The type 2 iodothyronine deiodinase is expressed primarily in glial cells in the neonatal rat brain. Proc Natl Acad Sci U S A *94*, 10391-10396.

Guillery, R.W., and Herrup, K. (1997). Quantification without pontification: choosing a method for counting objects in sectioned tissues. J Comp Neurol *386*, 2-7.

Haddow, J.E., Palomaki, G.E., Allan, W.C., Williams, J.R., Knight, G.J., Gagnon, J., O'Heir, C.E., Mitchell, M.L., Hermos, R.J., Waisbren, S.E., *et al.* (1999). Maternal thyroid deficiency during pregnancy and subsequent neuropsychological development of the child. N Engl J Med *341*, 549-555.

Hannemann, A., Friedrich, N., Haring, R., Krebs, A., Völzke, H., Alte, D., Nauck, M., Kohlmann, T., Schober, H.C., Hoffmann, W., *et al.* (2010). Thyroid function tests in patients taking thyroid medication in Germany: Results from the population-based Study of Health in Pomerania (SHIP). BMC Res Notes *3*, 227.

Harder, L., Dudazy-Gralla, S., Müller-Fielitz, H., Hjerling Leffler, J., Vennström, B., Heuer, H., and Mittag, J. (2018a). Maternal Thyroid Hormone is Required for Parvalbumin Neuron Development in the Anterior Hypothalamic Area. J Neuroendocrinol.

Harder, L., Schanze, N., Sarsenbayeva, A., Kugel, F., Köhrle, J., Schomburg, L., Mittag, J., and Hoefig, C.S. (2018b). In vivo Effects of Repeated Thyronamine Administration in Male C57BL/6J Mice. European Thyroid Journal *7*, 3-12.

Heinonen, A.M., Rahman, M., Dogbevia, G., Jakobi, H., Wolfl, S., Sprengel, R., and Schwaninger, M. (2014). Neuroprotection by rAAV-mediated gene transfer of bone morphogenic protein 7. BMC Neurosci *15*, 38.

Heizmann, C.W. (1984). Parvalbumin, an intracellular calcium-binding protein; distribution, properties and possible roles in mammalian cells. Experientia *40*, 910-921.

Hirsch, D., Levy, S., Nadler, V., Kopel, V., Shainberg, B., and Toledano, Y. (2013). Pregnancy outcomes in women with severe hypothyroidism. Eur J Endocrinol *169*, 313-320.

Hoefig, C.S., Harder, L., Oelkrug, R., Meusel, M., Vennström, B., Brabant, G., and Mittag, J. (2016a). Thermoregulatory and Cardiovascular Consequences of a Transient Thyrotoxicosis and Recovery in Male Mice. Endocrinology *157*, 2957-2967.

Hoefig, C.S., Jacobi, S.F., Warner, A., Harder, L., Schanze, N., Vennström, B., and Mittag, J. (2015a). 3-Iodothyroacetic acid lacks thermoregulatory and cardiovascular effects in vivo. Br J Pharmacol *172*, 3426-3433.

Hoefig, C.S., Köhrle, J., Brabant, G., Dixit, K., Yap, B., Strasburger, C.J., and Wu, Z. (2011). Evidence for extrathyroidal formation of 3-iodothyronamine in humans as provided by a novel monoclonal antibody-based chemiluminescent serum immunoassay. J Clin Endocrinol Metab *96*, 1864-1872.

Hoefig, C.S., Wuensch, T., Rijntjes, E., Lehmphul, I., Daniel, H., Schweizer, U., Mittag, J., and Köhrle, J. (2015b). Biosynthesis of 3-Iodothyronamine From T4 in Murine Intestinal Tissue. Endocrinology *156*, 4356-4364.

Hoefig, C.S., Zucchi, R., and Köhrle, J. (2016b). Thyronamines and Derivatives: Physiological Relevance, Pharmacological Actions, and Future Research Directions. Thyroid *26*, 1656-1673.

Ioos, V., Das, V., Maury, E., Baudel, J.L., Guechot, J., Guidet, B., and Offenstadt, G. (2008). A thyrotoxicosis outbreak due to dietary pills in Paris. Ther Clin Risk Manag *4*, 1375-1379.

Jastroch, M., Hirschberg, V., and Klingenspor, M. (2012). Functional characterization of UCP1 in mammalian HEK293 cells excludes mitochondrial uncoupling artefacts and reveals no contribution to basal proton leak. Biochim Biophys Acta *1817*, 1660-1670.

Johns, L.E., Ferguson, K.K., Cantonwine, D.E., Mukherjee, B., Meeker, J.D., and McElrath, T.F. (2017). Subclinical Changes in Maternal Thyroid Function Parameters in Pregnancy and Fetal Growth. J Clin Endocrinol Metab.

Jones, I., Ng, L., Liu, H., and Forrest, D. (2007). An intron control region differentially regulates expression of thyroid hormone receptor beta2 in the cochlea, pituitary, and cone photoreceptors. Mol Endocrinol *21*, 1108-1119.

Karakosta, P., Alegakis, D., Georgiou, V., Roumeliotaki, T., Fthenou, E., Vassilaki, M., Boumpas, D., Castanas, E., Kogevinas, M., and Chatzi, L. (2012). Thyroid dysfunction and autoantibodies in early pregnancy are associated with increased risk of gestational diabetes and adverse birth outcomes. J Clin Endocrinol Metab *97*, 4464-4472.

Kelsom, C., and Lu, W. (2013). Development and specification of GABAergic cortical interneurons. Cell Biosci *3*, 19.

Khattak, R.M., Ittermann, T., Nauck, M., Below, H., and Völzke, H. (2016). Monitoring the prevalence of thyroid disorders in the adult population of Northeast Germany. Popul Health Metr *14*, 39.

Kim, B. (2008). Thyroid hormone as a determinant of energy expenditure and the basal metabolic rate. Thyroid *18*, 141-144.

Kimura, S., Hara, Y., Pineau, T., Fernandez-Salguero, P., Fox, C.H., Ward, J.M., and Gonzalez, F.J. (1996). The T/ebp null mouse: thyroid-specific enhancer-binding protein is essential for the organogenesis of the thyroid, lung, ventral forebrain, and pituitary. Genes Dev *10*, 60-69.

Klein, I., and Ojamaa, K. (2001). Thyroid hormone and the cardiovascular system. N Engl J Med *344*, 501-509.

Köhrle, J. (2000). The selenoenzyme family of deiodinase isozymes controls local thyroid hormone availability. Rev Endocr Metab Disord *1*, 49-58.

Köhrle, J. (2002). Iodothyronine deiodinases. Methods Enzymol *347*, 125-167.

Koibuchi, N., and M. Yen, P. (2016). Thyroid Hormone Disruption and Neurodevelopment.

Kopp, P. (2002). Perspective: genetic defects in the etiology of congenital hypothyroidism. Endocrinology *143*, 2019-2024.

Korevaar, T.I., Muetzel, R., Medici, M., Chaker, L., Jaddoe, V.W., de Rijke, Y.B., Steegers, E.A., Visser, T.J., White, T., Tiemeier, H., *et al.* (2016). Association of maternal thyroid function during early pregnancy with offspring IQ and brain morphology in childhood: a population-based prospective cohort study. Lancet Diabetes Endocrinol *4*, 35-43.

Korevaar, T.I.M., Medici, M., Visser, T.J., and Peeters, R.P. (2017). Thyroid disease in pregnancy: new insights in diagnosis and clinical management. Nat Rev Endocrinol *13*, 610-622.

Krashes, M.J., Koda, S., Ye, C., Rogan, S.C., Adams, A.C., Cusher, D.S., Maratos-Flier, E., Roth, B.L., and Lowell, B.B. (2011). Rapid, reversible activation of AgRP neurons drives feeding behavior in mice. J Clin Invest *121*, 1424-1428.

Lazar, M.A. (1993). Thyroid hormone receptors: multiple forms, multiple possibilities. Endocr Rev *14*, 184-193.

Lazarus, J., Brown, R.S., Daumerie, C., Hubalewska-Dydejczyk, A., Negro, R., and Vaidya, B. (2014). 2014 European thyroid association guidelines for the management of subclinical hypothyroidism in pregnancy and in children. Eur Thyroid J *3*, 76-94.

Lazarus, J.H., Bestwick, J.P., Channon, S., Paradice, R., Maina, A., Rees, R., Chiusano, E., John, R., Guaraldo, V., George, L.M., *et al.* (2012). Antenatal thyroid screening and childhood cognitive function. N Engl J Med *366*, 493-501.

Lee, D.A., Bedont, J.L., Pak, T., Wang, H., Song, J., Miranda-Angulo, A., Takiar, V., Charubhumi, V., Balordi, F., Takebayashi, H., *et al.* (2012). Tanycytes of the hypothalamic median eminence form a diet-responsive neurogenic niche. Nat Neurosci *15*, 700-702.

Leonard, J.L., and Rosenberg, I.N. (1981). Solubilization of a phospholipid-requiring enzyme, iodothyronine 5'-deiodinase, from rat kidney membranes. Biochim Biophys Acta *659*, 205-218.

Liang, F., Webb, P., Marimuthu, A., Zhang, S., and Gardner, D.G. (2003). Triiodothyronine increases brain natriuretic peptide (BNP) gene transcription and amplifies endothelin-dependent BNP gene transcription and hypertrophy in neonatal rat ventricular myocytes. J Biol Chem *278*, 15073-15083.

Liggett, S.B. (2004). The two-timing thyroid. Nat Med *10*, 582-583.

Lin, J.Z., Martagon, A.J., Cimini, S.L., Gonzalez, D.D., Tinkey, D.W., Biter, A., Baxter, J.D., Webb, P., Gustafsson, J.A., Hartig, S.M., *et al.* (2015). Pharmacological Activation of Thyroid Hormone Receptors Elicits a Functional Conversion of White to Brown Fat. Cell Rep *13*, 1528-1537.

Lischinsky, J.E., Skocic, J., Clairman, H., and Rovet, J. (2016). Preliminary Findings Show Maternal Hypothyroidism May Contribute to Abnormal Cortical Morphology in Offspring. Front Endocrinol (Lausanne) *7*, 16.

Lopez, M., Alvarez, C.V., Nogueiras, R., and Dieguez, C. (2013). Energy balance regulation by thyroid hormones at central level. Trends Mol Med *19*, 418-427.

Lopez, M., Varela, L., Vazquez, M.J., Rodriguez-Cuenca, S., Gonzalez, C.R., Velagapudi, V.R., Morgan, D.A., Schoenmakers, E., Agassandian, K., Lage, R., *et al.* (2010). Hypothalamic AMPK and fatty acid metabolism mediate thyroid regulation of energy balance. Nat Med *16*, 1001-1008.

Luche, H., Weber, O., Nageswara Rao, T., Blum, C., and Fehling, H.J. (2007). Faithful activation of an extra-bright red fluorescent protein in "knock-in" Cre-reporter mice ideally suited for lineage tracing studies. Eur J Immunol *37*, 43-53.

Ludwig, A., Budde, T., Stieber, J., Moosmang, S., Wahl, C., Holthoff, K., Langebartels, A., Wotjak, C., Munsch, T., Zong, X., *et al.* (2003). Absence epilepsy and sinus dysrhythmia in mice lacking the pacemaker channel HCN2. EMBO J *22*, 216-224.

Madisen, L., Zwingman, T.A., Sunkin, S.M., Oh, S.W., Zariwala, H.A., Gu, H., Ng, L.L., Palmiter, R.D., Hawrylycz, M.J., Jones, A.R., *et al.* (2010). A robust and high-throughput Cre reporting and characterization system for the whole mouse brain. Nat Neurosci *13*, 133-140.

Maenhaut, C., Christophe, D., Vassart, G., Dumont, J., Roger, P.P., and Opitz, R. (2000). Ontogeny, Anatomy, Metabolism and Physiology of the Thyroid. In Endotext, L.J. De Groot, G. Chrousos, K. Dungan, K.R. Feingold, A. Grossman, J.M. Hershman, C. Koch, M. Korbonits, R. McLachlan, M. New, *et al.*, eds. (South Dartmouth (MA)).

Man, E.B., Brown, J.F., and Serunian, S.A. (1991). Maternal hypothyroxinemia: psychoneurological deficits of progeny. Ann Clin Lab Sci *21*, 227-239.

Mansouri, A., Chowdhury, K., and Gruss, P. (1998). Follicular cells of the thyroid gland require Pax8 gene function. Nat Genet *19*, 87-90.

Manvich, D.F., Webster, K.A., Foster, S.L., Farrell, M.S., Ritchie, J.C., Porter, J.H., and Weinshenker, D. (2018). The DREADD agonist clozapine N-oxide (CNO) is reverse-metabolized to clozapine and produces clozapine-like interoceptive stimulus effects in rats and mice. Sci Rep *8*, 3840.

Mariotta, L., Ramadan, T., Singer, D., Guetg, A., Herzog, B., Stoeger, C., Palacin, M., Lahoutte, T., Camargo, S.M., and Verrey, F. (2012). T-type amino acid transporter TAT1 (Slc16a10) is essential for extracellular aromatic amino acid homeostasis control. J Physiol *590*, 6413-6424.

Mark, P.B., Watkins, S., and Dargie, H.J. (2005). Cardiomyopathy induced by performance enhancing drugs in a competitive bodybuilder. Heart *91*, 888.

Martino, E., Safran, M., Aghini-Lombardi, F., Rajatanavin, R., Lenziardi, M., Fay, M., Pacchiarotti, A., Aronin, N., Macchia, E., Haffajee, C., *et al.* (1984). Environmental iodine intake and thyroid dysfunction during chronic amiodarone therapy. Ann Intern Med *101*, 28-34.

Mayerl, S., Müller, J., Bauer, R., Richert, S., Kassmann, C.M., Darras, V.M., Buder, K., Boelen, A., Visser, T.J., and Heuer, H. (2014). Transporters MCT8 and OATP1C1 maintain murine brain thyroid hormone homeostasis. J Clin Invest *124*, 1987-1999.

Mayr, F.B., Domanovits, H., and Laggner, A.N. (2012). Hypokalemic paralysis in a professional bodybuilder. Am J Emerg Med *30*, 1324 e1325-1328.

McKillop, G. (1987). Drug abuse in body builders in the West of Scotland. Scott Med J *32*, 39-41.

Messier, N., Laflamme, L., Hamann, G., and Langlois, M.F. (2001). In vitro effect of Triac on resistance to thyroid hormone receptor mutants: potential basis for therapy. Mol Cell Endocrinol *174*, 59-69.

Meszar, Z., Girard, F., Saper, C.B., and Celio, M.R. (2012). The lateral hypothalamic parvalbumin-immunoreactive (PV1) nucleus in rodents. J Comp Neurol *520*, 798-815.

Mittag, J., Friedrichsen, S., Strube, A., Heuer, H., and Bauer, K. (2009). Analysis of hypertrophic thyrotrophs in pituitaries of athyroid Pax8-/- mice. Endocrinology *150*, 4443-4449.

Mittag, J., Lyons, D.J., Sällström, J., Vujovic, M., Dudazy-Gralla, S., Warner, A., Wallis, K., Alkemade, A., Nordström, K., Monyer, H., *et al.* (2013). Thyroid hormone is required for hypothalamic neurons regulating cardiovascular functions. J Clin Invest *123*, 509-516.

Miyoshi, G., Butt, S.J., Takebayashi, H., and Fishell, G. (2007). Physiologically distinct temporal cohorts of cortical interneurons arise from telencephalic Olig2-expressing precursors. J Neurosci *27*, 7786-7798.

Morley, J.E. (1981). Neuroendocrine control of thyrotropin secretion. Endocr Rev *2*, 396-436.

Müller-Fielitz, H., Stahr, M., Bernau, M., Richter, M., Abele, S., Krajka, V., Benzin, A., Wenzel, J., Kalies, K., Mittag, J., *et al.* (2017). Tanycytes control the hormonal output of the hypothalamic-pituitary-thyroid axis. Nat Commun *8*, 484.

Müller, J., Mayerl, S., Visser, T.J., Darras, V.M., Boelen, A., Frappart, L., Mariotta, L., Verrey, F., and Heuer, H. (2014). Tissue-specific alterations in thyroid hormone homeostasis in combined Mct10 and Mct8 deficiency. Endocrinology *155*, 315-325.

Munoz-Manchado, A.B., Foldi, C., Szydlowski, S., Sjulson, L., Farries, M., Wilson, C., Silberberg, G., and Hjerling Leffler, J. (2016). Novel Striatal GABAergic Interneuron Populations Labeled in the 5HT3a(EGFP) Mouse. Cereb Cortex *26*, 96-105.

Musatov, S., Roberts, J., Pfaff, D., and Kaplitt, M. (2002). A cis-acting element that directs circular adeno-associated virus replication and packaging. J Virol *76*, 12792-12802.

Nakagawa, O., Ogawa, Y., Itoh, H., Suga, S., Komatsu, Y., Kishimoto, I., Nishino, K., Yoshimasa, T., and Nakao, K. (1995). Rapid transcriptional activation and early mRNA turnover of brain natriuretic peptide in cardiocyte hypertrophy. Evidence for brain natriuretic peptide as an "emergency" cardiac hormone against ventricular overload. J Clin Invest *96*, 1280-1287.

Ng, L., Lyubarsky, A., Nikonov, S.S., Ma, M., Srinivas, M., Kefas, B., St Germain, D.L., Hernandez, A., Pugh, E.N., Jr., and Forrest, D. (2010). Type 3 deiodinase, a thyroid-hormone-inactivating enzyme, controls survival and maturation of cone photoreceptors. J Neurosci *30*, 3347-3357.

Nicoloff, J.T., Low, J.C., Dussault, J.H., and Fisher, D.A. (1972). Simultaneous measurement of thyroxine and triiodothyronine peripheral turnover kinetics in man. J Clin Invest *51*, 473-483.

Nilsson, M., and Fagman, H. (2017). Development of the thyroid gland. Development *144*, 2123-2140.

Nishimura, M., and Naito, S. (2008). Tissue-specific mRNA expression profiles of human solute carrier transporter superfamilies. Drug Metab Pharmacokinet *23*, 22-44.

Obregon, M.J. (2014). Adipose tissues and thyroid hormones. Front Physiol *5*, 479.

Okamatsu-Ogura, Y., Fukano, K., Tsubota, A., Uozumi, A., Terao, A., Kimura, K., and Saito, M. (2013). Thermogenic ability of uncoupling protein 1 in beige adipocytes in mice. PLoS One *8*, e84229.

Panas, H.N., Lynch, L.J., Vallender, E.J., Xie, Z., Chen, G.L., Lynn, S.K., Scanlan, T.S., and Miller, G.M. (2010). Normal thermoregulatory responses to 3-iodothyronamine, trace amines and amphetamine-like psychostimulants in trace amine associated receptor 1 knockout mice. J Neurosci Res *88*, 1962-1969.

Paxinos, G., and Franklin, K.B.J. (2004). The Mouse Brain in Stereotaxic Coordinates, 2 edn (USA: Elsevier Science).

Pearce, S.H., Brabant, G., Duntas, L.H., Monzani, F., Peeters, R.P., Razvi, S., and Wemeau, J.L. (2013). 2013 ETA Guideline: Management of Subclinical Hypothyroidism. Eur Thyroid J *2*, 215-228.

Piehl, S., Heberer, T., Balizs, G., Scanlan, T.S., Smits, R., Koksch, B., and Köhrle, J. (2008). Thyronamines Are Isozyme-Specific Substrates of Deiodinases. Endocrinology *149*, 3037-3045.

Pilo, A., Iervasi, G., Vitek, F., Ferdeghini, M., Cazzuola, F., and Bianchi, R. (1990). Thyroidal and peripheral production of 3,5,3'-triiodothyronine in humans by multicompartmental analysis. Am J Physiol *258*, E715-726.

Pizzagalli, F., Hagenbuch, B., Stieger, B., Klenk, U., Folkers, G., and Meier, P.J. (2002). Identification of a novel human organic anion transporting polypeptide as a high affinity thyroxine transporter. Mol Endocrinol *16*, 2283-2296.

Pop, V.J., Brouwers, E.P., Vader, H.L., Vulsma, T., van Baar, A.L., and de Vijlder, J.J. (2003). Maternal hypothyroxinaemia during early pregnancy and subsequent child development: a 3-year follow-up study. Clin Endocrinol (Oxf) *59*, 282-288.

Pyner, S. (2009). Neurochemistry of the paraventricular nucleus of the hypothalamus: implications for cardiovascular regulation. J Chem Neuroanat *38*, 197-208.

Rathmann, D., Rijntjes, E., Lietzow, J., and Köhrle, J. (2015). Quantitative Analysis of Thyroid Hormone Metabolites in Cell Culture Samples Using LC-MS/MS. Eur Thyroid J *4*, 51-58.

Refetoff, S. (1994). Resistance to thyroid hormone: an historical overview. Thyroid *4*, 345-349.

Richard, S., and Flamant, F. (2018). Regulation of T3 Availability in the Developing Brain: The Mouse Genetics Contribution. Front Endocrinol (Lausanne) *9*, 265.

Roland, B.L., and Sawchenko, P.E. (1993). Local origins of some GABAergic projections to the paraventricular and supraoptic nuclei of the hypothalamus in the rat. J Comp Neurol *332*, 123-143.

Ross, D.S., Burch, H.B., Cooper, D.S., Greenlee, M.C., Laurberg, P., Maia, A.L., Rivkees, S.A., Samuels, M., Sosa, J.A., Stan, M.N., *et al.* (2016). 2016 American Thyroid Association Guidelines for Diagnosis and Management of Hyperthyroidism and Other Causes of Thyrotoxicosis. Thyroid *26*, 1343-1421.

Rotaru, D.C., Lewis, D.A., and Gonzalez-Burgos, G. (2012). The role of glutamatergic inputs onto parvalbumin-positive interneurons: relevance for schizophrenia. Rev Neurosci *23*, 97-109.

Roth, B.L. (2016). DREADDs for Neuroscientists. Neuron *89*, 683-694.

Royaux, I.E., Suzuki, K., Mori, A., Katoh, R., Everett, L.A., Kohn, L.D., and Green, E.D. (2000). Pendrin, the protein encoded by the Pendred syndrome gene (PDS), is an apical porter of iodide in the thyroid and is regulated by thyroglobulin in FRTL-5 cells. Endocrinology *141*, 839-845.

Rudy, B., Fishell, G., Lee, S., and Hjerling Leffler, J. (2011). Three groups of interneurons account for nearly 100% of neocortical GABAergic neurons. Dev Neurobiol *71*, 45-61.

Rytter, D., Andersen, S.L., Bech, B.H., Halldorsson, T.I., Henriksen, T.B., Laurberg, P., and Olsen, S.F. (2016). Maternal thyroid function in pregnancy may program offspring blood pressure, but not adiposity at 20 y of age. Pediatr Res *80*, 7-13.

Saba, A., Chiellini, G., Frascarelli, S., Marchini, M., Ghelardoni, S., Raffaelli, A., Tonacchera, M., Vitti, P., Scanlan, T.S., and Zucchi, R. (2010). Tissue distribution and cardiac metabolism of 3-iodothyronamine. Endocrinology *151*, 5063-5073.

Sakurada, T., Rudolph, M., Fang, S.-L.L., Vagenakis, A.G., Braverman, L.E., and Ingbar, S.H. (1978). Evidence That Triiodothyronine and Reverse Triiodothyronine Are Sequentially Deiodinated in Man*. The Journal of Clinical Endocrinology & Metabolism *46*, 916-922.

Sap, J., Munoz, A., Damm, K., Goldberg, Y., Ghysdael, J., Leutz, A., Beug, H., and Vennström, B. (1986). The c-erb-A protein is a high-affinity receptor for thyroid hormone. Nature *324*, 635-640.

Sarlieve, L.L., Rodriguez-Pena, A., and Langley, K. (2004). Expression of thyroid hormone receptor isoforms in the oligodendrocyte lineage. Neurochem Res *29*, 903-922.

Scanlan, T.S., Suchland, K.L., Hart, M.E., Chiellini, G., Huang, Y., Kruzich, P.J., Frascarelli, S., Crossley, D.A., Bunzow, J.R., Ronca-Testoni, S., *et al.* (2004). 3-Iodothyronamine is an endogenous and rapid-acting derivative of thyroid hormone. Nat Med *10*, 638-642.

Schanze, N., Jacobi, S.F., Rijntjes, E., Mergler, S., Del Olmo, M., Hoefig, C.S., Khajavi, N., Lehmphul, I., Biebermann, H., Mittag, J., *et al.* (2017). 3-Iodothyronamine Decreases Expression of Genes Involved in Iodide Metabolism in Mouse Thyroids and Inhibits Iodide Uptake in PCCL3 Thyrocytes. Thyroid *27*, 11-22.

Schneider, C.A., Rasband, W.S., and Eliceiri, K.W. (2012). NIH Image to ImageJ: 25 years of image analysis. Nat Methods *9*, 671-675.

Schussler, G.C. (2000). The thyroxine-binding proteins. Thyroid *10*, 141-149.

Schwartz, C.E., May, M.M., Carpenter, N.J., Rogers, R.C., Martin, J., Bialer, M.G., Ward, J., Sanabria, J., Marsa, S., Lewis, J.A., *et al.* (2005). Allan-Herndon-Dudley syndrome and the monocarboxylate transporter 8 (MCT8) gene. Am J Hum Genet *77*, 41-53.

Schwartz, H.L., Strait, K.A., Ling, N.C., and Oppenheimer, J.H. (1992). Quantitation of rat tissue thyroid hormone binding receptor isoforms by immunoprecipitation of nuclear triiodothyronine binding capacity. J Biol Chem *267*, 11794-11799.

Shepard, T.H. (1967). Onset of function in the human fetal thyroid: biochemical and radioautographic studies from organ culture. J Clin Endocrinol Metab *27*, 945-958.

Shimada, M., and Nakamura, T. (1973). Time of neuron origin in mouse hypothalamic nuclei. Exp Neurol *41*, 163-173.

Shine, B., McKnight, R.F., Leaver, L., and Geddes, J.R. (2015). Long-term effects of lithium on renal, thyroid, and parathyroid function: a retrospective analysis of laboratory data. Lancet *386*, 461-468.

Siegmund-Schultze, N. (2013). Leistungsbeeinflussende Substanzen im Breiten- und Freizeitsport: Trainieren mit allen Mitteln. Dtsch Arztebl International *110*, A-1422-A-1425.

Silva, J.E. (2003). The thermogenic effect of thyroid hormone and its clinical implications. Ann Intern Med *139*, 205-213.

Silva, J.E. (2006). Thermogenic mechanisms and their hormonal regulation. Physiol Rev *86*, 435-464.

Simonds, S.E., Pryor, J.T., Ravussin, E., Greenway, F.L., Dileone, R., Allen, A.M., Bassi, J., Elmquist, J.K., Keogh, J.M., Henning, E., *et al.* (2014). Leptin mediates the increase in blood pressure associated with obesity. Cell *159*, 1404-1416.

Solmonson, A., and Mills, E.M. (2016). Uncoupling Proteins and the Molecular Mechanisms of Thyroid Thermogenesis. Endocrinology *157*, 455-462.

Sommeijer, J.P., and Levelt, C.N. (2012). Synaptotagmin-2 is a reliable marker for parvalbumin positive inhibitory boutons in the mouse visual cortex. PLoS One *7*, e35323.

Song, M.K., Dozin, B., Grieco, D., Rall, J.E., and Nikodem, V.M. (1988). Transcriptional activation and stabilization of malic enzyme mRNA precursor by thyroid hormone. J Biol Chem *263*, 17970-17974.

Srichomkwun, P., Anselmo, J., Liao, X.H., Hones, G.S., Moeller, L.C., Alonso-Sampedro, M., Weiss, R.E., Dumitrescu, A.M., and Refetoff, S. (2017). Fetal Exposure to High Maternal

Thyroid Hormone Levels Causes Central Resistance to Thyroid Hormone in Adult Humans and Mice. J Clin Endocrinol Metab *102*, 3234-3240.

Südhof, T.C. (2015). Reproducibility: Experimental mismatch in neural circuits. Nature *528*, 338-339.

Sun, Z.Q., Ojamaa, K., Nakamura, T.Y., Artman, M., Klein, I., and Coetzee, W.A. (2001). Thyroid hormone increases pacemaker activity in rat neonatal atrial myocytes. J Mol Cell Cardiol *33*, 811-824.

Sussel, L., Marin, O., Kimura, S., and Rubenstein, J.L. (1999). Loss of Nkx2.1 homeobox gene function results in a ventral to dorsal molecular respecification within the basal telencephalon: evidence for a transformation of the pallidum into the striatum. Development *126*, 3359-3370.

Symons, C., Olsen, E.G., and Hawkey, C.M. (1975). The production of cardiac hypertrophy by tri-iodothyroacetic acid. J Endocrinol *65*, 341-346.

Takeuchi, Y., Murata, Y., Sadow, P., Hayashi, Y., Seo, H., Xu, J., O'Malley, B.W., Weiss, R.E., and Refetoff, S. (2002). Steroid receptor coactivator-1 deficiency causes variable alterations in the modulation of T(3)-regulated transcription of genes in vivo. Endocrinology *143*, 1346-1352.

Taurog, A., Dorris, M.L., and Doerge, D.R. (1996). Mechanism of simultaneous iodination and coupling catalyzed by thyroid peroxidase. Arch Biochem Biophys *330*, 24-32.

Taylor, P.N., Albrecht, D., Scholz, A., Gutierrez-Buey, G., Lazarus, J.H., Dayan, C.M., and Okosieme, O.E. (2018). Global epidemiology of hyperthyroidism and hypothyroidism. Nat Rev Endocrinol *14*, 301-316.

Tinnikov, A., Nordström, K., Thoren, P., Kindblom, J.M., Malin, S., Rozell, B., Adams, M., Rajanayagam, O., Pettersson, S., Ohlsson, C.*, et al.* (2002). Retardation of post-natal development caused by a negatively acting thyroid hormone receptor alpha1. EMBO J *21*, 5079-5087.

Trajkovic, M., Visser, T.J., Mittag, J., Horn, S., Lukas, J., Darras, V.M., Raivich, G., Bauer, K., and Heuer, H. (2007). Abnormal thyroid hormone metabolism in mice lacking the monocarboxylate transporter 8. J Clin Invest *117*, 627-635.

Trueba, S.S., Auge, J., Mattei, G., Etchevers, H., Martinovic, J., Czernichow, P., Vekemans, M., Polak, M., and Attie-Bitach, T. (2005). PAX8, TITF1, and FOXE1 gene expression patterns during human development: new insights into human thyroid development and thyroid dysgenesis-associated malformations. J Clin Endocrinol Metab *90*, 455-462.

van den Boogaard, E., Vissenberg, R., Land, J.A., van Wely, M., van der Post, J.A., Goddijn, M., and Bisschop, P.H. (2011). Significance of (sub)clinical thyroid dysfunction and thyroid autoimmunity before conception and in early pregnancy: a systematic review. Hum Reprod Update *17*, 605-619.

Van Der Vies, J. (1954). Two methods for the determination of glycogen in liver. Biochem J *57*, 410-416.

van Mullem, A., van Heerebeek, R., Chrysis, D., Visser, E., Medici, M., Andrikoula, M., Tsatsoulis, A., Peeters, R., and Visser, T.J. (2012). Clinical phenotype and mutant TRalpha1. N Engl J Med *366*, 1451-1453.

Vassart, G. (1972). Specific synthesis of thyroglobulin on membrane bound thyroid ribosomes. FEBS Lett *22*, 53-56.

Venero, C., Guadano-Ferraz, A., Herrero, A.I., Nordström, K., Manzano, J., de Escobar, G.M., Bernal, J., and Vennström, B. (2005). Anxiety, memory impairment, and locomotor dysfunction caused by a mutant thyroid hormone receptor alpha1 can be ameliorated by T3 treatment. Genes Dev *19*, 2152-2163.

Vulsma, T., Gons, M.H., and de Vijlder, J.J. (1989). Maternal-fetal transfer of thyroxine in congenital hypothyroidism due to a total organification defect or thyroid agenesis. N Engl J Med *321*, 13-16.

Wagner, M.S., Morimoto, R., Dora, J.M., Benneman, A., Pavan, R., and Maia, A.L. (2003). Hypothyroidism induces type 2 iodothyronine deiodinase expression in mouse heart and testis. J Mol Endocrinol *31*, 541-550.

Wallis, K., Dudazy, S., van Hogerlinden, M., Nordström, K., Mittag, J., and Vennström, B. (2010). The thyroid hormone receptor alpha1 protein is expressed in embryonic postmitotic neurons and persists in most adult neurons. Mol Endocrinol *24*, 1904-1916.

Wallis, K., Sjögren, M., van Hogerlinden, M., Silberberg, G., Fisahn, A., Nordström, K., Larsson, L., Westerblad, H., Morreale de Escobar, G., Shupliakov, O., *et al.* (2008). Locomotor deficiencies and aberrant development of subtype-specific GABAergic interneurons caused by an unliganded thyroid hormone receptor alpha1. J Neurosci *28*, 1904-1915.

Warner, A., Rahman, A., Solsjo, P., Gottschling, K., Davis, B., Vennström, B., Arner, A., and Mittag, J. (2013). Inappropriate heat dissipation ignites brown fat thermogenesis in mice with a mutant thyroid hormone receptor alpha1. Proc Natl Acad Sci U S A *110*, 16241-16246.

Watson, C. (2010). The brain : an introduction to functional neuroanatomy / Charles Watson, Matthew Kirkcaldie, George Paxinos (Amsterdam ; Boston: Academic).

Wikström, L., Johansson, C., Salto, C., Barlow, C., Campos Barros, A., Baas, F., Forrest, D., Thoren, P., and Vennström, B. (1998). Abnormal heart rate and body temperature in mice lacking thyroid hormone receptor alpha 1. EMBO J *17*, 455-461.

Wood, W.J., Geraci, T., Nilsen, A., DeBarber, A.E., and Scanlan, T.S. (2009). Iodothyronamines are oxidatively deaminated to iodothyroacetic acids in vivo. Chembiochem *10*, 361-365.

Wu, S.Y., Green, W.L., Huang, W.S., Hays, M.T., and Chopra, I.J. (2005). Alternate pathways of thyroid hormone metabolism. Thyroid *15*, 943-958.

Xu, Q., Cobos, I., De La Cruz, E., Rubenstein, J.L., and Anderson, S.A. (2004). Origins of cortical interneuron subtypes. J Neurosci *24*, 2612-2622.

Yen, P.M. (2001). Physiological and molecular basis of thyroid hormone action. Physiol Rev *81*, 1097-1142.

Zhao, L., Jiang, G., Tian, X., Zhang, X., Zhu, T., Chen, B., Wang, Y., and Ma, Q. (2018). Initiation timing effect of levothyroxine treatment on subclinical hypothyroidism in pregnancy. Gynecol Endocrinol, 1-4.

6. Non-Standard Abbreviations

3-T_1AM	3-iodothyronamine
$5HT_{3a}$	serotonin receptor 3a
AAV	adeno-associated virus
AHA	anterior hypothalamic area
AHDS	Allen-Herndon-Dudley syndrome
AUC	area under the curve
bpm	beats per minute
BrdU	bromodeoxyuridine
cDNA	complementary deoxyribonucleic acid
CGE	caudal ganglionic eminance
CH	congenital hypothyrodism
CNO	Clozapine-N-oxid
cnts	counts
DAB	3,3′-diaminobenzidine
DIO 1-3	iodothyronine deiodinases type 1-3
dko	double knock out
DNA	deoxyribonucleic acid
DREADD	designer receptors exclusively activated by designer drugs
E	embryonic day
GABA	gamma-aminobutyric acid
GAD67	glutamate decarboxylase 67
GAPDH	glyceraldehyde-3-phosphate dehydrogenase
i.p.	intraperitoneal injection
iBAT	interscapular brown adipose tissue
IgG	immunoglobulin G
IQ	intelligence quotient
ko	knock out
LGE	lateral ganglionic eminence
M/O dko	Mct8/Oatp1c1 double knock out
mAKT	murine thymoma viral proto-oncogene 1
MAO	monoamine oxidase
Mct8/10	monocarboxylate transport protein 8/10
MGE	median ganglionic eminance
mRNA	messenger ribonucleic acid
Oatp1c1	organic anion transporting peptides 1c1
ObRb	leptin receptor b
OD	optical density
ODC	ornithine decarboxylase
P	postnatal day
PV	parvalbumin
PVN	paraventricular nucleus

qPCR	quantitative polymerase chain reaction
RNA	ribonucleic acid
RT	room temperature
RTHβ	resistance to thyroid hormone syndrome β
SST	somatostatin
T_0AM	L-thyronamine
T_3	3,3′,5-triiodo-L-thyronine
T_4	3,3′,5,5′-tetraiodo-L-thyronine (thyroxine)
TA_1	3-iodothyroacetic acid
TAAR1	receptor trace amine-associated receptor 1
TAM	thyronamines
TH	thyroid hormone
TR	thyroid hormone receptor
TRH	thyrotropin-releasing hormone
TSH	thyroid stimulating hormone
UCP1	uncoupling protein 1
VGLUT2	vesicular glutamate transporter 2
wt	wild-type

7. Danksagung

Ich möchte mich bei all den Menschen bedanken, die mir in der Zeit meiner Doktorarbeit zur Seite standen und ohne die diese Arbeit nicht möglich gewesen wäre.

An erster Stelle steht hierbei mein Doktorvater Prof. Jens Mittag, der mich immer unterstützte und motivierte, nie die Geduld mit mir verlor, und mich unermüdlich antrieb, bis ich über mich hinausgewachsen bin, danke! Ich werde die Jagd nach „catchy" Abstract-Titeln und all die gratis Allgemeinbildung aus den 80gern vermissen.

Mein Dank gilt außerdem den Mitgliedern des Prüfungsausschusses, die sich bereit erklärt haben, mich zu prüfen.

Ich möchte mich bei Prof. Hendrik Lehnert sowie dem ehemaligen und dem aktuellen Program Committee und allen Mitgliedern des GRK1957 Adipocyte-Brain Crosstalk bedanken. Die Aufnahme als assoziiertes Mitglied in das Programm hat mir vielfältige Möglichkeiten geboten, um mich über mein Projekt hinaus fortzubilden und einen Forschungsaufenthalt am Karolinska Institutet in Stockholm ermöglicht. Ein besonderer Dank geht hierbei an Prof. Olaf Jöhren, der mein Projekt als Zweitbetreuer begleitet hat und Dr. Nina Perwitz und Chaoqun Jiang zu denen man immer und mit jeder Frage gehen konnte.

Im Rahmen meines Projektes durfte ich mit verschieden Kollaborationspartnern zusammenarbeiten, bei denen ich mich für die großartige Unterstützung bedanken möchte. Vielen Dank Prof. Björn Vennström und Dr. Susi Dudazy-Gralla für die Zeit in Stockholm; Prof. Jens Hjerling Leffler für die Doppel-Reporter Mäuse und das Feedback zum Paper; Prof. Heike Heuer für die Mäuse rund ums AHD-Syndrom; Prof. Markus Schwaninger und Dr. Helge Müller-Fielitz für die rAAVs und viel nützliches Knowhow zum Thema stereotaktische Injektionen; Dr. Kostja Renko für die angenehme Zusammenarbeit; Prof. Georg Brabant, Prof. Josef Köhrle und Prof. Lutz Schomburg für konstruktives Feedback zu verschiedensten Paper-Entwürfen und viele spannende Diskussionen auf zahlreichen Konferenzen. Außerdem geht ein großer Dank an die GTH Lübeck, Sven, Yannick, Heiko und Kathi, die den Laden geschmissen haben wann immer es nötig war!

Ich möchte mich natürlich auch bei allen ehemaligen und aktuellen Mitgliedern der Arbeitsgruppe bedanken, die immer eine helfende Hand und ein ermutigendes Wort erübrigen konnten und jede Mittagspause geduldig ausharrten, bis auch ich aufgegessen hatte. Dr. Carolin Höfig, die mich am ersten Arbeitstag Klausuren korrigieren ließ und mir in einem atemberaubenden Tempo all das Rüstzeug an die Hand gab, das für mich später so unverzichtbar werden sollte. Dr. Rebecca Ölkrug, die mein Fels in der Brandung ist, nicht

nur weil wir gegenseitig unsere Sätze beenden können und uns fragen was wohl der Sentinel vom Käfigwechsel hält, sondern weil ich ausnahmslos immer und mit allem zu ihr kommen konnte. Sogol Gachkar, die Drahtzieherin der großartigsten Minion-Aktionen, die man sich vorstellen kann, und unfehlbar darin mich aufzuheitern. Beate Herrmann, eine fantastische Last-minute Korrektorin, die immer ein offenes Ohr hatte, nie müde wurde ihre unerschütterliche Zuversicht mit mir zu teilen und mir gezeigt hat, dass man auch in Socken pusten kann. Kornelia Johann, die für den sportlichen Ausgleich sorgte und immer für eine hitzige Diskussion zu haben war. Francesca Raffaelli, deren unendliche Flut an Anekdoten mir regelmäßig Fernweh beschert. PD Alexander Iwen, der immer für eine Überraschung gut war. Julia Resch, die mir mit einem simplen Western Blot die Schweißperlen auf die Stirn treiben kann, aber immer genau dann tatkräftig in die Bresche springt, wenn es nötig ist. Ihr habt die Zeit meiner Doktorarbeit zu einer großartigen Erfahrung gemacht und dafür bin ich euch unendlich dankbar!

Auch außerhalb der Grenzen dieses Labors sind mir viele wunderbare Menschen begegnet, die mich auf meinem Weg unterstützt haben. Danke Prof. Henrik Oster, dass du mich dazu motiviert hast den größten Schritt von allen zu tun, den Ersten; Danke Dr. Carla Schulz, dass du mich im richtigen Moment dem richtigen Menschen vorgestellt hast, und natürlich für den besten „Doktorarbeits-Motivations-Kalender" den man sich nur vorstellen kann; Danke Jana-Thabea Kiehn, dass du mir das „Ende der Welt" gezeigt hast und dass ich immer auf dich zählen kann, vor allem wenn man sich mal wieder so richtig in was reinsteigern muss. Danke Dr. Isa Kolbe und Isabel Heyde, für aufmunternde Worte und Ablenkung in der Kletterwand. Danke Helen Sievert, das du es so lange mit mir ausgehalten hast, dafür gesorgt hast, dass ich nicht verhungere und manchmal sogar noch wach warst, wenn ich nach Hause kam.

Die letzten Worte hier sollen an meine Eltern und meine Familie gehen, ohne die nichts von alledem möglich gewesen wäre, weil sie mich immer unterstützen und immer hinter mir stehen, obwohl sie „nicht ganz verstehen was sie da eigentlich macht" und sich fragen „wann sie den endlich mal mit dem Studium fertig ist". Und natürlich an Sebastian, weil es jetzt nicht mehr nur Sinn macht, sondern auch Sinn ergibt. Danke für euer Vertrauen und eure uneingeschränkte Liebe!

8. Publisher Licence

OXFORD UNIVERSITY PRESS LICENSE
TERMS AND CONDITIONS

Jun 19, 2018

This Agreement between Ms. Lisbeth Harder ("You") and Oxford University Press ("Oxford University Press") consists of your license details and the terms and conditions provided by Oxford University Press and Copyright Clearance Center.

License Number	4362561104045
License date	Jun 05, 2018
Licensed content publisher	Oxford University Press
Licensed content publication	Endocrinology
Licensed content title	Thermoregulatory and Cardiovascular Consequences of a Transient Thyrotoxicosis and Recovery in Male Mice
Licensed content author	Hoefig, Carolin S.; Harder, Lisbeth
Licensed content date	Jul 1, 2016
Type of Use	Thesis/Dissertation
Institution name	
Title of your work	Layered Interactions of Systemic and Brain Effects by Thyroid Hormones
Publisher of your work	University of Lübeck
Expected publication date	Jul 2018
Permissions cost	0.00 EUR
Value added tax	0.00 EUR
Total	0.00 EUR
Title	Layered Interactions of Systemic and Brain Effects by Thyroid Hormones
Instructor name	Prof. Dr. Jens Mittag
Institution name	University of Lübeck
Expected	Jul 2018

presentation date	
Portions	Figure 1., 2., 3., 4., Table 1., Supplemental Table 1., Supplemental Figure 1., Supplemental Figure 2.
Specific Languages	English, German
Requestor Location	Ms. Lisbeth Harder Roentgenstraße 31 Luebeck, Schleswig-Holstein 23562 Germany Attn: Ms. Lisbeth Harder
Publisher Tax ID	GB125506730
Billing Type	Invoice
Billing Address	Ms. Lisbeth Harder Roentgenstraße 31 Luebeck, Germany 23562 Attn: Ms. Lisbeth Harder
Total	0.00 EUR

Terms and Conditions

STANDARD TERMS AND CONDITIONS FOR REPRODUCTION OF MATERIAL FROM AN OXFORD UNIVERSITY PRESS JOURNAL

1. Use of the material is restricted to the type of use specified in your order details.
2. This permission covers the use of the material in the English language in the following territory: world. If you have requested additional permission to translate this material, the terms and conditions of this reuse will be set out in clause 12.
3. This permission is limited to the particular use authorized in (1) above and does not allow you to sanction its use elsewhere in any other format other than specified above, nor does it apply to quotations, images, artistic works etc that have been reproduced from other sources which may be part of the material to be used.
4. No alteration, omission or addition is made to the material without our written consent. Permission must be re-cleared with Oxford University Press if/when you decide to reprint.
5. The following credit line appears wherever the material is used: author, title, journal, year, volume, issue number, pagination, by permission of Oxford University Press or the sponsoring society if the journal is a society journal. Where a journal is being published on behalf of a learned society, the details of that society must be included in the credit line.
6. For the reproduction of a full article from an Oxford University Press journal for whatever purpose, the corresponding author of the material concerned should be informed of the proposed use. Contact details for the corresponding authors of all Oxford University Press journal contact can be found alongside either the abstract or full text of the article concerned, accessible from www.oxfordjournals.org Should there be a problem clearing these rights, please contact journals.permissions@oup.com
7. If the credit line or acknowledgement in our publication indicates that any of the figures, images or photos was reproduced, drawn or modified from an earlier source it will be necessary for you to clear this permission with the original publisher as well. If this permission has not been obtained, please note that this material cannot be included in your publication/photocopies.
8. While you may exercise the rights licensed immediately upon issuance of the license at the end of the

licensing process for the transaction, provided that you have disclosed complete and accurate details of your proposed use, no license is finally effective unless and until full payment is received from you (either by Oxford University Press or by Copyright Clearance Center (CCC)) as provided in CCC's Billing and Payment terms and conditions. If full payment is not received on a timely basis, then any license preliminarily granted shall be deemed automatically revoked and shall be void as if never granted. Further, in the event that you breach any of these terms and conditions or any of CCC's Billing and Payment terms and conditions, the license is automatically revoked and shall be void as if never granted. Use of materials as described in a revoked license, as well as any use of the materials beyond the scope of an unrevoked license, may constitute copyright infringement and Oxford University Press reserves the right to take any and all action to protect its copyright in the materials.
9. This license is personal to you and may not be sublicensed, assigned or transferred by you to any other person without Oxford University Press's written permission.
10. Oxford University Press reserves all rights not specifically granted in the combination of (i) the license details provided by you and accepted in the course of this licensing transaction, (ii) these terms and conditions and (iii) CCC's Billing and Payment terms and conditions.
11. You hereby indemnify and agree to hold harmless Oxford University Press and CCC, and their respective officers, directors, employs and agents, from and against any and all claims arising out of your use of the licensed material other than as specifically authorized pursuant to this license.
12. Other Terms and Conditions:
v1.4

Questions? customercare@copyright.com or +1-855-239-3415 (toll free in the US) or +1-978-646-2777.

KARGER PUBLISHERS LICENSE TERMS AND CONDITIONS

Jun 19, 2018

This Agreement between Ms. Lisbeth Harder ("You") and Karger Publishers ("Karger Publishers") consists of your license details and the terms and conditions provided by Karger Publishers and Copyright Clearance Center.

License Number	4364380114450
License date	Jun 08, 2018
Licensed Content Publisher	Karger Publishers
Licensed Content Publication	European Thyroid Journal
Licensed Content Title	In vivo Effects of Repeated Thyronamine Administration in Male C57BL/6J Mice
Licensed copyright line	Copyright © 2017, © 2017 European Thyroid Association Published by S. Karger AG, Basel
Licensed Content Author	Harder Lisbeth, Schanze Nancy, Sarsenbayeva Assel, et al
Licensed Content Date	Dec 5, 2017
Licensed Content Volume	7
Licensed Content Issue	1
Special issue or supplement	
Type of Use	Thesis/Dissertation
Requestor type	author of requested content
Format	Print, Electronic
Portion	full article
Include PDF	no
Rights for	Main product and any product related to main product
Duration of use	Life of current edition/presentation
Creation of copies for the disabled	no
For distribution to	Worldwide
In the following language(s)	Original language plus one translation
Specific languages	English, German
The lifetime unit quantity of new product	100
The requesting person/organization is:	Lisbeth Harder
Order reference number	
Title of your thesis / dissertation	Layered Interactions of Systemic and Brain Effects by Thyroid Hormones
Expected completion date	Jul 2018

Estimated size (pages)	120
Requestor Location	Ms. Lisbeth Harder Roentgenstraße 31 Luebeck, Schleswig-Holstein 23562 Germany Attn: Ms. Lisbeth Harder
Publisher Tax ID	980406204
Billing Type	Invoice
Billing Address	Ms. Lisbeth Harder Roentgenstraße 31 Luebeck, Germany 23562 Attn: Ms. Lisbeth Harder
Total	0.00 EUR
Terms and Conditions	

STANDARD TERMS AND CONDITIONS FOR REPRODUCTION OF MATERIAL

Introduction

The Publisher for this copyrighted material is Karger Publishers. By clicking "accept" in connection with completing this licensing transaction, you agree that the following terms and conditions apply to this transaction (along with the Billing and Payment terms and conditions established by Copyright Clearance Center, Inc. ("CCC"), at the time that you opened your CCC account and that are available at any time at http://myaccount.copyright.com.

Limited License

Publisher hereby grants to you a non-exclusive license to use this material. Licenses are for one-time use only with a maximum distribution equal to the number that you identified in the licensing process. It is explicitly forbidden to reuse and/or translate a complete book or journal issue by separately obtaining permission for each book chapter or journal article. Any further use, edition, translation or distribution, either in print or electronically requires written permission again and may be subject to another permission fee. This permission applies only to copyrighted content that Karger Publishers owns, and not to copyrighted content from other sources. If any material in our work appears with credit to another source, you must also obtain permission from the original source cited in our work. All content reproduced from copyrighted material owned by Karger Publishers remains the sole and exclusive property of Karger Publishers. The right to grant permission to a third party is reserved solely by Karger Publishers.

Geographic Rights

Licenses may be exercised anywhere in the world with particular exceptions in China.

Altering/Modifying Material

• You may not alter or modify the material in any manner (except that you may use, within the scope of the license granted, one or more excerpts from the copyrighted material, provided that the process of excerpting does not alter the meaning of the material or in any way reflect negatively on the Publisher or any writer of the material), nor may you translate the material into another language, unless your license specifically grants translation rights.
• Other minor editing modifications are allowed when reusing figures/tables and illustrations (e.g. redesigning, reformation, coloring/recoloring) and can be made at the Licensee's

discretion.

Reservation of Rights

All rights reserved. Publisher hereby grants to you a non-exclusive license to use this material. Licenses are for one-time use exclusively. No part of this publication may be translated into other languages, reproduced or utilized in any form or by any means, electronically or mechanically, including photocopying, recording, micro-copying, or by any information storage and retrieval system, without permission in writing from the Publisher.

License Contingent on Payment

While you may exercise the rights licensed immediately upon issuance of the license at the end of the licensing process for the transaction, provided that you have disclosed complete and accurate details of your proposed use, no license is finally effective unless and until full payment is received from you (either by Publisher or by CCC) as provided in CCC's Billing and Payment terms and conditions. If full payment is not received on a timely basis, then any license preliminarily granted shall be deemed automatically revoked and shall be void as if never granted. Further, in the event that you breach any of these terms and conditions or any of CCC's Billing and Payment terms and conditions, the license is automatically revoked and shall be void as if never granted. Use of materials as described in a revoked license, as well as any use of the materials beyond the scope of an unrevoked license, may constitute copyright infringement and Publisher reserves the right to take any and all action to protect its copyright in the materials.

Copyright Notice

• You must give full credit to the original source of the article/book chapter and include the following copyright notice in connection with any reproduction of the licensed material: "Copyright © 2012 (or other relevant year) Karger Publishers, Basel, Switzerland."

• In case of translations you must additionally include the following disclaimer:"The article/book chapter printed herein has been translated into (relevant language) from the original by (Name of Licensee).KARGER PUBLISHERS CANNOT BE HELD RESPONSIBLE FOR ANY ERRORS OR INACCURACIES THAT MAY HAVE OCCURRED DURING TRANSLATION. THIS ARTICLE/BOOK CHAPTER IS COPYRIGHT PROTECTED AND ANY FURTHER DISTRIBUTION REQUIRES A WRITTEN CONSENT FROM KARGER PUBLISHERS.

Warranties

Publisher makes no representations or warranties with respect to the licensed material and adopts on its own behalf the limitations and disclaimers established by CCC on its behalf in its Billing and Payment terms and conditions for this licensing transaction.

Indemnity

You hereby indemnify and agree to hold harmless Publisher and CCC, and their respective officers, directors, employees and agents, from and against any and all claims arising out of your use of the licensed material other than as specifically authorized pursuant to this license.

No Transfer of License

This license is personal to you and may not be sublicensed, assigned, or transferred by you to any other person without Publisher's written permission.

No Amendment Except in Writing

This license may not be amended except in a writing signed by both parties (or, in the case of Publisher, by CCC on Publisher's behalf).

Objection to Contrary Terms

Publisher hereby objects to any terms contained in any purchase order, acknowledgment, check endorsement or other writing prepared by you, which terms are inconsistent with these terms and conditions or CCC's Billing and Payment terms and conditions. These terms and

conditions, together with CCC's Billing and Payment terms and conditions (which are incorporated herein), comprise the entire agreement between you and Publisher (and CCC) concerning this licensing transaction. In the event of any conflict between your obligations established by these terms and conditions and those established by CCC's Billing and Payment terms and conditions, these terms and conditions shall control.

Content Delivery

• Content Delivery Requested content such as a figure/table/cover or PDF of a full article will be provided to you by the Publisher directly via e-mail in high resolution quality.
• Delivery will be processed within five (5) working days from the date of your purchase.
• Subsequent cancellations of content delivery orders cannot be considered and will not be refunded.

Excluded Grants

• Exclusivity.
• Reuse/Translation of a complete book or journal issue.
• Reuse in another or in a future Edition.
• Reuse beyond the limitations within the license's scope, such as e.g. beyond the granted number of copies, beyond the granted format, beyond the chosen foreign language.
• Reuse of contents copyrighted by a third party without obtaining permission from the third party.
• Make any data available and authorize others to reuse the materials.

Karger Publishers Open Access Policy

Karger Open Access articles can be read and shared for all noncommercial purposes on condition that the author and journal are properly acknowledged. For most Open Access articles, the Creative Commons Attribution-NonCommercial 3.0 Unported license (CC BY-NC) applies. For commercial use however permission needs to be obtained.
For research funded by the Wellcome Trust, Research Councils UK (RCUK) and other organizations with the same requirements, papers are published under the Creative Commons Attribution 3.0 Unported (CC BY 3.0) license.

Service Description for Content Services

Subject to these terms of use, any terms set forth on the particular order, and payment of the applicable fee, you may make the following uses of the ordered materials:

• Content Rental: You may access and view a single electronic copy of the materials ordered for the time period designated at the time the order is placed. Access to the materials will be provided through a dedicated content viewer or other portal, and access will be discontinued upon expiration of the designated time period. An order for Content Rental does not include any rights to print, download, save, create additional copies, to distribute or to reuse in any way the full text or parts of the materials.

The materials may be accessed and used only by the person who placed the Order or the person on whose behalf the order was placed and only in accordance with the terms included in the particular order.

Other Terms and Conditions:

v1.3

Questions? customercare@copyright.com or +1-855-239-3415 (toll free in the US) or +1-978-646-2777.

JOHN WILEY AND SONS LICENSE TERMS AND CONDITIONS

Jun 19, 2018

This Agreement between Ms. Lisbeth Harder ("You") and John Wiley and Sons ("John Wiley and Sons") consists of your license details and the terms and conditions provided by John Wiley and Sons and Copyright Clearance Center.

License Number	4362560261094
License date	Jun 05, 2018
Licensed Content Publisher	John Wiley and Sons
Licensed Content Publication	Journal of Neuroendocrinology
Licensed Content Title	Maternal thyroid hormone is required for parvalbumin neurone development in the anterior hypothalamic area
Licensed Content Author	L. Harder, S. Dudazy-Gralla, H. Müller-Fielitz, et al
Licensed Content Date	Feb 27, 2018
Licensed Content Volume	30
Licensed Content Issue	3
Licensed Content Pages	10
Type of use	Dissertation/Thesis
Requestor type	Author of this Wiley article
Format	Print and electronic
Portion	Full article
Will you be translating?	Yes, including English rights
Number of languages	1
Languages	English, German
Title of your thesis / dissertation	Layered Interactions of Systemic and Brain Effects by Thyroid Hormones
Expected completion date	Jul 2018
Expected size (number of pages)	120
Requestor Location	Ms. Lisbeth Harder Roentgenstraße 31 Luebeck, Schleswig-Holstein 23562 Germany Attn: Ms. Lisbeth Harder
Publisher Tax ID	EU826007151
Total	0.00 EUR
Terms and Conditions	

TERMS AND CONDITIONS

This copyrighted material is owned by or exclusively licensed to John Wiley & Sons, Inc. or one of its group companies (each a"Wiley Company") or handled on behalf of a society with which a Wiley Company has exclusive publishing rights in relation to a particular work (collectively "WILEY"). By clicking "accept" in connection with completing this licensing transaction, you agree that the following terms and conditions apply to this transaction (along with the billing and payment terms and conditions established by the Copyright Clearance Center Inc., ("CCC's Billing and Payment terms and conditions"), at the time that you opened your RightsLink account (these are available at any time at http://myaccount.copyright.com).

Terms and Conditions

- The materials you have requested permission to reproduce or reuse (the "Wiley Materials") are protected by copyright.

- You are hereby granted a personal, non-exclusive, non-sub licensable (on a stand-alone basis), non-transferable, worldwide, limited license to reproduce the Wiley Materials for the purpose specified in the licensing process. This license, **and any CONTENT (PDF or image file) purchased as part of your order,** is for a one-time use only and limited to any maximum distribution number specified in the license. The first instance of republication or reuse granted by this license must be completed within two years of the date of the grant of this license (although copies prepared before the end date may be distributed thereafter). The Wiley Materials shall not be used in any other manner or for any other purpose, beyond what is granted in the license. Permission is granted subject to an appropriate acknowledgement given to the author, title of the material/book/journal and the publisher. You shall also duplicate the copyright notice that appears in the Wiley publication in your use of the Wiley Material. Permission is also granted on the understanding that nowhere in the text is a previously published source acknowledged for all or part of this Wiley Material. Any third party content is expressly excluded from this permission.

- With respect to the Wiley Materials, all rights are reserved. Except as expressly granted by the terms of the license, no part of the Wiley Materials may be copied, modified, adapted (except for minor reformatting required by the new Publication), translated, reproduced, transferred or distributed, in any form or by any means, and no derivative works may be made based on the Wiley Materials without the prior permission of the respective copyright owner.**For STM Signatory Publishers clearing permission under the terms of the STM Permissions Guidelines only, the terms of the license are extended to include subsequent editions and for editions in other languages, provided such editions are for the work as a whole in situ and does not involve the separate exploitation of the permitted figures or extracts,** You may not alter, remove or suppress in any manner any copyright, trademark or other notices displayed by the Wiley Materials. You may not license, rent, sell, loan, lease, pledge, offer as security, transfer or assign the Wiley Materials on a stand-alone basis, or any of the rights granted to you hereunder to any other person.

- The Wiley Materials and all of the intellectual property rights therein shall at all times remain the exclusive property of John Wiley & Sons Inc, the Wiley Companies, or their respective licensors, and your interest therein is only that of having possession of and the right to reproduce the Wiley Materials pursuant to Section 2 herein during the continuance of this Agreement. You agree that you own no right, title or interest in or

to the Wiley Materials or any of the intellectual property rights therein. You shall have no rights hereunder other than the license as provided for above in Section 2. No right, license or interest to any trademark, trade name, service mark or other branding ("Marks") of WILEY or its licensors is granted hereunder, and you agree that you shall not assert any such right, license or interest with respect thereto

- NEITHER WILEY NOR ITS LICENSORS MAKES ANY WARRANTY OR REPRESENTATION OF ANY KIND TO YOU OR ANY THIRD PARTY, EXPRESS, IMPLIED OR STATUTORY, WITH RESPECT TO THE MATERIALS OR THE ACCURACY OF ANY INFORMATION CONTAINED IN THE MATERIALS, INCLUDING, WITHOUT LIMITATION, ANY IMPLIED WARRANTY OF MERCHANTABILITY, ACCURACY, SATISFACTORY QUALITY, FITNESS FOR A PARTICULAR PURPOSE, USABILITY, INTEGRATION OR NON-INFRINGEMENT AND ALL SUCH WARRANTIES ARE HEREBY EXCLUDED BY WILEY AND ITS LICENSORS AND WAIVED BY YOU.

- WILEY shall have the right to terminate this Agreement immediately upon breach of this Agreement by you.

- You shall indemnify, defend and hold harmless WILEY, its Licensors and their respective directors, officers, agents and employees, from and against any actual or threatened claims, demands, causes of action or proceedings arising from any breach of this Agreement by you.

- IN NO EVENT SHALL WILEY OR ITS LICENSORS BE LIABLE TO YOU OR ANY OTHER PARTY OR ANY OTHER PERSON OR ENTITY FOR ANY SPECIAL, CONSEQUENTIAL, INCIDENTAL, INDIRECT, EXEMPLARY OR PUNITIVE DAMAGES, HOWEVER CAUSED, ARISING OUT OF OR IN CONNECTION WITH THE DOWNLOADING, PROVISIONING, VIEWING OR USE OF THE MATERIALS REGARDLESS OF THE FORM OF ACTION, WHETHER FOR BREACH OF CONTRACT, BREACH OF WARRANTY, TORT, NEGLIGENCE, INFRINGEMENT OR OTHERWISE (INCLUDING, WITHOUT LIMITATION, DAMAGES BASED ON LOSS OF PROFITS, DATA, FILES, USE, BUSINESS OPPORTUNITY OR CLAIMS OF THIRD PARTIES), AND WHETHER OR NOT THE PARTY HAS BEEN ADVISED OF THE POSSIBILITY OF SUCH DAMAGES. THIS LIMITATION SHALL APPLY NOTWITHSTANDING ANY FAILURE OF ESSENTIAL PURPOSE OF ANY LIMITED REMEDY PROVIDED HEREIN.

- Should any provision of this Agreement be held by a court of competent jurisdiction to be illegal, invalid, or unenforceable, that provision shall be deemed amended to achieve as nearly as possible the same economic effect as the original provision, and the legality, validity and enforceability of the remaining provisions of this Agreement shall not be affected or impaired thereby.

- The failure of either party to enforce any term or condition of this Agreement shall not constitute a waiver of either party's right to enforce each and every term and condition of this Agreement. No breach under this agreement shall be deemed waived or excused by either party unless such waiver or consent is in writing signed by the party

granting such waiver or consent. The waiver by or consent of a party to a breach of any provision of this Agreement shall not operate or be construed as a waiver of or consent to any other or subsequent breach by such other party.

- This Agreement may not be assigned (including by operation of law or otherwise) by you without WILEY's prior written consent.
- Any fee required for this permission shall be non-refundable after thirty (30) days from receipt by the CCC.
- These terms and conditions together with CCC's Billing and Payment terms and conditions (which are incorporated herein) form the entire agreement between you and WILEY concerning this licensing transaction and (in the absence of fraud) supersedes all prior agreements and representations of the parties, oral or written. This Agreement may not be amended except in writing signed by both parties. This Agreement shall be binding upon and inure to the benefit of the parties' successors, legal representatives, and authorized assigns.
- In the event of any conflict between your obligations established by these terms and conditions and those established by CCC's Billing and Payment terms and conditions, these terms and conditions shall prevail.
- WILEY expressly reserves all rights not specifically granted in the combination of (i) the license details provided by you and accepted in the course of this licensing transaction, (ii) these terms and conditions and (iii) CCC's Billing and Payment terms and conditions.
- This Agreement will be void if the Type of Use, Format, Circulation, or Requestor Type was misrepresented during the licensing process.
- This Agreement shall be governed by and construed in accordance with the laws of the State of New York, USA, without regards to such state's conflict of law rules. Any legal action, suit or proceeding arising out of or relating to these Terms and Conditions or the breach thereof shall be instituted in a court of competent jurisdiction in New York County in the State of New York in the United States of America and each party hereby consents and submits to the personal jurisdiction of such court, waives any objection to venue in such court and consents to service of process by registered or certified mail, return receipt requested, at the last known address of such party.

WILEY OPEN ACCESS TERMS AND CONDITIONS

Wiley Publishes Open Access Articles in fully Open Access Journals and in Subscription journals offering Online Open. Although most of the fully Open Access journals publish open access articles under the terms of the Creative Commons Attribution (CC BY) License only, the subscription journals and a few of the Open Access Journals offer a choice of Creative Commons Licenses. The license type is clearly identified on the article.

The Creative Commons Attribution License

The Creative Commons Attribution License (CC-BY) allows users to copy, distribute and transmit an article, adapt the article and make commercial use of the article. The CC-BY license permits commercial and non-

Creative Commons Attribution Non-Commercial License

The Creative Commons Attribution Non-Commercial (CC-BY-NC)License permits use, distribution and reproduction in any medium, provided the original work is properly cited and is not used for commercial purposes.(see below)

Creative Commons Attribution-Non-Commercial-NoDerivs License
The Creative Commons Attribution Non-Commercial-NoDerivs License (CC-BY-NC-ND) permits use, distribution and reproduction in any medium, provided the original work is properly cited, is not used for commercial purposes and no modifications or adaptations are made. (see below)
Use by commercial "for-profit" organizations
Use of Wiley Open Access articles for commercial, promotional, or marketing purposes requires further explicit permission from Wiley and will be subject to a fee.
Further details can be found on Wiley Online Library
http://olabout.wiley.com/WileyCDA/Section/id-410895.html

Other Terms and Conditions:

v1.10 Last updated September 2015

Questions? customercare@copyright.com or +1-855-239-3415 (toll free in the US) or +1-978-646-2777.